8-2020

Protecting Crops from Abiotic Stress: Copper Oxide Nanoparticle Effects on Wheat and a Beneficial Rhizobacterium

Matthew Potter
Utah State University

Utah State University
MERRILL-CAZIER LIBRARY

PROTECTING CROPS FROM ABIOTIC STRESS: COPPER OXIDE

NANOPARTICLE EFFECTS ON WHEAT AND A BENEFICIAL

RHIZOBACTERIUM

by

Matthew Potter

A thesis submitted in partial fulfillment
of the requirements for the degree

of

MASTER OF SCIENCE

In

Biological Engineering

Approved:

_____   _____
David Britt, Ph.D.   Elizabeth Vargis, Ph.D.
Major Professor   Committee Member

_____   _____
Astrid Jacobson, Ph.D.   Joan E. McLean, M.S.
Committee Member   Committee Member

_____
Richard S. Inouye, Ph.D.
Vice Provost for Graduate Studies

UTAH STATE UNIVERSITY
Logan, Utah

2020

ABSTRACT

Protecting crops from abiotic stress: copper oxide nanoparticle effects on wheat and a

beneficial rhizosphere bacterium

by

Matthew Potter, Master of Science

Utah State University, 2020

Major Professor: David Britt
Department: Biological Engineering

CuO nanoparticles (NPs) have possible applications in agriculture as

micronutrient sources, pesticides, and enhancers of crop stress tolerance. Here, three

aspects of CuO NP agricultural applications are studied: 1) CuO-induced lignification,

the formation of the structural polymer lignin, in wheat; 2) CuO NP-induced drought

tolerance of wheat seedlings; and 3) the effects of CuO NPs on outer membrane vesicle

(OMV) production by *Pseudomonas chlororaphis* O6 (*Pc*O6), a plant-health promoting

bacterium.

Wheat seedlings (*Triticum aestivum* v. Dolores) grown 7 d exposed to CuO NPs

(300 mg Cu/kg) exhibited increased lignification, specifically in leaf sclerenchyma cells-

considered the strengthening cells of the plant. This increased lignification corresponded

with increases in the strength and toughness of the wheat shoots, measured with tensile

testing. CuO NP-induced lignification may be employed to prevent lodging in mature

cereal crops and reduce pathogen invasion.

Wheat seedlings (*Triticum aestivum* v. Juniper) inoculated with *Pc*O6 were grown

14 d in a sand growth matrix with a nutrient solution then exposed to simulated drought

for 8 d. Drought tolerance was quantified with chlorophyll fluorescence parameters of Φ_{PSII} and F_v/F_m, which represent operating and maximum photosystem II efficiencies respectively. Results showed that wheat seedling drought tolerance was unaffected by the investigated CuO NP dosages (0, 0.5, 5, 15, and 30 mg Cu/kg) in the growth matrix under these conditions. An absence of phytotoxic effects at these controlled CuO NP dosages showing that these NPs may be applied to soils without negative effects for crops.

The effects of CuO NPs (30 mg Cu/L) and H_2O_2 (3% v/v), a metabolite involved in plant stress responses, on PcO6 and its subsequent production of OMVs under stress were quantified by Raman spectroscopy coupled with linear discriminant analysis (LDA). Raman spectroscopy coupled with LDA was able to discriminate between PcO6 cells and isolated OMVs according to the cellular stressor with 83.3% and 71.1% accuracy respectively. OMVs showed unique Raman spectra peaks compared to PcO6 cells, indicating that PcO6 cell components are selectively enriched or excluded from OMVs. These results show the utility of Raman spectroscopy and LDA in characterizing OMVs according to the cellular stressor and thus understanding OMV roles in cell stress responses.

(164 pages)

PUBLIC ABSTRACT

Protecting crops from abiotic stress: copper oxide nanoparticle effects on wheat and a

beneficial rhizosphere bacterium

Matthew Potter

Nanoparticles (NPs) are defined as particles less than 100 nm in at least one

dimension. CuO NPs have possible applications in agriculture as micronutrient sources,

pesticides, and enhancers of crop stress tolerance. Here, three aspects of CuO NP

agricultural applications are studied: 1) the potential of CuO NPs to prevent wheat

lodging- when crops irreversibly fall over; 2) CuO NP-induced drought tolerance in

wheat seedlings; and 3) the effects of CuO NPs on outer membrane vesicle (OMV)

production by *Pseudomonas chlororaphis* O6 (*Pc*O6), a plant-health promoting

bacterium.

Wheat grown 7 d exposed to CuO NPs in the growth matrix exhibited increased

lignification, or formation of the plant structural polymer lignin, in wheat sclerenchyma

cells which are considered the strengthening cells of the plant. This increased

lignification also corresponded with stronger wheat shoots. These results, though

conducted on wheat seedlings, show promise for use of CuO NPs in preventing lodging

in mature wheat.

Wheat drought tolerance was measured with chlorophyll fluorescence, a method

that quantifies the photochemical reactions in a plant. This method showed that these low

CuO NPs dosages had no effect on drought tolerance of wheat grown 14 d then exposed

to simulated drought for 8 d. However, CuO NPs did not exhibit phytotoxic effects at

these controlled dosages showing that these NPs may be used for other agricultural purposes including pesticides and micronutrient sources.

The effects of CuO NPs, an agriculturally relevant NP, and H_2O_2, a metabolite involved in plant stress responses, on PcO6 and subsequent OMV production were studied with Raman spectroscopy. This spectroscopy method gives a "chemical fingerprint" and with subsequent analysis, Raman spectra can then be used to identify unknown samples. Raman spectroscopy with linear discriminant analysis was able to identify PcO6 cells and isolated OMVs according to the cellular stressor with an 83.3% accuracy and a 71.1% accuracy respectively. OMVs showed unique Raman spectra peaks compared to PcO6 cells, indicating that PcO6 cell components are selectively enriched or excluded from OMVs. These results show the power of Raman spectroscopy in characterizing OMVs according to cell stressor and thus understanding OMV roles in cell stress responses.

ACKNOWLEDGMENTS

I would like to thank everyone who supported me during this endeavor. I am very grateful for Dr. Britt who gave me the chance to start research as an undergraduate student and continue this research as a graduate student. His guidance and support have been crucial as I performed research and wrote the results in this thesis. I am also grateful to Dr. Vargis, Dr. Jacobson, and Prof. McLean who formed the remainder of my committee. Their suggestions and feedback have been instrumental throughout my time as a graduate student.

I would also like to thank my parents, Kent and Laurel Potter, who supported my decision to continue my education and were always happy to advise on balancing my studies, career goals, and my personal life. I also want to thank my wonderful new wife, Brandallyn Potter, who has been a support and helped me manage my time as I worked to balance our courtship and my studies.

Matthew Potter

TABLE OF CONTENTS

LIST OF TABLES

LIST OF FIGURES

CHAPTER 1

INTRODUCTION

Nanoparticles and agriculture

As the world population continues to increase, food security is a primary concern. The growing demand for food coincides with decreasing amounts of arable lands, leading to pressure to maximize crop yields in existing fields. This pressure has led to the development and common use of many unsustainable agricultural practices including excessive nutrient application (Bergstrom, Bowman, and Sims 2005) and groundwater overuse (Steward et al. 2013) that cause potentially irreversible environmental damage including topsoil loss and water pollution (Goodland 1997). Developing and implementing sustainable agricultural practices is of the highest priority (Bowler 2002) and will require multiple approaches. Nanotechnology is a promising solution for sustainable agriculture that leverages the unique properties of nanoparticles (NPs) as fertilizers, pesticides, and plant gene regulators to improve crop health while reducing environmental consequences.

NPs are defined as particles that are less than 100 nm in at least one dimension. Although compositionally similar to bulk materials, NPs often exhibit unique properties and higher reactivity than their bulk counterparts, largely due to their high surface area to volume ratio (Brunner et al. 2006). Multiple engineered metal and metal oxide NPs are considered for application in agriculture. Although nano-agriculture is relatively new, interest in this field has grown quickly (Figure 1 - 1). NPs in agriculture are generally studied for at least one of four applications: 1) pathogen suppression, 2) nutrient delivery, 3) crop growth or yield enhancement, or 4) crop stress tolerance enhancement.
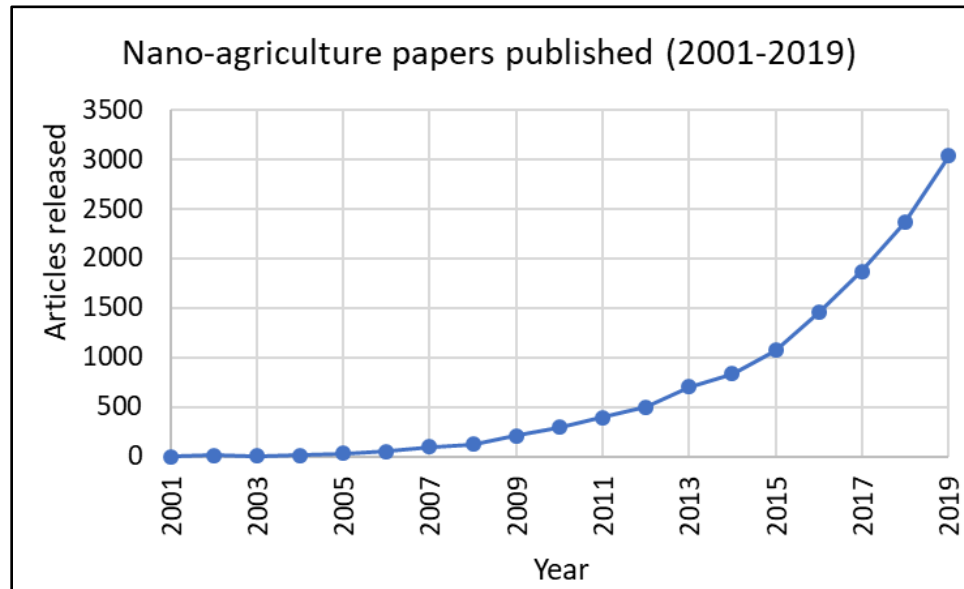
Figure 1 - 1: Number of journal articles published on nanotechnology in agriculture each year from 2001-2019. Only final releases of peer-reviewed articles are included (Scopus database, all potential fields, "nanotechnology AND agriculture", reviews excluded, accessed April 13, 2020).

One of the potential applications for NPs in agriculture is to fight crop pathogens. Some examples of this NP application include antifungal activities of CuO NPs (Elmer and White 2016), Cu-polymer composite NPs (Cioffi et al. 2004), Ag NPs (Jo, Kim, and Jung 2009), and complexed Ag-Si NPs (Park et al. 2006). Soda-lime glass containing Cu NPs exhibit both antibacterial and antifungal properties (Esteban-Tejeda et al. 2009). Unlike traditional chemical pesticides, fungicidal and bactericidal NPs can be engineered to adsorb to leaf surfaces allowing prolonged release. This approach was recently demonstrated with abamectin poly(lactic acid) NPs on cucumber leaves (Yu et al. 2017). This adhesion prevents NP pesticides from being washed away in the rain which is a large source of pollution from traditional chemical pesticides (Sekhon 2014).

Another potential NP innovation is nano-fertilizers for crops. NPs may be added to existing fertilizers or used as separate amendments. Currently, nutrient overuse is a major cause of phosphorus and nitrogen pollution in the environment (Bergstrom et al. 2005). This overuse is largely due to the low plant uptake rates and high runoff of current fertilizers that use salts and bulk materials. Though the amounts vary largely by crop and irrigation practices, it has been estimated that only about 50-70% of N, 10-25% of P, and 50-60% of K are utilized by crops. (Trenkel 1997). NPs are potential sources for providing nutrients (Liu and Lal 2015) including macronutrients, which are required by plants in large amounts, and micronutrients, which are required in small amounts. A list of essential plant macronutrients and micronutrients with their major functions in plant physiology is shown in Table 1 - 1.

Multiple NP properties may be exploited for fertilizer applications. Studies into the dissolution of NPs have shown that this complex process is affected by soil pH as well as NP size, aggregation, surface area, and surface charge (Misra et al. 2012) including NP coatings (Hortin 2017). These properties could be exploited to create NPs ideal for controlled nutrient release under specific agricultural environments. Another useful property of NPs is their ability to adsorb to plant seeds (Wu et al. 2012) and roots (Hortin 2017). NPs can also be engineered to adsorb to plant leaves (Yu et al. 2017). This NP adsorption allows the direct and localized release of macronutrients and micronutrients to the crop.

Table 1 - 1: List of major macronutrient roles in plant physiology (adapted from Tripathi et al., 2014) and major micronutrient roles in plant physiology (adapted from Hänsch and Mendel, 2009). This table focuses on nutrients commonly added in fertilizers and is not meant to be exhaustive.

Macronutrients	Major roles in plant physiology
Nitrogen (N)	A constituent of chlorophyll; an essential component of proteins and enzymes
Phosphorus (P)	Forms backbone of DNA, RNA, and ATP; a constituent of phospholipids
Potassium (K)	Linked to protein synthesis, enzyme activation, and cell membrane transportation; necessary for opening and closing stomata
Calcium (Ca)	Required for cell growth, division, and elongation; contributes to normal root system development
Magnesium (Mg)	The central atom of chlorophyll; active part of the electron transport chain
Sulfur (S)	An essential part of amino acids methionine and cysteine which are involved in plant defense against pathogens; crucial for photosynthesis
Micronutrients	Major roles in plant physiology
Boron (B)	Involved in sugar transport, protein synthesis, respiration, cell wall synthesis, lignification, and plant hormone metabolism
Chlorine (Cl)	Provides electrical charge balance; component of photosystem II
Copper (Cu)	Essential for mitochondrial respiration, C & N metabolism, and cell wall synthesis; cofactor of many proteins including many structures of the electron transport chain
Zinc (Zn)	Component of enzymes for protein synthesis, energy production, DNA transcription, and RNA processing and translation
Iron (Fe)	Involved in photosynthesis, mitochondrial respiration, nitrogen assimilation, production and scavenging of reactive oxygen species, and pathogen defense
Manganese (Mn)	Reacts with proteins either as a catalytically active metal or as an enzyme activator
Molybdenum (Mo)	Cofactor in proteins involved in nitrogen assimilation, sulfur metabolism, phytohormone biosynthesis, and stress reactions
Nickel (Ni)	Involved with plant ureases that protect against pathogens

Several researchers have also reported increased macronutrient and micronutrient uptake of crops exposed to micronutrient NP fertilizers. Uptake of N, P, K, Mg, Mn, Fe, and Zn by *Moringa peregrina* increased in plants treated with foliar-applied ZnO and Fe_3O_4 NPs compared to plants treated with salts of these nutrients (Soliman, El-feky, and Darwish 2015). Treatment with ZnO NPs increased leaf Zn concentrations in cucumber (Zhao et al. 2013) and wheat (Dimkpa, McLean, Latta, et al. 2012) compared to negative controls.

Nutrient-providing NPs may enhance plant health, yield, and quality compared to bulk or salts currently in use. For example, foliar-applied Fe NPs on black-eyed peas increased pod numbers per plant, and chlorophyll content compared to a bulk Fe control (Delfani et al. 2014) and Mn NPs increased root length, leaf length, rootlet number, and biomass in mung bean compared to Mn salts (Pradhan et al. 2013). These changes are likely due to the higher availability of the nutrients from NPs. However, changes in plant growth may also be attributed to the ability of NPs to enter cells, including plant cells, and alter gene expression (Van Aken 2015). These changes in gene expressions explain enhancements in plant growth by NPs that release no essential nutrients. Spinach exposed to TiO_2 NPs showed increases in biomass, nitrogen content, and chlorophyll content (Yang et al. 2007) even though Ti is not considered an essential micronutrient.

NP-induced gene expression changes also explain NP-induced changes in plant stress tolerance, allowing growth in conditions that would generally give inferior crop quality and yield. Various NPs can be utilized to lessen or prevent stress due to drought, soil salinity, heat, heavy metals, and UV-B radiation (Khan et al. 2017). NP-induced drought resistance is particularly notable, as this stressor is one of the most widespread

and damaging threats to crop yield and quality (Kim et al. 2012). Drought causes water stress in crops, defined as the inability of plants to efficiently perform physiological processes such as photosynthesis when adequate H_2O is unavailable. Drought severity will only continue to increase with the warming climate (Le Houerou 1996; Wang 2005).

Copper oxide nanoparticles and wheat

Amendments of CuO NPs have the potential to increase wheat drought tolerance. Cu is an essential micronutrient for plants (Hänsch and Mendel 2009). Though Cu occurs naturally in soil, it is largely unavailable to plants grown in calcareous and alkaline soils (Printz et al. 2016), largely because Cu ions bind to organic matter and carbonates (Mengel and Kirkby 2001) limiting availability to crops. Previous studies conducted in our research group have investigated CuO NP toxicity profiles and the subsequent effects on crops and microbiome bacteria (Dimkpa et al. 2013; Dimkpa, McLean, Britt, et al. 2012; Dimkpa, Mclean, et al. 2012; Dimkpa, McLean, Latta, et al. 2012; Stewart et al. 2015). Results of these studies led to investigations of potential applications of these NPs, at controlled doses, in agriculture (Anderson, McLean, et al. 2017; Hortin 2017; McManus et al. 2018) including enhancing wheat drought tolerance with CuO NPs (Jacobson et al. 2018; Yang et al. 2018).

Numerous genes related to mechanisms that protect against water stress are upregulated in wheat grown in sand amended with CuO NPs (Yang et al. 2018). During these drought studies, it was observed that introduction of CuO NPs to the growth matrix also results in leaves that are more rigid than the negative control (Jacobson et al. 2018; Yang et al. 2018) despite the H_2O content in wheat leaves decreasing as CuO NP concentration in the growth matrix increases (Jacobson et al. 2018). This CuO NP-

induced change in rigidity could be a method to prevent wind-caused lodging, a term for

when cereal crops irreversibly fall over which reduces photosynthetic output and exposes

crops to soil pests and pathogens (Fischer and Stapper 1987).

Crop microbiomes

During agricultural studies, it is important to consider the influence of the plant

microbiome, a term for the community of microorganisms that colonize multicellular

organisms including plants. Crop microbiome bacteria are studied for their value in

controlling pathogens (Fravel 2005; Pal and Gardener 2006) as well as enhancing plant

stress tolerance (Timmusk et al. 2017) including drought (Kim et al. 2012) and heavy

metal stress (Wright et al. 2016). Understanding the importance of the crop microbiome

may allow identification and implementation of beneficial microorganisms to improve

crop quality (Compant et al. 2005; Timmusk et al. 2017), another sustainable agricultural

practice.

Despite the integral nature of the crop microbiome, as NPs are studied for

application in agriculture, many researchers overlook the roles and impacts of NPs on the

microbiome. Understanding the three-way interactions among NPs, crops, and the

microbiome is essential as various NPs influence gene expression in various beneficial

and antagonistic microorganisms (Van Aken 2015) which may in turn affect the host

plant. In field-scale and laboratory-scale soil studies, the microbiome is present but often

ill-defined or uncharacterized. In laboratory-scale studies that use other growth mediums,

such as hydroponics or sand growth matrices, there is no microbiome. Implementing the

microbiome in these types of studies is extremely difficult. A majority of soil bacteria are

unculturable by traditional laboratory techniques, therefore simply identifying the many

diverse microbes that form communities in soil requires next-generation sequencing techniques (Knight et al. 2018; Rondon, Goodman, and Handelsman 1999). Instead of a complete representation, a model microbiome can be created. In these studies, the microbiome was modeled by a single beneficial bacterium, *Pseudomonas chlororaphis* O6.

Pseudomonas chlororaphis O6

Pseudomonas chlororaphis O6 (*Pc*O6) is a beneficial rhizobacterium originally isolated from roots of dryland wheat grown in Cache Valley, UT, USA (Spencer et al. 2003). *Pc*O6 increases wheat health including promoting drought tolerance (Anderson and Kim, 2018). Two primary mechanisms have been identified in *Pc*O6 that promote plant drought tolerance: 1) release of 2R,3R-butanediol that triggers stomatal closure in plants (Cho et al., 2008), and 2) formation of a biofilm matrix on the plant root (Kim et al., 2014; Jacobson et al., 2018). Biofilm formation may promote crop drought tolerance as the biofilm matrix maintains moisture around plant roots (Costa, Raaijmakers, and Kuramae 2018; Timmusk et al. 2015).

Previous studies by our research group have noted changes in *Pc*O6 metabolism upon exposure to CuO NPs (Anderson, McLean, et al. 2017). These changes elicited by CuO NPs include increased *Pc*O6 cell size (Bonebrake et al. 2018), decreased production of the metal scavenging siderophore pyoverdine (Dimkpa, McLean, Britt, et al. 2012), and increased production of the plant growth regulator indole-3-acetic acid (Dimkpa, Zeng, et al. 2012). *Pc*O6 viability is not affected in mature biofilms exposed to CuO NPs (300 mg Cu/L) (Bonebrake et al. 2018).

Biofilms in the environment

Biofilm is a term for a surface-bound microbial community surrounded by a self-produced extracellular matrix. Biofilms form when a sufficient number of individual, planktonic bacteria are present and detect each other through quorum sensing molecules. Bacteria then attach to a surface and produce an encasing extracellular matrix, a collection of secreted biomolecules including polysaccharides, DNA, and proteins. The biofilm matures as cells divide and differentiate. During this stage, biofilm bacteria take on different roles to support the microbial community while others become physiologically inactive. In many ways, the biofilm community begins to act similarly to a multicellular organism. At the final stage, the biofilm proliferates by releasing planktonic cells to further colonize other areas of the surrounding environment. These stages of biofilm formation are illustrated in Figure 1 - 2.

In soil, biofilm bacteria often form symbiotic relationships with plants that they colonize (Bonebrake et al. 2018; Timmusk et al. 2017). Aside from promoting drought tolerance (Timmusk et al. 2017), biofilm bacteria may protect plants from pathogens and pests. For example, *Pc*O6 biofilms produce phenazines, a class of antibiotic and antifungal compounds, and several insecticidal proteins (Anderson and Kim 2018). There are several methods that the biofilm may communicate with the host plant, including hormones (Hughes and Sperandio 2008) and quorum sensing molecules (Hughes and Sperandio 2008; Schikora, Schenk, and Hartmann 2016). These signals and other communication molecules may be excreted directly into the extracellular environment or released from the bacterium through outer membrane vesicles (OMVs).
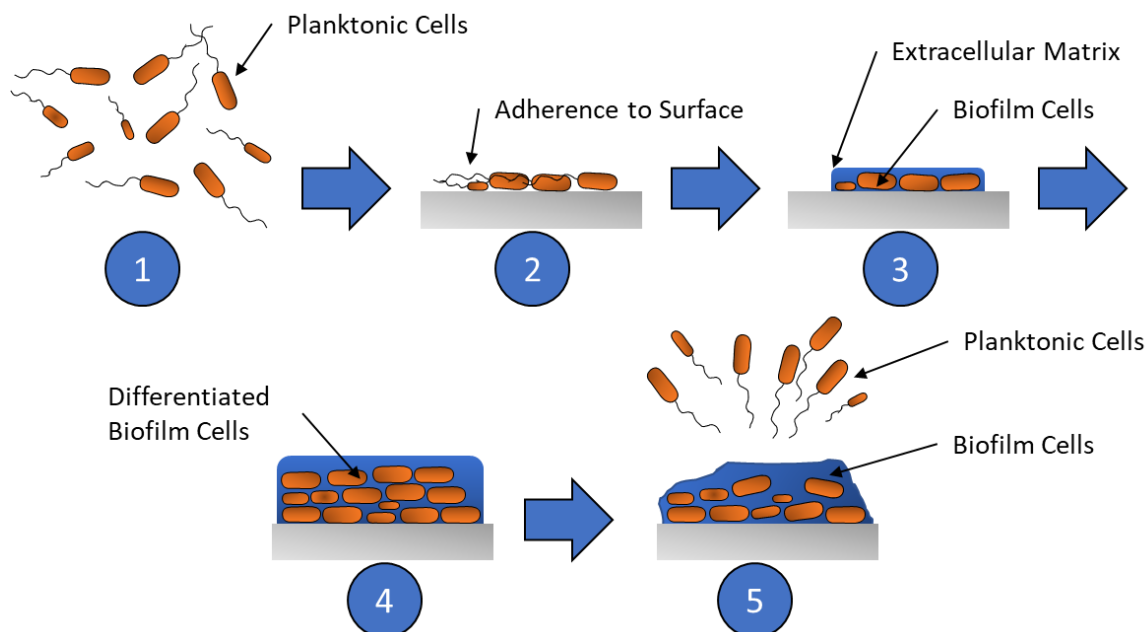
Figure 1 - 2: Illustration of biofilm formation stages which are 1) a sufficient number of planktonic bacteria are present and detect each other with quorum sensing molecules, 2) attachment of the bacteria to a surface, 3) formation of an extracellular matrix around the bacteria, 4) maturation of the biofilm and differentiation of biofilm cells, and 5) proliferation of the biofilm by releasing planktonic bacteria to colonize and form biofilms in other areas.

Outer membrane vesicles (OMVs)

OMVs are nonviable extracellular envelopes produced by all Gram-negative bacteria (Bahar et al. 2016; Bonnington and Kuehn 2014; Chutkan et al. 2013; McBroom et al. 2006) by pinching off a portion of their outer membrane (Figure 1 - 3). OMVs have shown many other unique functions including discarding waste from the bacteria, communicating between bacteria and eukaryotic cells (Klimentová and Stulík 2015; Kulp and Kuehn 2010), transferring DNA and RNA (Kulp and Kuehn 2010), and delivering toxins to pathogens and competing organisms (Horstman and Kuehn 2000; Li, Clarke, and Beveridge 1998). OMV release by *Pc*O6 has been reported previously (Dimkpa,

McLean, Britt, et al. 2012; Gade et al. 2016) but the roles of OMVs produced by this

bacterium have yet to be thoroughly studied.
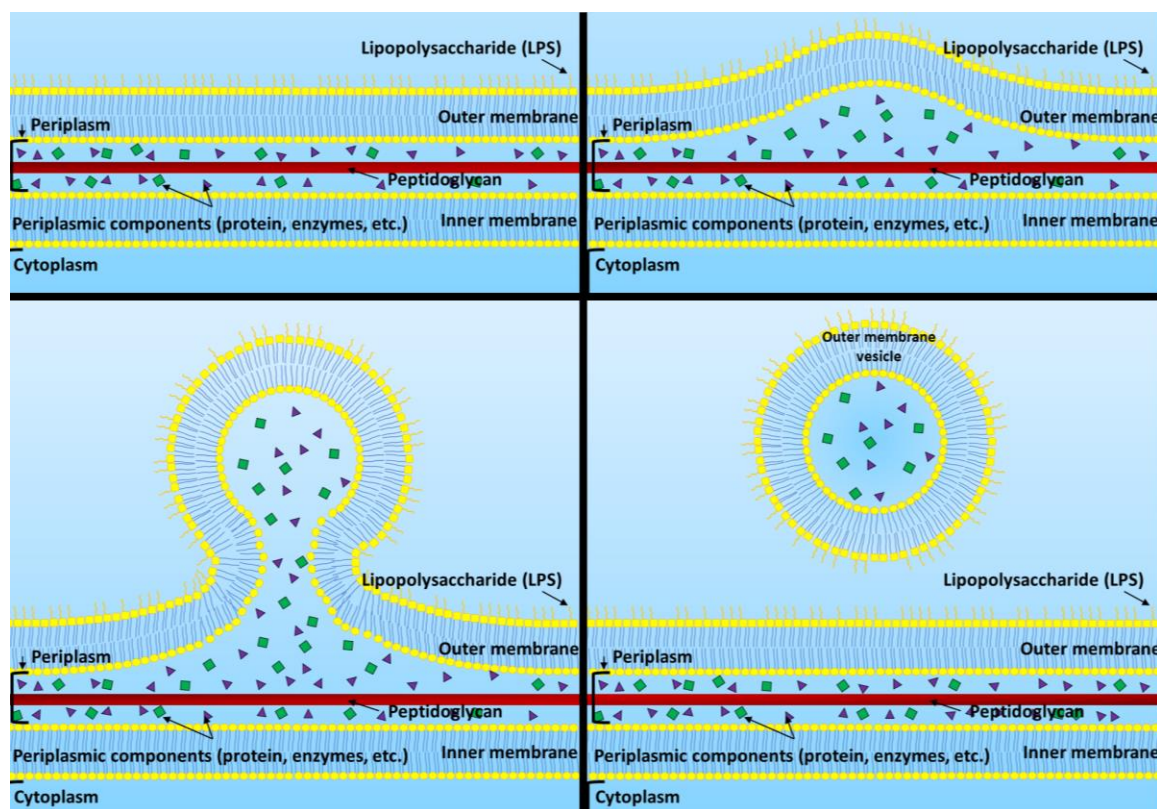
Figure 1 - 3: An illustration of the steps involved in the creation and separation of a bacterial outer membrane vesicle from the outer membrane. These stages are: A) the inner and outer membranes begin intact, B) an outward bulging of the outer membrane, C) the budding of the outer membrane, and D) the release of the OMV from the bacterium.

While it is established that OMV production and biofilm formation are integrally

related in Gram-negative bacteria, the details of this relationship are still being studied

(Wang, Chanda, and Zhong 2015). OMVs are found as a structural part of the biofilm

matrix (Schooling and Beveridge 2006) and may alter surface adhesiveness thus

promoting biofilm formation (Ionescu et al. 2014). OMV production by several *H. pylori*

strains correlates with the ability to form and maintain a biofilm state (Yonezawa et al. 2009). One of the quorum-sensing molecules of *Pseudomonas aeruginosa*, used for communication during biofilm formation, is released by the bacterium using OMVs (Mashburn-Warren et al. 2008).

OMV production is increased by Gram-negative bacteria as a response to stress. In these responses, OMVs exhibit a protective role. For example, OMV production is increased in bacteria under environmental stresses, including heat (McMahon et al. 2012) and nutrient depletion (van de Waterbeemd et al. 2013), and bacteria exposed to toxins and harmful chemical agents such as antibiotics (Bonnington and Kuehn 2014) or reactive oxygen species (MacDonald and Kuehn 2013). The release of OMVs is believed to be a method to quickly release misfolded periplasmic proteins (Klimentová and Stulík 2015; McBroom and Kuehn 2007). Some bacteria package enzymes into OMVs that breakdown antibiotics (Bonnington and Kuehn 2014; Schaar et al. 2011). OMVs may also serve as decoys to prevent attachment of membrane-binding antimicrobial agents and bacteriophages to the bacteria (Kulp and Kuehn 2010; Manning and Kuehn 2011).

Thesis aims

The goal of this thesis was to study the effects of CuO NPs in protecting wheat seedlings from abiotic stresses. This overarching goal was pursued through three specific aims: 1) evaluate the effect of CuO NPs on wheat seedling lignification, 2) quantify the effects of CuO NPs on wheat seedling drought tolerance, and 3) assess the effects of CuO NPs on biofilm architecture and OMV composition of a wheat microbiome bacterium, *Pc*O6. These aims are illustrated in Figure 1 - 4.
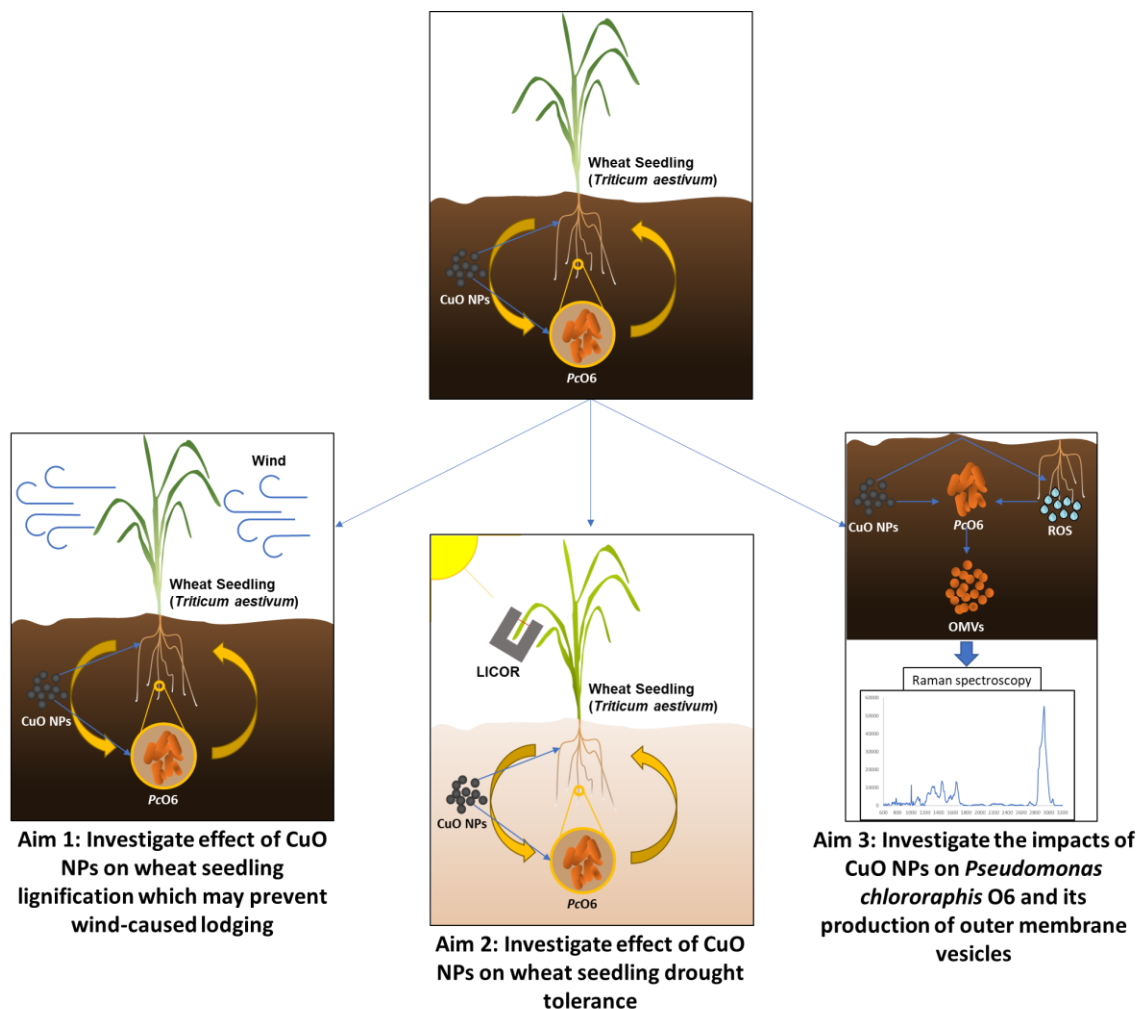
Figure 1 - 4: Illustration of the thesis aims- to understand the effect of CuO NPs in protecting wheat from abiotic stresses.

The first aim of this thesis is derived from the results of prior studies by our research group. It was observed that introduction of CuO NPs to the rhizosphere results in wheat leaves that are more rigid than the negative control (Jacobson et al. 2018; Yang et al. 2018) despite the H_2O content in the leaves decreasing as CuO NP concentration in the growth matrix increases (Jacobson et al. 2018). This decrease in H_2O content in wheat exposed to CuO NPs is mitigated when PcO6 is also present in the growth matrix (Yang et al. 2018), an example of the importance of the plant microbiome in crop health. It was

hypothesized that this increased rigidity was the result of CuO NP-induced lignification, the polymerization of the plant cell wall structural polymer lignin. Higher lignin content in crops is associated with increased resistance to pathogen invasion (Hammerschmidt and Kuć 1982) and resistance to wind-caused lodging (Zheng et al. 2017).

To test this hypothesis and to quantify this change in rigidity, phloroglucinol staining and mechanical property tests were performed on wheat leaves. Phloroglucinol, a dye that colors lignin red, was used to qualitatively compare lignin content. Wheat leaf mechanical properties were measured with tensile testing, an engineering method commonly used to measure the strength of a material. Tensile tests are commonly used by other researchers to assess various properties of plant tissues (Cleland 1967, 1984; Cosgrove 2016; Harker et al. 1997; Harker and Hallett 1992; Keyes, Sorrells, and Setter 1990; Köhler and Spatz 2002).

The second aim of this thesis was to investigate CuO NP effects on wheat drought tolerance. To quantify changes in wheat seedling drought tolerance caused by CuO NPs, gas exchange and chlorophyll fluorescence were measured with the LI-6800 Portable Photosynthesis Unit from LICOR. These methods analyze the photosynthetic efficiency of plants, defined as the number of photosynthetic reactions occurring in a plant compared to the maximum reactions possible, and are commonly used to quantify plant responses to water stress (Lu and Zhang 1998; Maxwell and Johnson 2000; Woo, Badger, and Pogson 2008). These measurements quantified wheat seedling drought response and whether CuO NPs, at dosages of 0, 0.5, 5, 15, and 30 mg Cu/kg growth medium, in the growth matrix mitigate drought stress in a Cu-sufficient growth medium.

Previous studies of CuO NPs have shown that the rhizosphere interactions

between plants and CuO NPs are complex and are in part dependent on the release of Cu

from the NPs that varies according to soil pH (Anderson, Britt, et al. 2017), organic

compounds (Hortin 2017), the composition of root exudates (McManus et al. 2018), and

the activities of the plant's microbiome (Anderson, McLean, et al. 2017; Wright et al.

2016). To limit the influence of these variables and improve experiment reproducibility, a

model growth system was developed and used in these studies. A Sand growth matrix

was used as sand is largely homogenous and lacks compounds that could bind or

precipitate Cu, thus decreasing plant availability. The crop microbiome was reduced to a

single beneficial soil microbe, PcO6, by surface sterilizing wheat seeds and inoculating

these with PcO6 at a controlled dosage (~10^4 CFUs/mL). These conditions were used in

all plant growth studies and allowed greater insight into the three-way interactions of

CuO NPs, wheat, and the microbiome.

The final aim of this thesis was to study the effects of CuO NPs on PcO6

biofilms, namely OMV release and composition. PcO6 was grown on solid media plates

as this culture technique allows the bacteria to grow in a quasi-biofilm state (Schooling

and Beveridge 2006), similar to natural PcO6 biofilms on plant roots. PcO6 biofilm cells

were exposed to either CuO NPs (30 mg Cu/L), or H_2O_2 (3% v/v)- a model of the release

of reactive oxygen species by plants as a response to exposure by CuO NPs (Adams et al.

2017) and contrasted with biofilms treated with sterile deionized H_2O. OMV composition

was characterized by atomic force microscopy, scanning electron microscopy, dynamic

light scattering, and Raman spectroscopy. These methods gave insight into the effect of

CuO NPs on OMV composition. To the knowledge of the author, this OMV study was

the first attempt to understand the effects of any NP on OMV formation and the first

attempt to characterize OMVs with Raman spectroscopy.

References

Adams, Josh, Melanie Wright, Hannah Wagner, Jonathan Valiente, David Britt, and Anne Anderson. 2017. "Cu from Dissolution of CuO Nanoparticles Signals Changes in Root Morphology." Plant Physiology and Biochemistry 110:108–17.

Van Aken, Benoit. 2015. "Gene Expression Changes in Plants and Microorganisms Exposed to Nanomaterials." Current Opinion in Biotechnology 33:206–19.

Anderson, Anne J., David Britt, Joan E. McLean, and Paul McManus. 2017. "Soil Chemistry Influences the Phytotoxicity of Metal Oxide Nanoparticles." International Journal of Nanotechnology 14:15–21.

Anderson, Anne J. and Young Cheol Kim. 2018. "Biopesticides Produced by Plant-Probiotic Pseudomonas Chlororaphis Isolates." Crop Protection 105(November 2017):62–69.

Anderson, Anne J., Joan E. McLean, Astrid R. Jacobson, and David W. Britt. 2017. "CuO and ZnO Nanoparticles Modify Interkingdom Cell Signaling Processes Relevant to Crop Production." Journal of Agricultural and Food Chemistry acs.jafc.7b01302.

Bahar, Ofir, Gideon Mordukhovich, Dee Dee Luu, Benjamin Schwessinger, Arsalan Daudi, Anna Kristina Jehle, Georg Felix, and Pamela C. Ronald. 2016. "Bacterial Outer Membrane Vesicles Induce Plant Immune Responses." Molecular Plant-Microbe Interactions 29(5):374–84.

Bergstrom, L., B. T. Bowman, and J. T. Sims. 2005. "Definition of Sustainable and Unsustainable Issues in Nutrient Management of Modern Agriculture." Soil Use and Management 21:76–81.

Bonebrake, Michelle, Kaitlyn Anderson, Jonathan Valiente, Astrid Jacobson, Joan E. McLean, Anne Anderson, and David W. Britt. 2018. "Biofilms Benefiting Plants Exposed to ZnO and CuO Nanoparticles Studied with a Root-Mimetic Hollow Fiber Membrane." Journal of Agricultural and Food Chemistry 66(26):6619–27.

Bonnington, K. E. and M. J. Kuehn. 2014. "Protein Selection and Export via Outer Membrane Vesicles." Biochimica et Biophysica Acta - Molecular Cell Research 1843(8):1612–19.

Bowler, Ian. 2002. "Developing Sustainable Agriculture." Geography 87(3):205–12.

Brunner, Tobias J., Peter Wick, Pius Manser, Philipp Spohn, Robert N. Grass, Ludwig K. Limbach, Arie Bruinink, and Wendelin J. Stark. 2006. "In Vitro Cytotoxicity of Oxide Nanoparticles: Comparison to Asbestos, Silica, and the Effect of Particle Solubility." Environmental Science and Technology 40(14):4374–81.

Chutkan, Halima, Ian MacDonald, Andrew Manning, and Meta J. Kuehn. 2013. "Quantitative and Qualitative Preparations of Bacterial Outer Membrane Vesicles." Methods in Molecular Biology.

Cioffi, Nicola, Luisa Torsi, Nicoletta Ditaranto, Luigia Sabbatini, Pier Giorgio Zambonin, Giuseppina Tantillo, Lina Ghibelli, Maria D'Alessio, Teresa Bleve-Zacheo, and Enrico Traversa. 2004. "Antifungal Activity of Polymer-Based Copper Nanocomposite Coatings." Applied Physics Letters 85(12):2417–19.

Cleland, Robert E. 1967. "Extensibility of Isolated Cell Walls: Measurement and Changes during Cell Elongation." Planta.

Cleland, Robert E. 1984. "The Instron Technique as a Measure of Immediate-Past Wall Extensibility." Planta 514–20.

Compant, Stéphane, Brion Duffy, Jerzy Nowak, Christophe Clement, and Essaid Ait Barka. 2005. "Use of Plant Growth-Promoting Bacteria for Biocontrol of Plant Diseases : Principles, Mechanisms of Action, and Future Prospects." Applied and Environmental Microbiology 71(9):4951–59.

Cosgrove, Daniel J. 2016. "Plant Cell Wall Extensibility: Connecting Plant Cell Growth with Cell Wall Structure, Mechanics, and the Action of Wall-Modifying Enzymes." Journal of Experimental Botany 67(2):463–76.

Costa, Ohana Y. A., Jos M. Raaijmakers, and Eiko E. Kuramae. 2018. "Microbial Extracellular Polymeric Substances – Ecological Functions and Impact on Soil Aggregation." Frontiers in Microbiology 9(July):1636.

Delfani, M., M. Baradarn Firouzabadi, N. Farrokhi, and H. Makarian. 2014. "Some Physiological Responses of Black-Eyed Pea to Iron and Magnesium Nanofertilizers." Communications in Soil Science and Plant Analysis 45(4):530–40.

Dimkpa, Christian O., Drew E. Latta, Joan E. Mclean, David W. Britt, Maxim I. Boyanov, and Anne J. Anderson. 2013. "Fate of CuO and ZnO Nano and Micro Particles in the Plant Environment." Environmental Science & Technology 47:4734–42.

Dimkpa, Christian O., Joan E. Mclean, David W. Britt, and Anne J. Anderson. 2012. "CuO and ZnO Nanoparticles Differently Affect the Secretion of Fluorescent Siderophores in the Beneficial Root Colonizer, Pseudomonas Chlororaphis O6." Nanotoxicology 6(6):635–42.

Dimkpa, Christian O., Joan E. McLean, David W. Britt, William P. Johnson, Bruce Arey, A. Scott Lea, and Anne J. Anderson. 2012. "Nanospecific Inhibition of Pyoverdine Siderophore Production in Pseudomonas Chlororaphis O6 by CuO Nanoparticles." Chemical Research in Toxicology 25(5):1066–74.

Dimkpa, Christian O., Joan E. McLean, Drew E. Latta, Eliana Manangón, David W. Britt, William P. Johnson, Maxim I. Boyanov, and Anne J. Anderson. 2012. "CuO and ZnO Nanoparticles: Phytotoxicity, Metal Speciation, and Induction of Oxidative Stress in Sand-Grown Wheat." Journal of Nanoparticle Research 14(9).

Dimkpa, Christian O., Jia Zeng, Joan E. McLean, David W. Britt, Jixun Zhan, and Anne J. Anderson. 2012. "Production of Indole-3-Acetic Acid via the Indole-3-Acetamide Pathway in the Plant-Beneficial Bacterium Pseudomonas Chlororaphis O6 Is Inhibited by ZnO Nanoparticles but Enhanced by CuO Nanoparticles." Applied and Environmental Microbiology 78(5):1404–10.

Elmer, Wade H. and Jason C. White. 2016. "The Use of Metallic Oxide Nanoparticles to Enhance Growth of Tomatoes and Eggplants in Disease Infested Soil or Soilless Medium." Environmental Science: Nano 3(5):1072–79.

Esteban-Tejeda, L., F. Malpartida, A. Esteban-Cubillo, C. Pecharromn, and J. S. Moya. 2009. "Antibacterial and Antifungal Activity of a Soda-Lime Glass Containing Copper Nanoparticles." Nanotechnology 20.

Fischer, R. A. and M. Stapper. 1987. "Lodging Effects on High-Yielding Crops of Irrigated Semidwarf Wheat." Field Crops Research 17(3–4):245–58.

Fravel, D. R. 2005. "Commercialization and Implementation of Biocontrol." Annual Review of Phytopathology 43(1):337–59.

Gade, Aniket, Joshua Adams, David W. Britt, Fen Ann Shen, Joan E. McLean, Astrid Jacobson, Young Cheol Kim, and Anne J. Anderson. 2016. "Ag Nanoparticles Generated Using Bio-Reduction and -Coating Cause Microbial Killing without Cell Lysis." BioMetals 29(2):211–23.

Goodland, Robert. 1997. "Environmental Sustainability in Agriculture: Diet Matters." Ecological Economics 23:189–200.

Hammerschmidt, R. and J. Kuć. 1982. "Lignification as a Mechanism for Induced Systemic Resistance in Cucumber." Physiological Plant Pathology.

Hänsch, Robert and Ralf R. Mendel. 2009. "Physiological Functions of Mineral Micronutrients (Cu, Zn, Mn, Fe, Ni, Mo, B, Cl)." Current Opinion in Plant Biology 12(3):259–66.

Harker, F. R. and I. C. Hallett. 1992. "Physiological Changes Associated with Development of Mealiness of Apple Fruit during Cool Storage." Hort Science 27(12):1291–94.

Harker, F. Roger, Margaret G. H. Stec, Ian C. Hallett, and Carey L. Bennett. 1997. "Texture of Parenchymatous Plant Tissue: A Comparison between Tensile and Other Instrumental and Sensory Measurements of Tissue Strength and Juiciness." Postharvest Biology and Technology 11(2):63–72.

Horstman, Amanda L. and Meta J. Kuehn. 2000. "Enterotoxigenic Escherichia Coli Secretes Active Heat-Labile Enterotoxin via Outer Membrane Vesicles." Journal of Biological Chemistry 275(17):12489–96.

Hortin, Joshua. 2017. "Behavior of Copper Oxide Nanoparticles in Soil Pore Waters as Influenced by Soil Characteristics, Bacteria, and Wheat Roots." Utah State University.

Le Houerou, Henry N. 1996. "Climate Change, Drought and Desertification." Journal of Arid Environments 34(2):133–85.

Hughes, David T. and Vanessa Sperandio. 2008. "Inter-Kingdom Signalling: Communication between Bacteria and Their Hosts." Nature Reviews Microbiology 6(February):111–20.

Ionescu, Michael, Paulo A. Zaini, Clelia Baccari, Sophia Tran, Aline M. da Silva, and Steven E. Lindow. 2014. "Xyllela Fastidiosa Outer Membrane Vesicles Modulate Plant Colonization by Blocking Attachment to Surfaces." Proceedings of the National Academy of Sciences 111(37):E3910–18.

Jacobson, Astrid, Stephanie Doxey, Matthew Potter, Joshua Adams, David Britt, Paul McManus, Joan McLean, and Anne Anderson. 2018. "Interactions between a Plant Probiotic and Nanoparticles on Plant Responses Related to Drought Tolerance." Industrial Biotechnology 14(3):148–56.

Jo, Young Ki, Byung H. Kim, and Geunhwa Jung. 2009. "Antifungal Activity of Silver Ions and Nanoparticles on Phytopathogenic Fungi." Plant Disease 93(10):1037–43.

Keyes, Geoff, Mark E. Sorrells, and Tim L. Setter. 1990. "Gibberellic Acid Regulates Cell Wall Extensibility in Wheat (Triticum Aestivum L.)." Plant Physiology 92(1):242–45.

Khan, M. Nasir, M. Mobin, Zahid Khorshid Abbas, Khalid A. AlMutairi, and Zahid H. Siddiqui. 2017. "Role of Nanomaterials in Plants under Challenging Environments." Plant Physiology and Biochemistry 110:194–209.

Kim, Young Cheol, Bernard R. Glick, Yoav Bashan, and Choong-Min Ryu. 2012. "Enhancement of Plant Drought Tolerance by Microbes." Pp. 383–413 in Plant Responses to Drought Stress: From Morphological to Molecular Features. Vol. 9783642326.

Klimentová, Jana and Jiří Stulík. 2015. "Methods of Isolation and Purification of Outer Membrane Vesicles from Gram-Negative Bacteria." Microbiological Research 170:1–9.

Knight, Rob, Alison Vrbanac, Bryn C. Taylor, Alexander Aksenov, Chris Callewaert, Justine Debelius, Antonio Gonzalez, Tomasz Kosciolek, Laura-Isobel McCall, Daniel McDonald, Alexey V. Melnik, James T. Morton, Jose Navas, Robert A. Quinn, Jon G. Sanders, Austin D. Swafford, Luke R. Thompson, Anupriya Tripathi, Zhenjiang Z. Xu, Jesse R. Zaneveld, Qiyun Zhu, J. Gregory Caporaso, and Pieter C. Dorrestein. 2018. "Best Practices for Analysing Microbiomes." Nature Reviews Microbiology 16(7):410–22.

Köhler, Lothar and Hanns Christof Spatz. 2002. "Micromechanics of Plant Tissues beyond the Linear-Elastic Range." Planta 215(1):33–40.

Kulp, Adam and Meta J. Kuehn. 2010. "Biological Functions and Biogenesis of Secreted Bacterial Outer Membrane Vesicles." Annual Review of Microbiology 64(1):163–84.

Li, Z., A. J. Clarke, and T. J. Beveridge. 1998. "Gram-Negative Bacteria Produce Membrane Vesicles Which Are Capable of Killing Other Bacteria." Journal of Bacteriology 180(20):5478–83.

Liu, Ruiqiang and Rattan Lal. 2015. "Potentials of Engineered Nanoparticles as Fertilizers for Increasing Agronomic Productions." Science of the Total Environment 514:131–39.

Lu, Congming and Jianhua Zhang. 1998. "Effects of Water Stress on Photosynthesis, Chlorophyll Fluorescence and Photoinhibition in Wheat Plants." Australian Journal of Plant Physiology 25:883–92.

MacDonald, Ian A. and Meta J. Kuehn. 2013. "Stress-Induced Outer Membrane Vesicle Production by Pseudomonas Aeruginosa." Journal of Bacteriology 195(13):2971–81.

Manning, Andrew J. and Meta J. Kuehn. 2011. "Contribution of Bacterial Outer Membrane Vesicles to Innate Bacterial Defense." BMC Microbiology 11(1):258.

Mashburn-Warren, Lauren, Jörg Howe, Patrick Garidel, Walter Richter, Frank Steiniger, Manfred Roessle, Klaus Brandenburg, and Marvin Whiteley. 2008. "Interaction of Quorum Signals with Outer Membrane Lipids: Insights into Prokaryotic Membrane Vesicle Formation." Molecular Microbiology 69(2):491–502.

Maxwell, Kate and Giles N. Johnson. 2000. "Chlorophyll Fluorescence—a Practical Guide." Journal of Experimental Botany 51(345):659–68.

McBroom, Amanda J., Alexandra P. Johnson, Sreekanth Vemulapalli, and Meta J. Kuehn. 2006. "Outer Membrane Vesicle Production by Escherichia Coli Is Independent of Membrane Instability." Journal of Bacteriology 188(15):5385–92.

McBroom, Amanda J. and Meta J. Kuehn. 2007. "Release of Outer Membrane Vesicles by Gram-Negative Bacteria Is a Novel Envelope Stress Response." Molecular Microbiology 63(2):545–58.

McMahon, Kenneth J., Maria E. Castelli, Eleonora García Vescovi, and Mario F. Feldman. 2012. "Biogenesis of Outer Membrane Vesicles in Serratia Marcescens Is Thermoregulated and Can Be Induced by Activation of the Rcs Phosphorelay System." Journal of Bacteriology 194(12):3241–49.

McManus, Paul, Joshua Hortin, Anne J. Anderson, Astrid R. Jacobson, David W. Britt, Joseph Stewart, and Joan E. McLean. 2018. "Rhizosphere Interactions between Copper Oxide Nanoparticles and Wheat Root Exudates in a Sand Matrix: Influences on Copper Bioavailability and Uptake." Environmental Toxicology and Chemistry 37(10):2619–32.

Mengel, Konrad and Ernest A. Kirkby. 2001. "Soil Copper." Pp. 599–611 in Principles of plant nutrition. Springer Science.

Misra, Superb K., Agnieszka Dybowska, Deborah Berhanu, Samuel N. Luoma, and Eugenia Valsami-Jones. 2012. "The Complexity of Nanoparticle Dissolution and Its Importance in Nanotoxicological Studies." Science of the Total Environment 438:225–32.

Pal, Kamal Krishna and Brian McSpadden Gardener. 2006. "Biological Control of Plant Pathogens." The Plant Health Instructor 1–25.

Park, Hae-Jun, Sung Ho Kim, Hwa Jung Kim, and Seong-Ho Choi. 2006. "A New Composition of Nanosized Silica-Silver for Control of Various Plant Diseases." Plant Pathology Journal 22(3):295–302.

Pradhan, Saheli, Prasun Patra, Sumistha Das, Sourov Chandra, Shouvik Mitra, Kushal Kumar Dey, Shirin Akbar, Pratip Palit, and Arunava Goswami. 2013. "Photochemical Modulation of Biosafe Manganese Nanoparticles on Vigna Radiata: A Detailed Molecular, Biochemical, and Biophysical Study." Environmental Science and Technology 47(22):13122–31.

Printz, Bruno, Stanley Lutts, Jean-Francois Hausman, and Kjell Sergeant. 2016. "Copper Trafficking in Plants and Its Implication on Cell Wall Dynamics." Frontiers in Plant Science 7(May):1–16.

Rondon, Michelle R., Robert M. Goodman, and Jo Handelsman. 1999. "The Earth's Bounty: Assessing and Accessing Soil Microbial Diversity." Trends in Biotechnology 17(10):403–9.

Schaar, Viveka, Therése Nordström, Matthias Mörgelin, and Kristian Riesbeck. 2011. "Moraxella Catarrhalis Outer Membrane Vesicles Carry β-Lactamase and Promote Survival of Streptococcus Pneumoniae and Haemophilus Influenzae by Inactivating Amoxicillin." Antimicrobial Agents and Chemotherapy 55(8):3845–53.

Schikora, Adam, Sebastian T. Schenk, and Anton Hartmann. 2016. "Beneficial Effects of Bacteria-Plant Communication Based on Quorum Sensing Molecules of the N-Acyl Homoserine Lactone Group." Plant Molecular Biology 90(6):605–12.

Schooling, Sarah R. and Terry J. Beveridge. 2006. "Membrane Vesicles: An Overlooked Component of the Matrices of Biofilms." Journal of Bacteriology 188(16):5945–57.

Sekhon, Bhupinder Singh. 2014. "Nanotechnology in Agri-Food Production : An Overview." Nanotechnology, Science and Applications 7:31–53.

Soliman, Amir Sh, Souad A. El-feky, and Essam Darwish. 2015. "Alleviation of Salt Stress on Moringa Peregrina Using Foliar Application of Nanofertilizers." Journal of Horticulture and Forestry 7(2):36–47.

Spencer, Matthew, Choong-Min Ryu, Kwang Yeol Yang, Young Cheol Kim, Joseph W. Kloepper, and Anne J. Anderson. 2003. "Induced Defence in Tobacco by Pseudomonas Chlororaphis Strain O6 Involves at Least the Ethylene Pathway." Physiological and Molecular Plant Pathology 63(1):27–34.

Steward, David R., Paul J. Bruss, Xiaoying Yang, Scott A. Staggenborg, Stephen M. Welch, and Michael D. Apley. 2013. "Tapping Unsustainable Groundwater Stores for Agricultural Production in the High Plains Aquifer of Kansas, Projections to 2110." Proceedings of the National Academy of Sciences of the United States of America 110(37).

Stewart, Jacob, Trevor Hansen, Joan E. Mclean, Paul Mcmanus, Siddhartha Das, David W. Britt, Anne J. Anderson, and Christian O. Dimkpa. 2015. "Salts Affect the Interaction of ZnO or CuO Nanoparticles with Wheat." Environmental Toxicology and Chemistry 34(9):2116–25.

Timmusk, Salme, Lawrence Behers, Julia Muthoni, Anthony Muraya, and Anne-Charlotte Aronsson. 2017. "Perspectives and Challenges of Microbial Application for Crop Improvement." Frontiers in Plant Science 8(February):1–10.

Timmusk, Salme, Seong Bin Kim, Eviatar Nevo, Islam Abd El Daim, Bo Ek, Jonas Bergquist, and Lawrence Behers. 2015. "Sfp-Type PPTase Inactivation Promotes Bacterial Biofilm Formation and Ability to Enhance Wheat Drought Tolerance." Frontiers in Microbiology 6(MAY):1–13.

Trenkel, Martin E. 1997. Controlled-Release and Stabilized Fertilizers in Agriculture.

Tripathi, Durgesh Kuman, Vijay Pratap Singh, Devendra Kumar Chauhan, Sheo Mohan Prasad, and Nawal Kishor Dubey. 2014. "Role of Macronutrients in Plant Growth and Acclimation: Recent Advances and Future Perspective." Pp. 197–216 in Improvement of Crops in the Era of Climatic Changes. Vol. 2.

Wang, Guiling. 2005. "Agricultural Drought in a Future Climate: Results from 15 Global Climate Models

Participating in the IPCC 4th Assessment." Climate Dynamics 25(7–8):739–53.

Wang, Wendong, Warren Chanda, and Mintao Zhong. 2015. "The Relationship between Biofilm and Outer Membrane Vesicles: A Novel Therapy Overview." FEMS Microbiology Letters 362(15):1–6.

van de Waterbeemd, Bas, Gijsbert Zomer, Jan van den IJssel, Lonneke van Keulen, Michel H. Eppink, Peter van der Ley, and Leo A. van der Pol. 2013. "Cysteine Depletion Causes Oxidative Stress and Triggers Outer Membrane Vesicle Release by Neisseria Meningitidis; Implications for Vaccine Development." PLoS ONE 8(1).

Woo, Nick S., Murray R. Badger, and Barry J. Pogson. 2008. "A Rapid, Non-Invasive Procedure for Quantitative Assessment of Drought Survival Using Chlorophyll Fluorescence." Plant Methods 4(1):1–14.

Wright, Melanie, Joshua Adams, Kwang Yang, Paul McManus, Astrid Jacobson, Aniket Gade, Joan McLean, David Britt, and Anne Anderson. 2016. "A Root-Colonizing Pseudomonad Lessens Stress Responses in Wheat Imposed by CuO Nanoparticles." PLoS ONE 11(10):1–19.

Wu, Stephen G., Li Huang, Jennifer Head, Daren Chen, In Chul Kong, and Yinjie J. Tang. 2012. "Phytotoxicity of Metal Oxide Nanoparticles Is Related to Both Dissolved Metals Ions and Adsorption of Particles on Seed Surfaces." Journal of Petroleum & Environmental Biotechnology 03(04).

Yang, Fan, Chao Liu, Fengqing Gao, Mingyu Su, Xiao Wu, Lei Zheng, Fashui Hong, and Ping Yang. 2007. "The Improvement of Spinach Growth by Nano-Anatase TiO2 Treatment Is Related to Nitrogen Photoreduction." Biological Trace Element Research 119(1):77–88.

Yang, Kwang Yeol, Stephanie Doxey, Joan E. McLean, David Britt, Andre Watson, Dema Al Qassy, Astrid Jacobson, and Anne J. Anderson. 2018. "Remodeling of Root Morphology by CuO and ZnO Nanoparticles: Effects on Drought Tolerance for Plants Colonized by a Beneficial Pseudomonad." Botany 96:175–86.

Yonezawa, Hideo, Takako Osaki, Satoshi Kurata, Minoru Fukuda, Hayato Kawakami, Kuniyasu Ochiai, Tomoko Hanawa, and Shigeru Kamiya. 2009. "Outer Membrane Vesicles of Helicobacter Pylori TK1402 Are Involved in Biofilm Formation." BMC Microbiology 9:1–12.

Yu, Manli, Junwei Yao, Jie Liang, Zhanghua Zeng, Bo Cui, Xiang Zhao, Changjiao Sun, Yan Wang, Guoqiang Liu, and Haixin Cui. 2017. "Development of Functionalized Abamectin Poly(Lactic Acid) Nanoparticles with Regulatable Adhesion to Enhance Foliar Retention." RSC Advances 7(19):11271–80.

Zhao, Lijuan, Youping Sun, Jose A. Hernandez-Viezcas, Alia D. Servin, Jie Hong, Genhua Niu, Jose R. Peralta-Videa, Maria Duarte-Gardea, and Jorge L. Gardea-Torresdey. 2013. "Influence of CeO2 and ZnO Nanoparticles on Cucumber Physiological Markers and Bioaccumulation of Ce and Zn: A Life Cycle Study." Journal of Agricultural and Food Chemistry 61(49):11945–51.

Zheng, Mengjing, Jin Chen, Yuhua Shi, Yanxia Li, Yanping Yin, Dongqing Yang, Yongli Luo, Dangwei Pang, Xu Xu, Wenqian Li, Jun Ni, Yuanyuan Wang, Zhenlin Wang, and Yong Li. 2017. "Manipulation of Lignin Metabolism by Plant Densities and Its Relationship with Lodging Resistance in Wheat." Scientific Reports.

CHAPTER 2

MECHANICAL PROPERTIES OF WHEAT LEAVES EXPOSED TO COPPER

OXIDE NANOPARTICLES IN THE GROWTH MATRIX

Abstract

Lignification, the polymerization of the structural polymer lignin, within plant cell walls is impaired by Cu deficiency and may result in lodging of cereal crops. It was hypothesized that applications of CuO NPs would increase lignification in wheat (*Triticum aestivum* cv. doloris) grown for 7 d in a sand growth matrix. Increased lignification, examined with phloroglucinol staining, was observed in leaf sclerenchyma cells of wheat seedlings grown in sand containing CuO NPs (10 & 300 mg Cu/kg). This finding is significant as sclerenchyma are considered the strengthening tissues of the plant. Ultimate tensile strength and toughness of wheat leaves were measured on a mechanical testing frame and found to be higher for CuO NP-exposed plants (300 mg Cu/kg) showing that lignification corresponded not only with more rigid wheat leaves but also with stronger wheat leaves. These results indicate that CuO NPs present in the growth matrix are utilized by the wheat and result in stronger, more rigid plants through enhanced lignification. The changes in lignification in wheat seedlings also demonstrates the value in early amendments. This CuO NP-induced lignification may yield crops with greater resistance to pathogen invasion and lodging.

Background

Engineered nanoparticles (NPs), defined as particles less than 100 nm in at least one dimension, are widely studied for application in agriculture and have the potential to shield crops from pathogens (Sekhon 2014), deliver essential micronutrients and

macronutrients (Liu and Lal 2015), and protect crops from various stressors (Khan et al.

2017) including drought (Anderson et al. 2017; Jacobson et al. 2018; Sekhon 2014; Yang

et al. 2018). These effects are attributed in part to the ability of NPs to alter gene

expression in plants and microorganisms (Van Aken 2015). In wheat plants, CuO NPs

have demonstrated the ability to upregulate genes related to the crop's ability to

withstand drought stress (Yang et al. 2018).

Wheat seedlings exposed to CuO NPs have displayed more erect leaves during

drought compared to wheat exposed to ZnO NPs or the control without NPs (Yang et al.

2018). It was hypothesized that this change was due to increased lignin content in plant

cell walls. Lignin is a structural polymer formed from phenolic monomer units found in

plant cell walls. It has long been established that Cu deficiency impairs lignin synthesis

(Robson, Hartley, and Jarvis 1981) as phenolic monomer units are polymerized into

lignin, in part, through mechanisms involving Cu-containing enzymes called laccases

(Printz et al. 2016). Multiple forms of Cu are used to increase lignin synthesis in crops

(Moura et al. 2010; Printz et al. 2016) including $CuSO_4$, Cu metal dust, bulk CuO, and

Cu chelates (Mengel and Kirkby 2001). Increased lignification has been reported in roots

of several plant species exposed to toxic levels of CuO NPs including soybean (Nair and

Chung 2014a), *Arabidopsis thaliana* (Nair and Chung 2014b), and mustard (Nair and

Chung 2015) though this was believed to be a Cu ion effect rather than a NP effect.

In this study, CuO NP-induced lignification in wheat was confirmed with

phloroglucinol staining, which colors lignin red. The strength of lignified wheat leaves

was quantified using tensile testing on a mechanical load frame. Tensile testing is in an

engineering technique that is commonly used to quantify material strength, including

biological materials such as plant tissue (Cleland 1967, 1984; Cosgrove 2016; Genet et al. 2005; Harker et al. 1997; Harker and Hallett 1992). In this method, a material is uniaxially extended at a defined rate while recording the resulting force and extension of the material. These measurements during testing are normalized to stress (σ) and strain (ε):

$$\sigma = \frac{F}{A} \tag{1}$$

$$\varepsilon = \frac{l-l_0}{l_0} \tag{2}$$

where F is the applied force, A is the cross-sectional area, l is the total length of the material during testing, and l_0 is the original length of the material. Stress and strain were used to find the mechanical properties of the material including:

- Ultimate tensile strength- the highest stress the material endures before failure
- Modulus of elasticity- the amount of stress the material withstands per unit of strain
- Toughness- the amount of energy the material absorbs before failure

Ultimate tensile strength was recorded as the maximum stress measured during sample elongation before material failure. Modulus of elasticity was approximated with a trendline. Toughness is generally calculated by integrating under the stress v strain curve but was approximated with the trapezoidal rule in this study.

Most NP studies in agriculture underplay or ignore the presence of the crop microbiome, despite the importance of the microbiome in plant health and crop yield

(Costa, Raaijmakers, and Kuramae 2018). This may be a concern as NPs have been demonstrated to alter gene expression in various beneficial and antagonistic organisms (Van Aken 2015) which may have further downstream effects on the plant. For this study, *Pseudomonas chlororaphis* O6 (*Pc*O6), an isolate cultured from wheat roots grown in calcareous soil under dryland farming conditions (Spencer et al. 2003), was used as a simplified microbiome model. This beneficial bacterium provides drought tolerance to wheat (Yang et al. 2018) through at least two mechanisms. First, through the release of butanediol that triggers stomatal closure in plants (Cho et al., 2008). Second, through the formation of a biofilm matrix on the plant root (Kim et al., 2014; Jacobson et al., 2018), which may promote crop drought tolerance as the biofilm matrix maintains moisture around plant roots (Costa et al. 2018; Timmusk et al. 2015). *Pc*O6 biofilms also protect plants from pests and pathogens by producing phenazines and other antibacterial and antifungal compounds (Anderson and Kim 2018).

Materials and Methods

<u>Nanoparticle characterization</u>

CuO NPs (diameter < 100 nm, purity = 99.95%) were obtained from American Elements (Los Angeles, CA, USA) as a nanopowder and stored protected from light. NP size distribution and agglomeration profiles were confirmed with scanning electron microscopy (FEI Quanta FEG 650) (Figure A - 1). Elemental composition was determined by scanning electron microscopy with energy-dispersive X-ray spectroscopy using an X-Max Detector (Oxford Instruments).

<div align="center">Planting and growing wheat</div>

Quartz sand (4075 grit, Unimin Corp.) was rinsed of impurities with demineralized H_2O, dried at 100°C, and measured into clear, polycarbonate Magenta^{TM} GA-7 Plant Culture Boxes (Sigma Aldrich, V8505, 10x7x7 cm) (300 g sand/box) which were closed and autoclaved at 121°C for 50 min. CuO NPs (dosages varied by experiment), and 50 mL of sterile double distilled H_2O (ddH_2O) (resistance > 18 MΩ*cm) were added to each box and thoroughly dispersed through the sand by vigorous shaking the closed box. Wheat seeds (*Triticum aestivum* var. doloris) were surface sterilized with 10% H_2O_2 for 10 minutes, rinsed thoroughly with sterile ddH_2O, inoculated with *Pc*O6 previously grown to stationary phase (2 d) on minimal media then suspended in sterile ddH_2O (~10^4 CFUs/mL) for 10 minutes for appropriate treatments, and planted (15 seeds/box).

Wheat plants were grown for 7 days under soft white LED lights (Yescom USA) suspended 45 cm above the base of the pots (photon flux = 180-225 μmol/m^2/s) with a continuous 24 h light cycle. No additional nutrients were added to the crops because, at this stage of development, the nutrients within the seed are sufficient for growth.

<div align="center">Phloroglucinol staining</div>

Three growth studies were performed with the treatments: 1) *Pc*O6 and no NPs, 2) *Pc*O6 and 10 mg Cu/kg CuO NPs, 3) *Pc*O6 and 300 mg Cu/kg CuO NPs. Hand-cut sections of wheat leaves were immersed in a phloroglucinol-HCl solution then immediately imaged under a light microscope. Data and images shown are typical of all growth studies.

<u>Tensile testing</u>

Tests used the following treatments: 1) 300 mg Cu/kg CuO NPs and *Pc*O6, 2) 300 mg Cu/kg CuO NPs without added microbes, 3) *Pc*O6 and no NPs, and 4) a negative control with no NPs nor added microbes. Three growth studies were performed with these treatments after which *Pc*O6 treatments were eliminated as this factor did not significantly affect results. In total, seven independent growth studies were performed using CuO NPs and the negative control treatments with between 11 and 22 leaves tested per treatment in each study for a total of 121 control leaves and 108 leaves of CuO NP treated plants.

Tensile testing was performed on an Instron universal testing machine (Instron Model 5542 with Bluehill Operating System) equipped with a 50 N load cell. Wheat leaves were harvested individually and tested immediately to minimize H_2O loss. Leaves were cut at the coleoptile, sectioned to 50 mm lengths, and 10 mm of both ends were taped (Scotch Matte Finish Magic^{TM} Tape, 3M Co.) to prevent slipping within the grips of the Instron for a final gage length of 30 mm. The cross-sectional area was measured at 3 points along the gage length of the wheat leaf with digital calipers and averaged to allow determination of engineering stress. Samples were mounted in the Instron and tested at a rate of 3 mm/min until failure. Force and extension were measured at millisecond intervals and converted to stress and strain using the manually entered cross-sectional area and length.

<u>Mechanical properties</u>

Stress and strain data were graphed and examined using Microsoft Excel to determine the ultimate tensile strength and toughness of wheat leaves. Ultimate tensile

strength was calculated as the maximum stress for a sample before breaking. Modulus of elasticity was calculated with Microsoft Excel's trendline function, with a fixed y-intercept at the graph's origin. Toughness, which is the area under a stress-strain curve, was approximated with the trapezoidal rule:

$$Toughness = \sum_{t=1}^{t_f} \frac{1}{2}(\sigma_t + \sigma_{t-1})\Delta\varepsilon \qquad (3)$$

where σ_t is the stress at time t, σ_{t-1} is the stress at the previous time point, and $\Delta\varepsilon$ is the change in strain between the two time points.

Statistical analysis

JMP8 software was used for statistical analysis. Only data from wheat leaves without PcO6 were used for statistical analysis. One-way ANOVA tests were performed to determine if mechanical properties varied between growth studies CuO NP-exposure altered mechanical properties of wheat leaves. If there were no differences between growth studies (ANOVA p-value > 0.05), data were examined as one set with a student t-test.

Results and discussion

Lignification in wheat sclerenchyma cells

Phloroglucinol, which stains lignin red, was used to determine whether lignin production is altered in CuO NP treated wheat. Figure 2 - 1 shows the results of the phloroglucinol staining. These images show that wheat exposed to CuO NPs had high lignin content in the vascular bundles, though not notably higher than wheat without NPs.

However, the lignin content in sclerenchyma cells, considered the strengthening tissue of the plant, of wheat leaves exposed to CuO NPs was greater than the control without NPs. This observation is novel- no other literature reports lignification in sclerenchyma cells due to CuO NP exposure nor Cu ion exposure.

| *Pc*O6 (no NPs) | CuO NPs (10 mg Cu/kg) and *Pc*O6 | CuO NPs (300 mg Cu/kg) and *Pc*O6 |
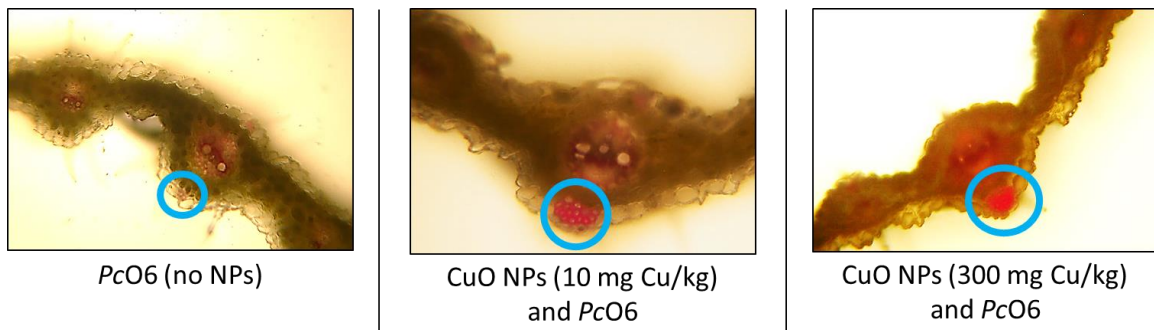
Figure 2 - 1: Transverse wheat leaf sections grown in a sand growth matrix with varying concentrations of CuO NPs after lignin staining. The stained sclerenchyma cells are circled.

Lignification of sclerenchyma is associated with more robust wheat leaves which are more able to withstand wind-caused lodging (Zheng et al. 2017), a term for when cereal crops fall over permanently. Lodging results in large economic losses in agriculture as it lowers crop yield (Baker et al. 1998) because fallen plants are shielded from sunlight (Fischer and Stapper 1987). Cell walls strengthened by increased lignin content also show increased resistance to invasion by pathogens (Hammerschmidt and Kuć 1982).

Stress-strain relationship in wheat leaves

Tensile testing was performed to determine whether changes in lignin content corresponded with differences in wheat mechanical properties. Figure 2 - 2 shows

examples of a wheat leaf during and after tensile testing. Approximately 90% of wheat

leaves broke at the Instron grip at the end corresponding to the wheat leaf tip, which is

the weakest part of the leaf. Wheat leaves that did not follow this trend would break

anywhere from the base to the middle of the gage length.
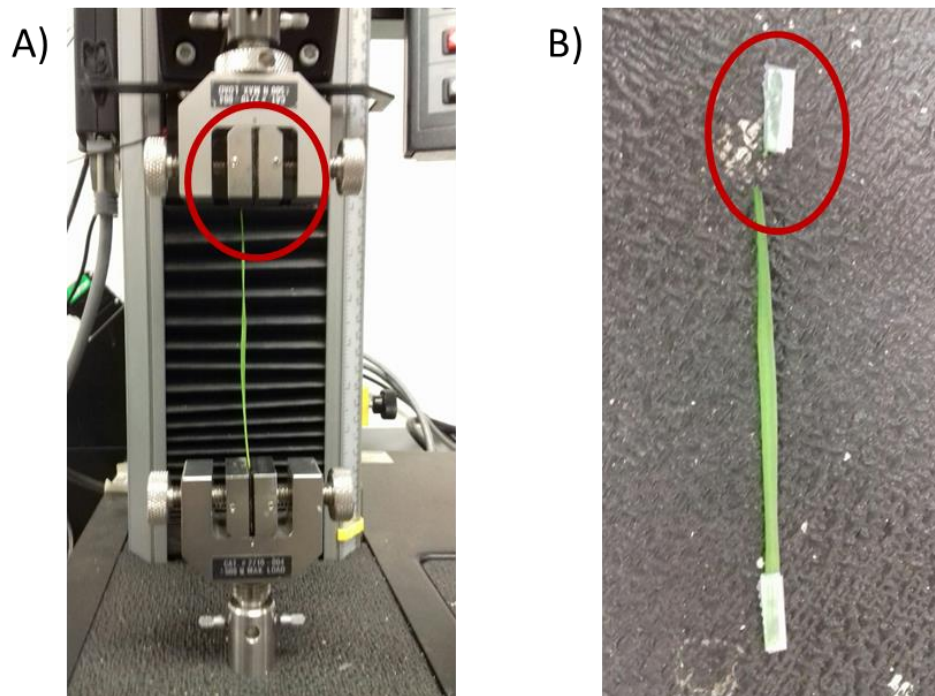
Figure 2 - 2: Images of mechanical testing of wheat leaves. A) Image of a wheat leaf in the
Instron grips after material failure. B) Image of a wheat leaf after removal of from the Instron
grips. The broken end of the wheat leaf is circled in both images. The end nearest the wheat tip
broke during the test, a result that was replicated in ~90% of tensile tests.

The irregularities in breakpoint were possibly due to stress risers in the leaf such

as microscopic tears. Furthermore, there were no statistical differences between the

mechanical properties of leaves that broke in other locations compared to those that broke

at the end corresponding to the wheat leaf tip (ANOVA p-value > 0.05) (data not shown).

As these trends were consistent between treatments and growth studies, the location of the break was not considered for statistical analysis of wheat leaf mechanical properties. During the first three trials, it was determined that colonization by *Pc*O6 did not affect wheat mechanical properties (data not shown). The stress and strain curves for all tests, only including wheat leaves of plants grown without added microbes, are presented in Figure 2 - 3.

All samples exhibited a generally linear relationship between stress and strain during testing. Most showed a sharp breakpoint that is consistent with previous studies of barley (Cleland 1984). Some samples exhibited a dip in stress followed by a subsequent increase in stress which most likely corresponds to samples slipping. This stress-strain relationship is indicative of a brittle material that undergoes little if any plastic deformation before mechanical failure. This relationship was consistent between all growth studies and both control and CuO NP-treated wheat leaves.
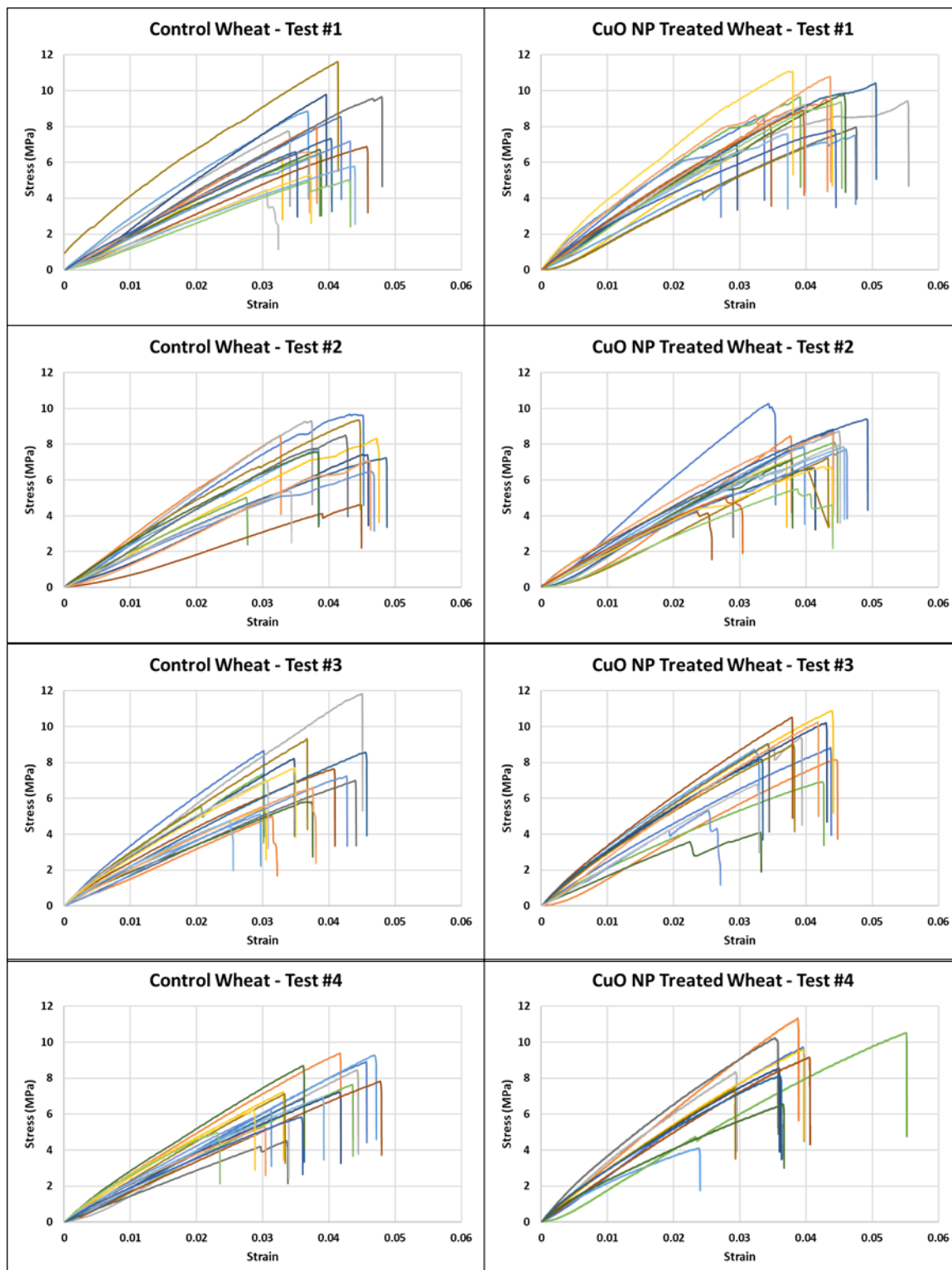
Figure 2 - 3: Stress v. strain curves for control and CuO NP treated wheat leaves of plants grown without added microbes. All x-axes and y-axes have the same scale (Stress: 0 – 12 MPa and strain: 0 – 0.06).
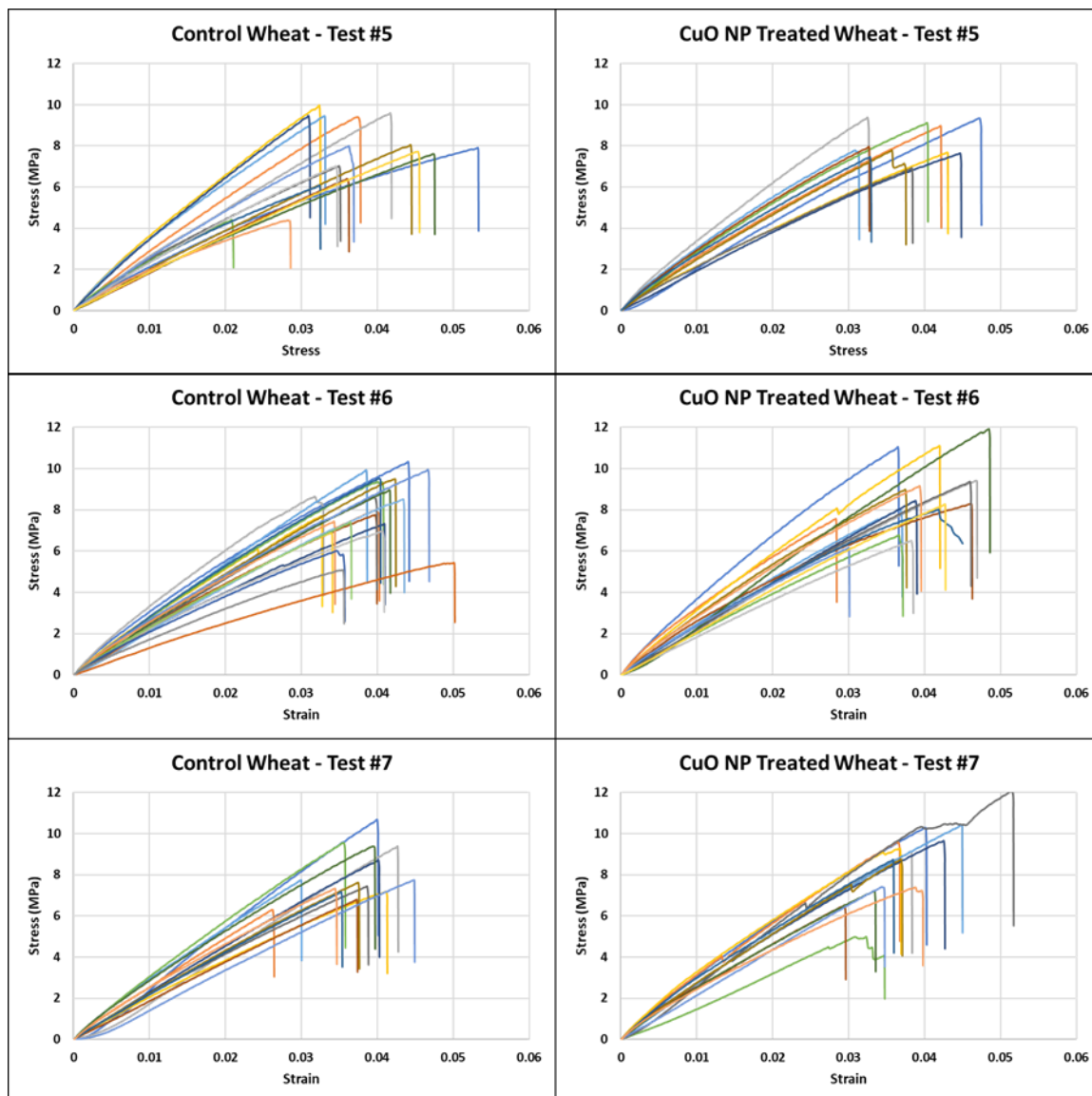
Figure 2 - 3: Stress v. strain curves for control and CuO NP treated wheat leaves of plants grown without added microbes. All x-axes and y-axes have the same scale (Stress: 0 – 12 MPa and strain: 0 – 0.06).

<u>Copper oxide NP-treated wheat leaf mechanical properties</u>

The mechanical properties of ultimate tensile strength, modulus of elasticity, and toughness were calculated using stress and strain results and used to determine the leaf strength of CuO NP-treated wheat. One-way ANOVA tests confirmed that there were no

significant differences in ultimate tensile strength and toughness according to growth study (ANOVA p-value > 0.05), so data from each trial were combined and examined as one set. Modulus of elasticity did vary according to growth study (ANOVA p-value < 0.05).

It was decided that modulus of elasticity would not be used to determine the effects of CuO NPs on wheat leaf strength. The trendlines used to calculate the modulus of elasticity regularly showed a poor fit for stress v strain curves ($r^2 < 0.95$) which limited the accuracy of this variable. Using moduli of curves that had high r^2 values was a potential option, but since the modulus of elasticity varied according to growth study these data could not be examined in one set which gave limited sample sizes (n < 15 per treatment) compared to the high sample sizes required for ultimate tensile strength and toughness measurements (n > 100).

Leaves of CuO NP treated wheat (n=108) showed a 12% increase in ultimate tensile strength and a 17% increase in toughness compared to the control (n=121) (ANOVA p-value < 0.001) (Figure 2 - 4). The increase in mechanical properties corresponds to the increased lignin content of CuO NP treated wheat. These results are supported by the relationship between mechanical strength and lignin content reported by Köhler and Spatz (2002) where lignin-deficient wheat cultivars had lower ultimate tensile strength than lignin-proficient cultivars.
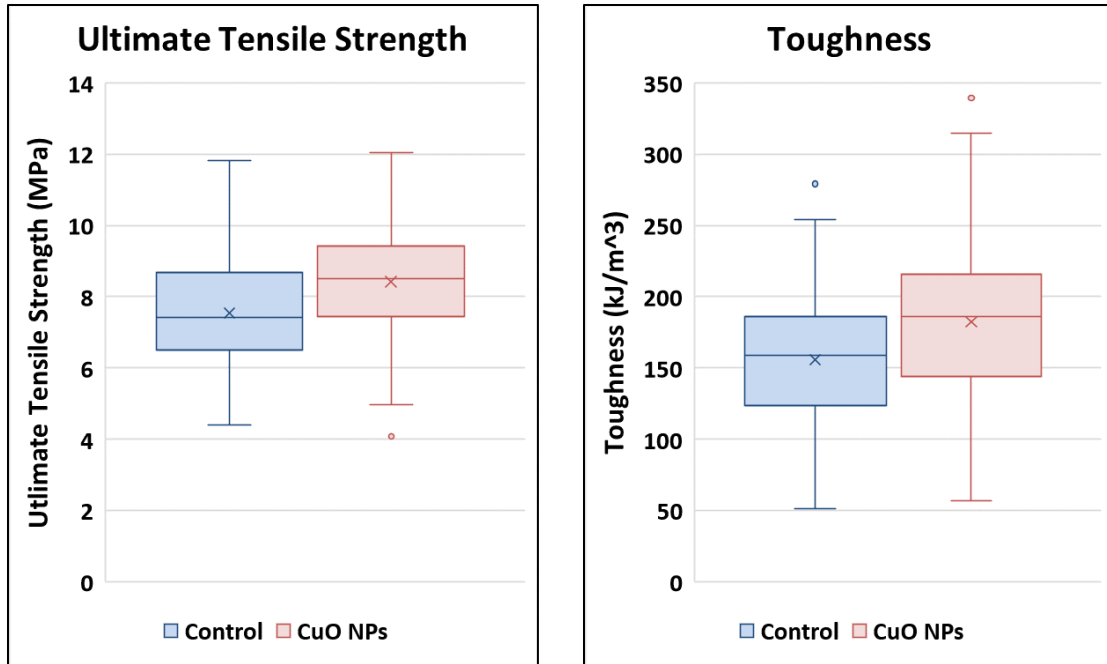
Figure 2 - 4: Box and whisker plots showing the ultimate tensile strength and toughness of control wheat leaves (n=121) and leaves of CuO NP treated wheat (n=108) from all 7 growth studies. The means are marked with an "x" and outliers are shown as distinct circles. Differences in ultimate tensile strength and toughness were statistically significant (ANOVA with posthoc student t-test p-value << 0.05).

These results indicate that increased lignin content corresponds with stronger wheat leaves. Further research will be necessary to determine if this a NP effect, or due to Cu ion release from NPs. In either case, this approach towards increasing wheat lignification has advantages over other methods to prevent lodging. Creation of lodging-resistant crop cultivars, such as shorter wheat by breeding with semi-dwarf cultivars, has upper limits in its success and is highly dependent on crop density (Zheng et al. 2017). By comparison, CuO NPs have the potential to decrease the risk of lodging in all wheat cultivars, a less time-consuming task compared to the trial-and-error approach of creating and testing new cultivars.

Conclusions

Lignin content in the sclerenchyma cells was increased in wheat seedlings grown for 7 d in a sand matrix containing CuO NPs. Although CuO NP-induced lignification has been reported in other plants, CuO NP-induced lignification in sclerenchyma cells has not been reported. This novel observation is significant as sclerenchyma are considered the strengthening tissues of the plant and increased lignification in sclerenchyma corresponds with resistance to wind-caused lodging. The influence of the CuO NP-induced lignification on mechanical properties was evaluated with tensile tests, which showed increased ultimate tensile strength and toughness in wheat leaves of plants treated with CuO NPs. Wheat root colonization by *Pc*O6 did not affect these results.

This enhancement in mechanical properties of wheat after only 7 d of growth is a demonstration of the value in early amendments. However, the agricultural impact of these findings is preliminary as lodging is a concern for mature wheat, not wheat seedlings. Further studies are required to prove the efficacy of CuO NP-induced lignification in mature wheat. Future studies should also include ionic Cu commonly used to increase lignification (Printz et al. 2016), such as $CuSO_4$ or $CuCl_2$, and bulk CuO to determine if these results are discrete nanoparticle effects. If these results are truly nanoparticle effects, then differing NP concentrations should also be attempted as the dosage used in these studies (300 mg Cu/kg growth matrix) is considered too high for field applications which are generally only 1-10 kg Cu/ha in mineral soils (Mengel and Kirkby 2001).

Acknowledgments

This chapter expands on results and conclusions I contributed towards the

publication "Interactions Between a Plant Probiotic and Nanoparticles on Plant

Responses Related to Drought Tolerance" (Jacobson et al. 2018). I would like to thank

Joshua Hortin for assisting me with statistical analysis. I also wish to thank Stephanie

Doxey, Dr. Astrid Jacobson, and Dr. Anne Anderson who performed the lignin stains.

References

Van Aken, Benoit. 2015. "Gene Expression Changes in Plants and Microorganisms Exposed to Nanomaterials." Current Opinion in Biotechnology 33:206–19.

Anderson, Anne J. and Young Cheol Kim. 2018. "Biopesticides Produced by Plant-Probiotic Pseudomonas Chlororaphis Isolates." Crop Protection 105(November 2017):62–69.

Anderson, Anne J., Joan E. McLean, Astrid R. Jacobson, and David W. Britt. 2017. "CuO and ZnO Nanoparticles Modify Interkingdom Cell Signaling Processes Relevant to Crop Production." Journal of Agricultural and Food Chemistry acs.jafc.7b01302.

Baker, C. J., P. M. Berry, J. H. Spink, R. Sylvester-Bradley, J. M. Griffin, R. K. Scott, and R. W. Clare. 1998. "A Method for the Assessment of the Risk of Wheat Lodging." Journal of Theoretical Biology 194(4):587–603.

Cleland, Robert E. 1967. "Extensibility of Isolated Cell Walls: Measurement and Changes during Cell Elongation." Planta.

Cleland, Robert E. 1984. "The Instron Technique as a Measure of Immediate-Past Wall Extensibility." Planta 514–20.

Cosgrove, Daniel J. 2016. "Plant Cell Wall Extensibility: Connecting Plant Cell Growth with Cell Wall Structure, Mechanics, and the Action of Wall-Modifying Enzymes." Journal of Experimental Botany 67(2):463–76.

Costa, Ohana Y. A., Jos M. Raaijmakers, and Eiko E. Kuramae. 2018. "Microbial Extracellular Polymeric Substances – Ecological Functions and Impact on Soil Aggregation." Frontiers in Microbiology 9(July):1636.

Fischer, R. A. and M. Stapper. 1987. "Lodging Effects on High-Yielding Crops of Irrigated Semidwarf Wheat." Field Crops Research 17(3–4):245–58.

Genet, Marie, Alexia Stokes, Franck Salin, Slobodan B. Mickovski, Thierry Fourcaud, Jean François Dumail, and Rens Van Beek. 2005. "The Influence of Cellulose Content on Tensile Strength in Tree Roots." Plant and Soil 278(1–2):1–9.

Hammerschmidt, R. and J. Kuć. 1982. "Lignification as a Mechanism for Induced Systemic Resistance in Cucumber." Physiological Plant Pathology.

Harker, F. R. and I. C. Hallett. 1992. "Physiological Changes Associated with Development of Mealiness of Apple Fruit during Cool Storage." Hort Science 27(12):1291–94.

Harker, F. Roger, Margaret G. H. Stec, Ian C. Hallett, and Carey L. Bennett. 1997. "Texture of Parenchymatous Plant Tissue: A Comparison between Tensile and Other Instrumental and Sensory Measurements of Tissue Strength and Juiciness." Postharvest Biology and Technology 11(2):63–72.

Jacobson, Astrid, Stephanie Doxey, Matthew Potter, Joshua Adams, David Britt, Paul McManus, Joan McLean, and Anne Anderson. 2018. "Interactions between a Plant Probiotic and Nanoparticles on Plant Responses Related to Drought Tolerance." Industrial Biotechnology 14(3):148–56.

Khan, M. Nasir, M. Mobin, Zahid Khorshid Abbas, Khalid A. AlMutairi, and Zahid H. Siddiqui. 2017. "Role of Nanomaterials in Plants under Challenging Environments." Plant Physiology and Biochemistry 110:194–209.

Köhler, Lothar and Hanns Christof Spatz. 2002. "Micromechanics of Plant Tissues beyond the Linear-Elastic Range." Planta 215(1):33–40.

Liu, Ruiqiang and Rattan Lal. 2015. "Potentials of Engineered Nanoparticles as Fertilizers for Increasing Agronomic Productions." Science of the Total Environment 514:131–39.

Mengel, Konrad and Ernest A. Kirkby. 2001. "Soil Copper." Pp. 599–611 in Principles of plant nutrition. Springer Science.

Moura, Jullyana Cristina Magalhães Silva, Cesar Augusto Valencise Bonine, Juliana de Oliveira Fernandes Viana, Marcelo Carnier Dornelas, and Paulo Mazzafera. 2010. "Abiotic and Biotic Stresses and Changes in the Lignin Content and Composition in Plants." Journal of Integrative Plant Biology 52(4):360–76.

Nair, Prakash M. Gopalakrishnan and Ill Min Chung. 2014a. "A Mechanistic Study on the Toxic Effect of Copper Oxide Nanoparticles in Soybean (Glycine Max L.) Root Development and Lignification of Root Cells." Biological Trace Element Research 162(1–3):342–52.

Nair, Prakash M. Gopalakrishnan and Ill Min Chung. 2014b. "Impact of Copper Oxide Nanoparticles Exposure on Arabidopsis Thaliana Growth, Root System Development, Root Lignification, and Molecular Level Changes." Environmental Science and Pollution Research 21(22):12709–22.

Nair, Prakash M. Gopalakrishnan and Ill Min Chung. 2015. "Study on the Correlation between Copper Oxide Nanoparticles Induced Growth Suppression and Enhanced Lignification in Indian Mustard (Brassica Juncea L.)." Ecotoxicology and Environmental Safety.

Printz, Bruno, Stanley Lutts, Jean-Francois Hausman, and Kjell Sergeant. 2016. "Copper Trafficking in Plants and Its Implication on Cell Wall Dynamics." Frontiers in Plant Science 7(May):1–16.

Robson, A. D., R. D. Hartley, and S. C. Jarvis. 1981. "Effect of Cu Deficiency on Phenolic and Other Constituents of Wheat Cell Walls." The New Phytologist 89:361–71.

Sekhon, Bhupinder Singh. 2014. "Nanotechnology in Agri-Food Production : An Overview." Nanotechnology, Science and Applications 7:31–53.

Spencer, Matthew, Choong-Min Ryu, Kwang Yeol Yang, Young Cheol Kim, Joseph W. Kloepper, and Anne J. Anderson. 2003. "Induced Defence in Tobacco by Pseudomonas Chlororaphis Strain O6 Involves at Least the Ethylene Pathway." Physiological and Molecular Plant Pathology 63(1):27–34.

Timmusk, Salme, Seong Bin Kim, Eviatar Nevo, Islam Abd El Daim, Bo Ek, Jonas Bergquist, and Lawrence Behers. 2015. "Sfp-Type PPTase Inactivation Promotes Bacterial Biofilm Formation and Ability to Enhance Wheat Drought Tolerance." Frontiers in Microbiology 6(MAY):1–13.

Yang, Kwang Yeol, Stephanie Doxey, Joan E. McLean, David Britt, Andre Watson, Dema Al Qassy, Astrid Jacobson, and Anne J. Anderson. 2018. "Remodeling of Root Morphology by CuO and ZnO Nanoparticles: Effects on Drought Tolerance for Plants Colonized by a Beneficial Pseudomonad." Botany 96:175–86.

Zheng, Mengjing, Jin Chen, Yuhua Shi, Yanxia Li, Yanping Yin, Dongqing Yang, Yongli Luo, Dangwei Pang, Xu Xu, Wenqian Li, Jun Ni, Yuanyuan Wang, Zhenlin Wang, and Yong Li. 2017. "Manipulation of Lignin Metabolism by Plant Densities and Its Relationship with Lodging Resistance in Wheat." Scientific Reports.

CHAPTER 3

EFFECTS OF COPPER OXIDE NANOPARTICLES ON DROUGHT TOLERANCE

OF WHEAT COLONIZED BY A BENEFICIAL RHIZOBACTERIUM

Abstract

Multiple genes relating to water stress tolerance are upregulated in wheat exposed to CuO nanoparticles (NPs) in the growth matrix. Here, the effects of CuO NPs on wheat seedling drought tolerance were examined and quantified with gas exchange and chlorophyll fluorescence. Wheat seeds (*Triticum aestivum* v. Juniper) were inoculated with *Pseudomonas chlororaphis* O6, a beneficial rhizobacterium that served as a model microbiome, and grown exposed to low CuO NP concentrations (0, 0.5, 5, 15, and 30 mg Cu/kg growth matrix) in a sand growth matrix for 14 d then droughted for 8 d. A half-strength Hoagland's solution including Cu ions was added during planting and on days 7 & 14 of growth to ensure that results were discrete NP effects and not merely nutrient effects. Due to the small size of 22 d old leaves, results showed that chlorophyll fluorescence measurements of Φ_{PSII} and F_v/F_m, which represent the operating and maximum photosystem II efficiency respectively, were more consistent for monitoring drought response than gas exchange measurements. Over the course of three growth studies, this method revealed that these low CuO NP dosages had no statistically significant effect on wheat seedling drought tolerance under these experimental conditions (restricted maximum likelihood method p-value > 0.05). CuO NPs did not prevent root colonization by *Pc*O6 and no Cu toxicity effects towards wheat were observed showing that CuO NPs at these concentrations can be used for other potential plant-health promoting effects.

Background

CuO NPs provide multiple benefits to crops including pathogen control (Cioffi et al. 2004; Esteban-Tejeda et al. 2009) and Cu ion sources (Adams et al. 2017), an essential micronutrient (Printz et al. 2016). Several genes related to water stress tolerance are upregulated in wheat (*Triticum aestivum*, Doloris cultivar) seedlings exposed to CuO NPs (Yang et al. 2018). This finding is significant as drought is one of the most significant threats to crop yield and quality (Kim et al. 2012). Water scarcity limits a crop's ability to perform basic physiological processes including photosynthesis and electron transport (Lu and Zhang 1998). Drought severity is predicted to worsen in the coming years with the warming climate (Le Houerou 1996; Wang 2005) making drought one of the largest obstacles to food security.

Wheat seedlings (*Triticum aestivum* var. Doloris) grown in a sand matrix containing CuO NPs have shown upregulation in genes relating to drought tolerance however, shoot moisture content did not vary between droughted wheat with or without CuO NPs (Yang et al. 2018). Further investigation is needed into the potential of CuO NPs to mitigate drought stress as this measurement was the only quantitative variable used in this study. Shoot moisture content is just one of several methods that can measure physiological changes caused by drought and by extension, a plant's drought tolerance. Other methods include leaf gas exchange (Flexas et al. 2002; Subrahmanyam et al. 2006), chlorophyll fluorescence (Maxwell and Johnson 2000; Woo, Badger, and Pogson 2008), and metabolite and protein production (Bowne et al. 2012; Vincent et al. 2005). Of these methods, gas exchange and chlorophyll fluorescence measurements can be conducted noninvasively throughout the drought period, whereas other methods require destructive

harvests.

Gas exchange and chlorophyll fluorescence may be measured in parallel with the LI-6800 Portable Photosynthesis System from LICOR. For gas exchange measurements, a plant leaf is clamped in an environmentally controlled chamber. The chamber is sealed around the leaf by a gasket and does not need to be harvested from the plant. Air with defined CO_2 and H_2O concentrations is passed through the chamber and changes in concentration of these gases due to plant respiration and transpiration are measured by infrared gas analyzers to calculate plant carbon assimilation (A), intercellular CO_2 concentration (C_i), and H_2O transpiration (E).

Chlorophyll fluorescence measurements are also performed on an intact leaf within an environmental chamber. The plant leaf is exposed to an incident light beam and the excitation of the chlorophyll is measured. F_v/F_m, a ratio of the maximum Photosystem II (PSII) efficiency, is measured on dark-adapted plants. Φ_{PSII}, a ratio of the operating PSII efficiency, is measured on light-adapted plants. Summaries of the variables measured by gas exchange and chlorophyll fluorescence are shown in Table 3 - 1. The effect of drought on these gas exchange and chlorophyll fluorescence variables is shown in Table 3 - 2.

Table 3 - 1: Variables measured using gas exchange and chlorophyll fluorescence

Variable		Description
Carbon assimilation	**A**	The rate that the plant takes up ambient CO_2
Intercellular CO_2 concentration	**C_i**	The CO_2 concentration of in the plant's intercellular air space
H_2O transpiration	**E**	The rate that the plant releases H_2O vapor
Maximum PSII efficiency	**F_v/F_m**	The maximum number of PSII that could be used compared to the total number of PSII
Operating PSII efficiency	**Φ_{PSII}**	The actual number of PSII that are used compared to the total number of PSII

Table 3 - 2: Effects of water stress on gas exchange and chlorophyll fluorescence of wheat and various other plants.

Plant	Growth Conditions	Parameter	Effect of water stress	Reference
Wheat	Lab	A	Lowered during drought	(Shangguan, Shao, and Dyckmans 2000)
		E	Lowered during drought	
		C_i	Increased during drought	
Wheat	Field	A	"Strongly lower" in drought conditions	(Monneveux et al. 2006)
		E	"Strongly lower" in drought conditions	
		A & E	Strong correlation in drought conditions; weaker correlation in irrigated conditions than in rainfed conditions	
Wheat	Lab	E	Regulated by abscisic acid during drought; increases upon rehydration after drought	(Henson, Jensen, and Turner 1989)
Wheat	Field	A	Decreased during drought; lesser decrease when Si is present during drought	(Gong and Chen 2012)
		E	Decreased during drought; lesser decrease when Si is present during drought	
		C_i	During the cycle of one day: initially higher during drought then lower than watered plants about midday; similar results for Si treated plants	
Grapevines	Field	F_v/F_m	Only slightly lowered by drought (0.8 to 0.74)	(Flexas et al. 2002)
		A and E	Highly correlated	
		E	Best indicator as to the inflection point between stomatal and non-stomatal limitations during drought	
Turkey Oak	Field	A	Similar in moderate water stress, lowered in strong water stress	(Valentini et al. 1995)
		C_i	Lowered in water stress	
		F_v/F_m	No changes during water stress	
		Φ_{PsII}	Lowered during water stress	
Tree	Lab	A	Decreased during drought	(Sánchez-Rodríguez, Pérez, and Martínez-Carrasco 1999)
		Φ_{PsII}	Similar for plants with and without water stress	
		C_i	No differences with or without water stress	
Arabidopsis	Lab	F_v/F_m	Water stress did not affect F_v/F_m during the early stages of water stress. A small decline in F_v/F_m then occurred followed by a sudden sharp decline before plant death	(Woo et al. 2008)
		Φ_{PsII}	Declines in $\Phi PsII$ preceded declines in F_v/F_m	
Key				
A: CO_2 assimilation E: H_2O transpiration C_i: Intercellular CO_2 concentration				
F_v/F_m: Maximum PSII efficiency Φ_{PsII}: Operating PSII efficiency				

Most NP studies underplay or ignore the importance of the crop microbiome, despite the importance of the microbiome in plant health and crop yield (Costa, Raaijmakers, and Kuramae 2018). This may be an oversight as NPs are known to alter gene expression in various beneficial and antagonistic microorganisms (Van Aken 2015). For this study, *Pseudomonas chlororaphis* O6 (*Pc*O6), an isolate cultured from wheat roots grown in calcareous soil under dryland farming conditions (Spencer et al. 2003), was used as a simplified microbiome model.

*Pc*O6 provides drought tolerance to wheat (Yang et al. 2018). Two primary mechanisms for *Pc*O6-induced drought tolerance have been previously identified: 1) release of 2R,3R-butanediol that triggers stomatal closure in plants (Cho et al., 2008), and 2) formation of a biofilm matrix on the plant root (Kim et al., 2014; Jacobson et al., 2018). Biofilm formation may promote crop drought tolerance as the biofilm matrix maintains moisture around plant roots (Costa et al. 2018; Timmusk et al. 2015).

In these studies, *Triticum aestivum* var. Juniper, which was bred to withstand low rainfall conditions, was examined. A single wheat growth experiment was performed to understand what gas exchange and chlorophyll fluorescence variables most reliably and reproducibly quantify wheat seedling drought tolerance and the effect of *Pc*O6 on these variables. With these results, three subsequent growth studies were performed to determine the effects of CuO NPs on wheat seedling drought tolerance.

Previous studies by our group have exposed wheat (*Triticum aestivum* var. Doloris) to CuO NP concentrations as high as 300 mg Cu/kg (Jacobson et al. 2018; Yang et al. 2018) which led to significant wheat root shortening (Yang et al. 2018). Root growth inhibition is one of the most rapid plant responses to Cu toxicity (Mengel and

Kirkby 2001). This concentration is also at the threshold of toxicity for soil microorganisms (Dimkpa et al. 2011). This study aimed to look at more realistic application dosages.

In Cu-deficient soils, recommended Cu dosages vary greatly according to crop and soil type. For mineral soils, a single application of $CuSO_4$ at 1-10 kg Cu/ha is usually sufficient while organic soils may require an application as high as 22 kg Cu/ha (Mengel and Kirkby 2001). However, the goal of this research was not providing this micronutrient in Cu deficient soils but rather on assessing the discrete NP effects of CuO NPs on wheat. To that end, a range of low, non-toxic CuO NP concentrations was used in a sand growth matrix that was Cu sufficient.

Wheat seeds were inoculated with *Pc*O6 and planted in a sand growth matrix containing CuO NP concentrations of 0, 0.5, 5, 15, and 30 mg Cu/kg and grown for 14 days. The plants in half the pots were then exposed to simulated drought and all plants were grown for another 8 days. Drought tolerance measurements were made with chlorophyll fluorescence every 2 days during the drought period. Results were examined with the restricted maximum likelihood method (REML) for repeated measurements. Plants were harvested at the end of the drought period to measure shoot wet mass, dry mass, and moisture content. Inductively coupled plasma mass spectrometry (ICP-MS) was performed to measure the effects of drought on dissolved Cu content of the growth matrix. Two-way ANOVA and posthoc Tukey tests were used to analyze these results.

Materials and Methods

<u>Nanoparticle characterization</u>

CuO NPs (diameter < 100 nm, purity = 99.95%) were obtained from American

Elements (Los Angeles, CA, USA) as a nanopowder and stored protected from light. NP

size distribution and agglomeration profiles were confirmed with scanning electron

microscopy (FEI Quanta FEG 650) (Figure A - 1). Elemental composition was

determined by scanning electron microscopy with energy-dispersive X-ray spectroscopy

using an X-Max Detector (Oxford Instruments).

Planting Wheat

Hard red winter wheat seeds (*Triticum aestivum* var. Juniper) were surface

sterilized with 10% H_2O_2 for 10 min then rinsed thoroughly with sterile double-distilled

H_2O (ddH_2O) (resistance > 18 MΩ*cm). Seeds were inoculated with *Pc*O6 that was

grown for 2 d to stationary phase on minimal media 2% agar plates at room temperature,

suspended in sterile ddH_2O, and diluted to 10^4 CFUs/mL. Seeds were left in the *Pc*O6

suspension for 10 min. 800 g of quartz sand (4075 grit; Unimin Corp; New Canaan, CT,

USA), previously washed of impurities with demineralized H_2O for 10 min and dried at

100°C, was measured into plastic pots (4.5" x 4.5" x 5.25"; United States Plastic Corp.,

Lima, OH, USA). CuO NPs (0, 0.5, 5, 15, or 30 mg Cu/kg sand) were added to each pot

then dispersed by vigorously shaking the closed pot. 150 mL of half-strength modified

Hoagland's solution (Hoagland and Arnon 1950) (FeCl$_3$ was used as the Fe source, see

Table A - 1 for full chemical composition) was added to the sand, which was then mixed

to homogeneity by hand. Nine inoculated wheat seeds were planted in each pot at a depth

of 1 cm.

Wheat growth conditions

Wheat plants were grown for 14 d under soft white LED light panels (Yescom

USA Inc; City of Industry, CA, USA) with a photocycle of 16/8h light/dark periods.

Light panels were hung 30 cm above the base of the pots for the first 7 d of growth

(photon flux = 250-350 μmol/m^2/s), then 45 cm above the base of the pots (photon flux =

180-225 μmol/m^2/s) until the end of the growth period. The temperature was monitored

with TP50 digital thermometers (ThermoPro; Toronto, Ontario, Canada) and controlled

with F422 mini USB desk fans (OPOLAR; Barking, Greater London, UK) suspended

above the wheat which maintained the growth chamber at 20-24°C. Moisture content was

maintained at 0.169 g H_2O/g growth matrix (135 g H_2O/pot) by adding ddH_2O daily by

weight. On days 7 and 14 of growth, 25 mL and 40 mL half-strength modified

Hoagland's solution was added respectively before restoring moisture content. After 14 d

of growth, half of the pots in each treatment were maintained in well-watered conditions

and the other pots were put into a simulated drought (0.025 g H_2O/g growth matrix, 20

mL H_2O/pot) for an additional 8 d.

<u>Preliminary wheat gas exchange and chlorophyll fluorescence study</u>

A preliminary study was performed to determine which gas exchange and

chlorophyll fluorescence variables best quantified wheat drought response. This

experiment began on day 14 of growth using the LI-6800 Portable Photosynthesis Unit

(LICOR Biosciences; Lincoln, NE, USA). F_v/F_m was measured on plants that had been

dark-adapted for at least 4 h. No gas exchange measurements were conducted on dark-

adapted plants. Leaf gas exchange and Φ_{PSII} were measured concurrently on plants that

had been light-adapted for at least 1 h. LI-6800 chamber environmental parameters were

set to:

- Flow: 600 µmol/s
- ΔP: 0.2 kPa
- H_2O: RH_{air} 55%
- CO_2: 500 µmol/mol
- Fan: 5000 rpm
- T_{air}: 25°C
- Light (light-adapted measurements only): 200 µmol/m^2/s, red- 90%, blue- 10%
- Fluorometer: dark mod rate of 500 Hz, light mod rate of 50 kHz

These measurements were performed on days 0, 3, 6, 9, and 10 of drought (this study was the only one performed with this drought length). This growth study was performed using 4 pots for each CuO NP concentration which were later divided into 2 droughted and 2 watered pots for each CuO NP concentration. For each pot, 3 randomly chosen wheat leaves were tested for dark-adapted measurements and light-adapted measurements. This study also used a control with no *Pc*O6 nor CuO NPs.

<u>Wheat chlorophyll fluorescence</u>

Three subsequent growth studies were performed using only chlorophyll fluorescence measurements. On day 14 of growth, dark-adapted (F_v/F_m) and light-adapted (Φ_{PsII}) chlorophyll fluorescence measurements began using the LI-6800 Portable Photosynthesis Unit. F_v/F_m was measured on plants that had been dark-adapted for at least 4 h. Φ_{PsII} was measured on plants that had been light-adapted for at least 1 h. LI-6800 chamber environmental parameters were identical to those used in the preliminary experiment using gas exchange and chlorophyll fluorescence measurements. Three independent growth studies were performed under these conditions with 6 pots used per CuO NP concentration, later divided into 3 watered and 3 drought pots, in each growth study. Three randomly chosen wheat leaves were used for each set of dark-adapted

measurements and each set of light-adapted measurements. These measurements were performed every 2 d for an 8 d drought period.

Harvesting methods

On the final day of drought (22 d of total growth, 8 d of drought), after gas exchange and chlorophyll fluorescence had been measured, the moisture content of all watered and drought pots was restored to 0.169 g H_2O/g growth matrix (135 g H_2O/pot). Wheat roots were removed from the sand growth matrix and the shoots were cut at the coleoptile. PcO6 colonization of roots was confirmed at harvest by clipping a small portion of the roots and placing it on LB 2% agar medium.

Growth matrix pore water analysis

Immediately after harvest, the growth matrix sand was mixed and placed in an acid-cleaned glass funnel with Fisherbrand P4 filter paper (Fisher Scientific International Inc; Pittsburgh, Pennsylvania, USA) and glass wool to extract the pore water into a sterile 50 mL polypropylene conical tube (Falcon Life Sciences; Corning, NY, USA) under vacuum. The solution was sterile filtered with a 0.2 μm nylon filter (Life Science Products Inc; Frederick, CO, USA) to remove remaining sand and microbes. Electroconductivity and pH were immediately measured after filtering. Samples were stored at 4°C until further use. Dissolved Cu content was measured with 7700x ICP-MS with an octopole reaction system (Agilent Technologies Inc; Santa Clara, CA, USA) after centrifugation (20,300 x g, 15 min) to remove remaining NPs. Appropriate standards and quality control samples including blanks, calibration verification samples, and matrix spikes were measured during analysis with ICP-MS. The reported Cu concentrations as μg/L were adjusted to the amount of H_2O in the pot at the time of harvest before moisture

content was restored to 0.169 g H_2O/g growth matrix (135 g H_2O/pot). The Cu

concentration was also expressed as µg/kg of sand growth matrix.

Growth matrix precipitation modeling

MINTEQ version 3.1 was used to evaluate the extent of precipitation of salts with

the loss of water from the drought pots. The subroutine model for evaporation loss was

used with inputs of all cation and anion data, including amino acids and low molecular

weight organic acids, pH, and EC.

Measuring wheat shoot moisture contents

After cutting the wheat shoots from the plant, the shoot tissues were weighed

immediately to obtain wet weights, trimmed of three leaf portions for metabolite analyses

not included in this thesis, and weighed again. Remaining shoot tissue was stored in

labeled paper bags, dried at 60°C for at least 48 h, and weighed again to obtain dry

weights. Moisture content was calculated as:

$$H_2O \text{ content in } \frac{g \ H_2O}{g \ dry \ tissue} = \frac{Remaining \ Wet \ Mass - Dry \ Mass}{Dry \ Mass}$$

Wheat shoot elemental analysis

Dry shoot tissues were stored in labeled paper bags in plastic storage bins for 1-2

months before further analysis. All available shoot tissues were compacted into the base

of glass 50 mL glass tubes, submerged in 1 mL nitric acid (ICP-OES for trace metal

analysis, Thermo Scientific) and 5 mL perchloric acid (70% purity, 11.7 normality,

Fisher Scientific), then covered with Parafilm[TM] (Bemis Company Inc.; Neenah, WI,

USA) for pre-digestion at room temperature for 12 h. Blanks and standards (NIST tomato

tissue) were also performed during each replicate.

After 12 h, Parafilm™ was removed, glass funnels were placed on tubes, and tubes were put on a heating block. The vials were heated at 50°C for 1 h, 100°C for 1.5 h, then 140°C for 1.5 h. The funnels were then removed, and the tubes were heated to 160°C for 1 h, then 180°C until < 0.5 mL of liquid remained (~3-5 h). A final volume of 50 mL was obtained by adding ddH$_2$O and mixing. Shoot elemental content was measured with a 7700x ICP-MS with an octopole reaction system alongside appropriate standards.

Statistical analysis

Results from the preliminary study using gas exchange and chlorophyll fluorescence were used to determine correlations between measured parameters of A, E, C$_i$, and Φ$_{PSII}$. Correlation coefficients were calculated via the Spearman correlation method using R. All data were used for calculations regardless of drought status, CuO NP concentration, or the presence of PcO6.

In the main study, a repeated measurement method was used to analyze Φ$_{PSII}$ and F$_v$/F$_m$ data: each pot was treated as a statistical unit so all measurements for each pot on a given day were averaged for a total statistical sample size of n=9 per treatment. The day 0 measurements were used as model parameters. Data were blocked by trial. The restricted maximum likelihood method (REML) was utilized to determine differences between the effects of drought status, days of drought, and CuO NP concentration using SAS (p-value < 0.05). Any significant differences were examined with posthoc Tukey HSD tests.

The dissolved Cu concentration, shoot Cu content, and shoot moisture content data were blocked by trial and analyzed with two-way ANOVA, main effects of CuO NP

concentration, and drought status using R. Post-hoc Tukey HSD tests were performed

accounting for the significant factors. Growth matrix dissolved Cu by H_2O volume,

growth matrix dissolved Cu by growth matrix mass, and shoot Cu concentration data

were log-transformed before statistical analysis to achieve a normal distribution.

Results and Discussion

<u>Correlations of gas exchange and chlorophyll fluorescence measurements</u>

A preliminary wheat growth study was performed measuring all potential gas

exchange and chlorophyll fluorescence variables defined in Table 3 - 1 to determine what

gas exchange and chlorophyll fluorescence variables would best quantify wheat drought

response. Plants were grown for 14 d then exposed to a 10 d simulated drought. While

performing measurements for this study, A and E often fell below the LI-6800 detection

limit for plants in drought (Figure 3 - 1). Gas exchange measurements on leaves that are

smaller than the environmental chamber are considered unreliable (Dr. Bruce Bugbee,

private communication, summer 2019). Wheat leaf width at this seedling stage is usually

only ~0.2-0.3 cm where the LI-6800 chamber is ~3.5 cm in diameter.

Chlorophyll fluorescence results did not have these limitations. The fluorescence

variables are ratios and therefore independent of leaf area. Measurements also never fell

below instrument detection limits during this study (Figure 3 - 1). Other researchers have

shown that chlorophyll fluorescence is a useful tool in assessing plant vigor drought

studies. F_v/F_m is shown to be a method for monitoring drought survival for several

Arabidopsis thaliana strains (Woo et al. 2008). Φ_{PSII} is also commonly measured in

drought studies, though generally this is measured alongside gas exchange.

Pairing Φ_{PSII} and gas exchange has also shown the ability to determine how the

relationships between plant respiration, transpiration, and photochemical reactions breakdown in certain conditions. For example, the relationship between Φ_{PSII} and A has been mathematically modeled for maize grown under laboratory conditions as this relationship is relatively linear (Edwards and Baker 1993). Alternatively, it was demonstrated that these relationships break down in field-grown maize during periods of chilling (Fryer et al. 1998).

In the case of wheat seedlings grown under these conditions, Φ_{PSII} proved to be correlated with A and E (Table 3 - 3). For both well-watered and droughted plants, Φ_{PSII} was the most reproducible variable measured and never fell below the instrument detection limit. Therefore, it was decided that measuring Φ_{PSII} was sufficient to quantify wheat photosynthetic activity under these conditions. F_v/F_m was also used to quantify wheat seedling drought tolerance after consulting literature as it is reported to be the best determinant of plant survivability during drought (Woo et al. 2008).

Table 3 - 3: Correlation coefficients (Spearman method) between H_2O transpiration (E), CO_2 assimilation (A), intercellular CO_2 concentration (C_i), and operating PSII efficiency (Φ_{PSII}). Green cells indicate a positive correlation between variables.

Variable	E	A	C_i	Φ_{PSII}
E	-	0.895	0.0846	0.785
A	0.895	-	0.00965	0.866
C_i	0.0846	0.00965	-	-0.0913
Φ_{PSII}	0.785	0.866	-0.0913	-

Effects of *Pseudomonas chlororaphis* O6 on wheat photochemistry during drought

Another goal of this preliminary test was to examine the effect of *Pc*O6 on wheat photochemistry. Previous studies have noted that *Pc*O6 releases 2R,3R-butanediol that triggers stomatal closure in plants (Cho et al., 2008) which would have a pronounced effect on wheat gas exchange measurements. The effects of *Pc*O6 on wheat seedling gas exchange and chlorophyll fluorescence during drought are shown in Figure 3 - 1.

The results for gas exchange of wheat are erratic, which presents challenges for concluding the effects of *Pc*O6 on gas exchange. In contrast, *Pc*O6 appears to have no effect or minimal effects on chlorophyll fluorescence. For this reason, it was decided that further tests would use wheat seeds inoculated by *Pc*O6 and that control without any added microbes was unneeded. This approach also gave a balanced experimental design that focused on the effect of CuO NPs on wheat while not discounting the three-way interactions between a crop, the microbiome, and added NPs.

This preliminary study also led to the decision to shorten drought periods in subsequent growth studies. A total of 12 d of drought were planned originally, but the plants were extremely wilted and desiccated after only 10 d of drought. The leaves were difficult to handle without ripping the leaves from the plant leading to the decision to take final gas exchange and chlorophyll fluorescence measurements that day and end the study early. Further studies used a drought period of 8 d with measurements taking place every 2 d.
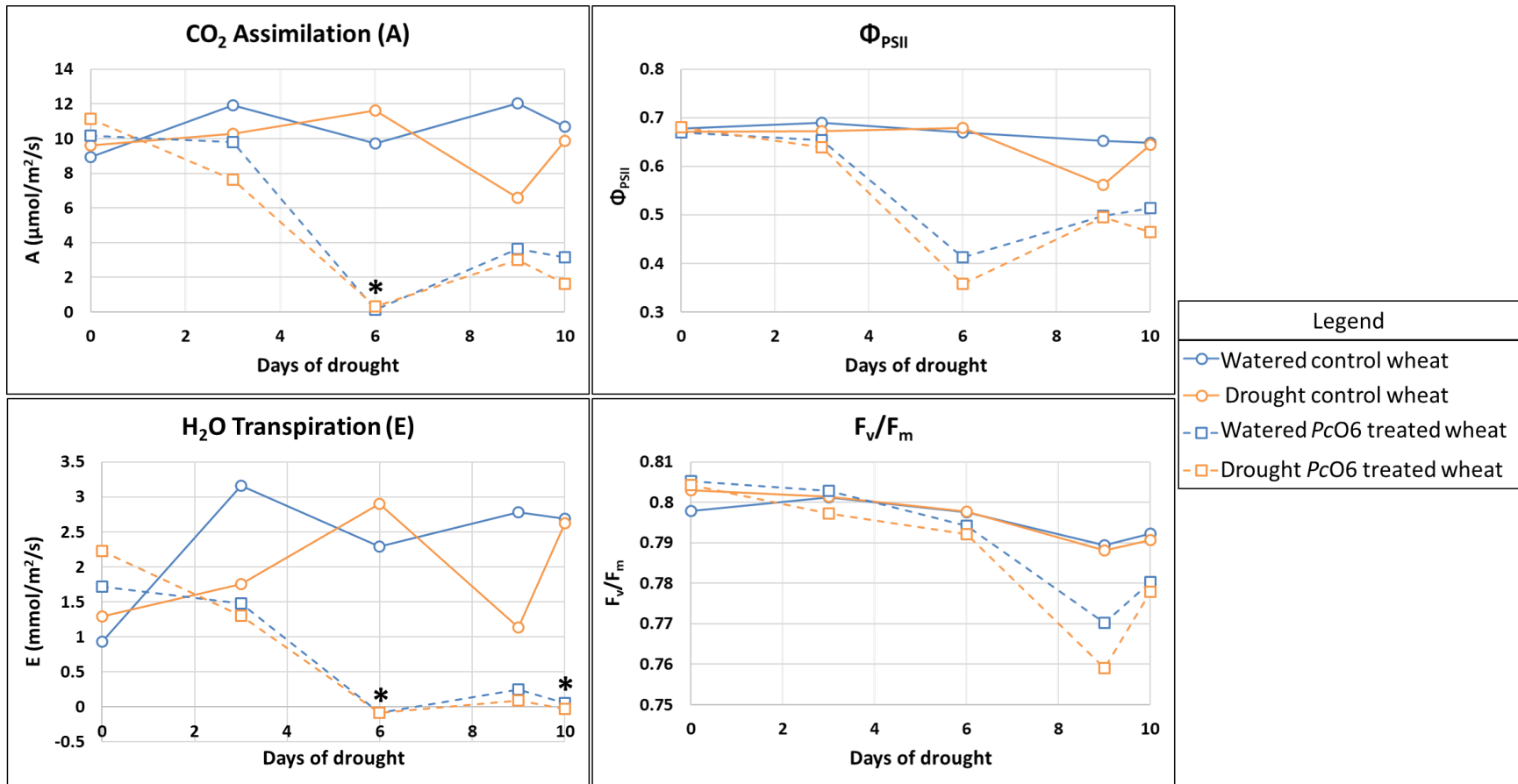
Figure 3 - 1: Effects of *Pc*O6 on wheat seedling gas exchange (A & E) and chlorophyll fluorescence (Φ_{PSII} & F_v/F_m) during a 10 d period with or without drought, after a 14 d of growth with daily watering. Days marked with an asterisk contain measurements below the LI-6800 Portable Photosynthesis Unit detection limits.

<u>Effects of copper oxide nanoparticles on wheat drought tolerance</u>

Following the preliminary study, three growth studies were performed with 14 d of growth followed by 8 days of growth with or without drought. CuO NP concentrations of 0, 0.5, 5, 15, and 30 mg Cu/kg were used in these studies. The effects of CuO NPs on Φ_{PSII} and F_v/F_m are shown in Figure 3 - 2. Drought effects are clear in both variables however, the REML results showed that there were no significant differences in Φ_{PSII} nor F_v/F_m according to CuO NP concentration over the course of the drought period except in the CuO NP concentration-drought interaction (REML results summarized in Table A - 2). However, pairwise comparisons showed that this was merely the result of differences between CuO NP concentrations of 0.5 & 15 mg Cu/kg (REML with posthoc Tukey p-value < 0.05) and neither of these treatments differed from the control (REML with posthoc Tukey p-value > 0.05).

At the end of the drought period, the wheat seedlings were harvested for further analysis. PcO6 colonization was confirmed by placing small root portions on LB 2% agar medium plates. After 2 d of growth, PcO6 colonies covered the plate with the distinct orange color from the phenazines this bacterium produces on rich medium (Kim et al. 2014). Wheat shoots were weighed, then dried, and weighed again to measure shoot moisture content (Figure 3 - 3). There were no statistically significant differences in moisture content between the watered plants at different NP concentrations (Tukey p-value >> 0.05) nor the drought plants at the differing NP dosages (Tukey p-value >> 0.05). Moisture content was reduced in drought plants at CuO NP concentrations of 0, 5, and 30 mg Cu/kg compared to watered controls (Tukey p-value < 0.05) but not in drought plants exposed to 0.5 and 15 kg Cu/kg (Tukey p-value >> 0.05).
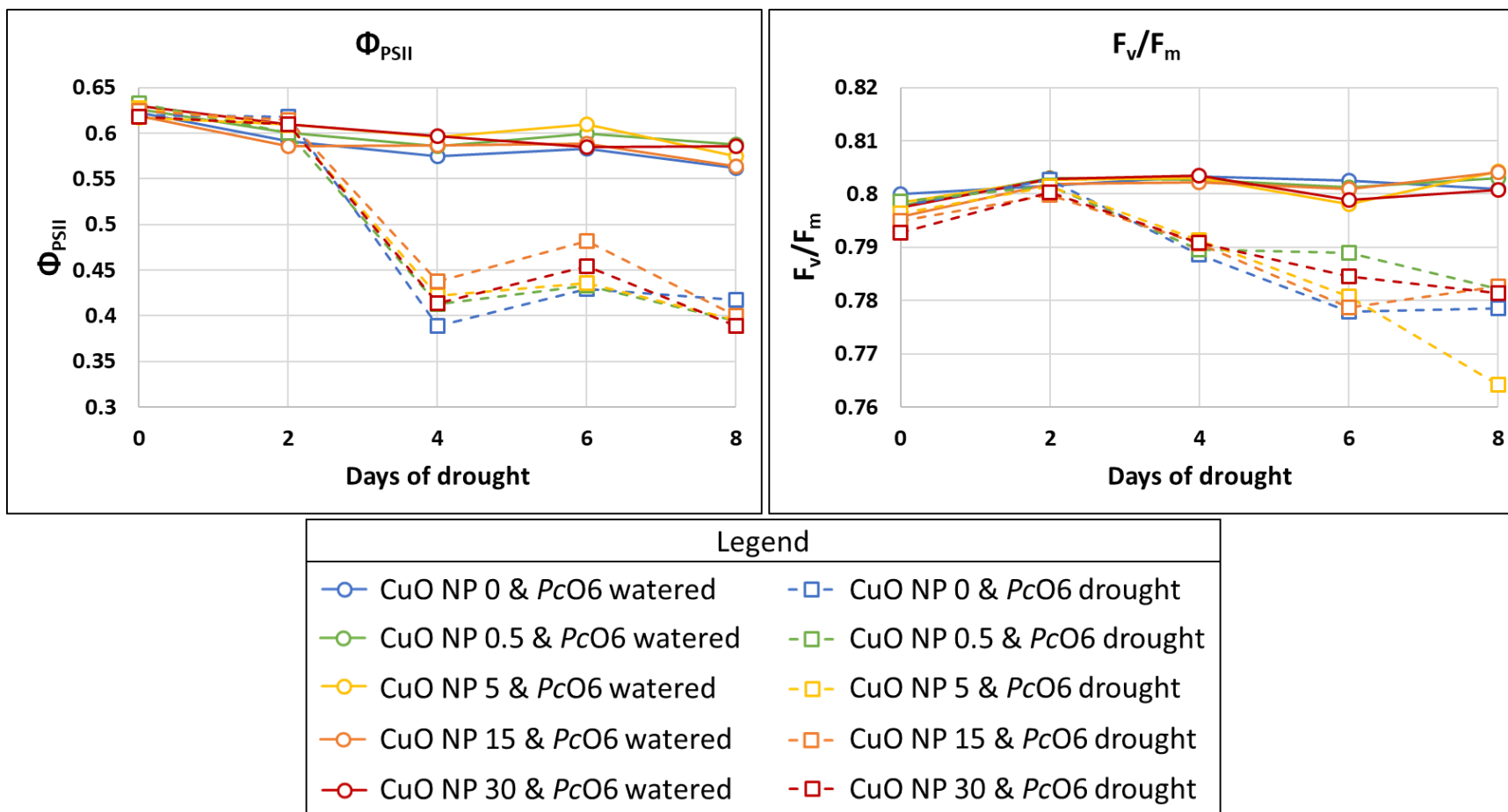
Figure 3 - 2: Average chlorophyll fluorescence (averages of measurements from n=3 pots per each of the 3 trials for a total of n=9 pots) of wheat during drought after 14 d of growth followed by an 8 d drought (22 d total growth). CuO NP concentrations are in units of mg Cu/kg.

CuO NP effect on leaf water content

Figure 3 - 3: Shoot moisture contents after 14 d of growth followed by 8 d of growth with or without drought (22 d of growth total). Error bars denote one standard deviation. Treatments sharing letters have no statistical difference (Two-way ANOVA with posthoc Tukey test, p-value > 0.05). CuO NP concentrations are in units of mg Cu/kg growth matrix.

Although shoot moisture content was not decreased by drought in wheat exposed to CuO NPs at 0.5 and 15 mg Cu/kg, there were still decreases in PSII activity as measured by Φ_{PSII} and F_v/F_m. These results show chlorophyll fluorescence parameters, which are measured throughout the drought period, are more defining of drought than parameters requiring destructive harvests including plant moisture content. Therefore, it can be concluded that CuO NPs do not significantly affect wheat drought tolerance at the seedling stages of growth under these growth conditions.

Although CuO NPs did not affect wheat drought tolerance under these conditions, this result is not inherently negative. At these controlled doses, CuO NPs showed no visible effect on root development (data not shown), one of the most visible and rapid

responses to Cu toxicity (Mengel and Kirkby 2001). Root shortening has been one of the

most notable signs of Cu toxicity in previous studies of CuO NP-treated wheat (Adams et

al. 2017; Yang et al. 2018).

These results indicate that CuO NPs do not affect wheat seedling drought

response at this stage of growth. However, these results do leave questions as to whether

CuO NPs affect drought tolerance of wheat at later growth stages or whether CuO NPs

could affect wheat recovery from drought to well-watered conditions. The absence of

these toxicity symptoms is also promising: CuO NPs can be used at controlled dosages

for other agricultural purposes without damage to the crops. CuO NPs have shown

potential as fertilizers due to the release of Cu ions (Adams et al. 2017), an essential

micronutrient that is often unavailable to plants despite its natural occurrence in the

Earth's crust (Printz et al. 2016). CuO NPs also exhibit pesticidal activity (Elmer and

White 2016). This property has been further explored and innovated with Cu-composite

NPs. Polymer-Cu nanocomposites have shown fungicidal activity (Cioffi et al. 2004) and

soda-lime glass containing Cu NPs have shown both antibacterial and antifungal activity

(Esteban-Tejeda et al. 2009).

<div align="center">Cu availability to wheat seedlings</div>

To determine the available Cu to the plant, growth matrix pore water was

extracted under vacuum after removing the roots from the matrix. The concentration of

dissolved Cu ions in the pore water was measured with ICP-MS. Since all pots were

restored to the original moisture content of 0.169 g H_2O/g growth matrix (135 g

H_2O/pot), ICP-MS results were corrected to the original volume of water in the pot

before harvest. For droughted boxes, this was approximately a 14-fold dilution. The Cu

concentration was also calculated according to the growth matrix mass. The final

concentrations of dissolved Cu in the growth matrix as µg/L and µg/kg are shown in

Figure 3 - 4A and Figure 3 - 4B respectively.
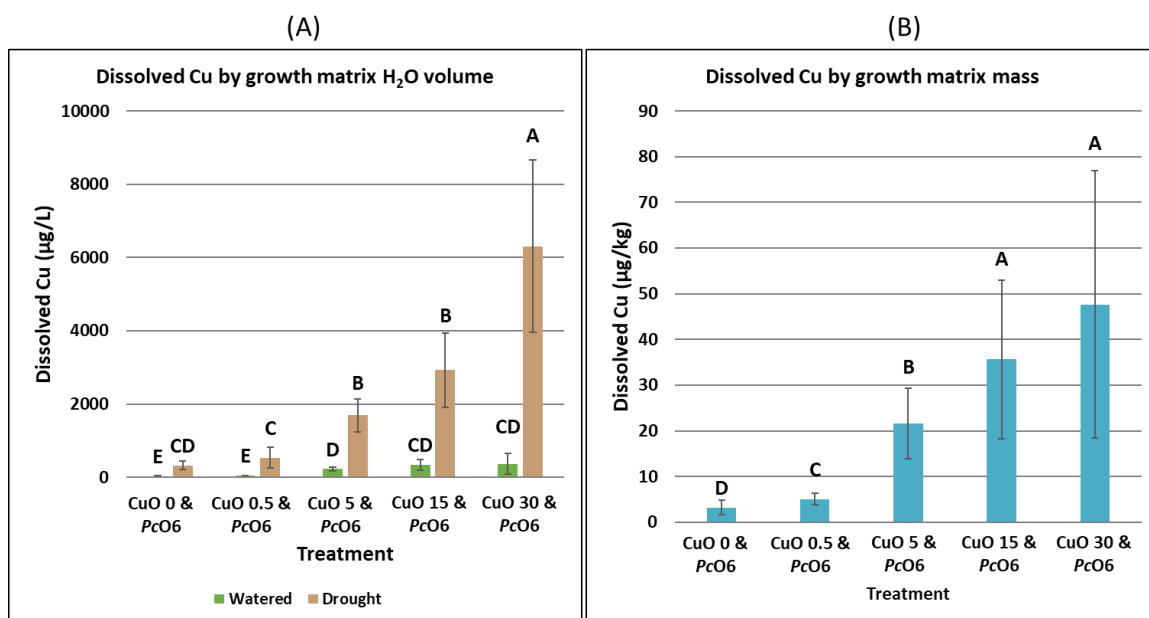
Figure 3 - 4: Dissolved Cu in growth matrix after 14 d of growth followed by 8 d of growth according to A) H_2O concentration in the pot before harvest (n=9 pots per treatment) and B) according to growth matrix mass (n=18 pots per treatment). Treatments are separated according to statistically significant factors of drought, CuO NP concentration, and/or the interaction of these variables (log-transformed two-way ANOVA p-value < 0.05). Treatments that share letters have no statistical differences (log-transformed Tukey HSD p-value > 0.05). Error bars denote one standard deviation. CuO NP concentrations are in units of mg Cu/kg.

On a volume basis, the amount of dissolved Cu in the solution increases with CuO

NP concentration and dramatically increases in drought pots. The same trend of

increasing dissolved Cu with increasing CuO NP concentration is seen when the data are

normalized to the mass of the sand growth matrix. However, no effect is observed from

drought status (two-way ANOVA p-value > 0.05). This is noteworthy as models of the growth system (accounting for all present cations and anions, amino acids, low molecular weight organic acids, pH, and electroconductivity) showed that Cu and all other introduced ions did not precipitate out of the solution. Therefore, the wheat roots in droughted pots were exposed to highly concentrated nutrient solutions and high amounts of Cu though less of the root surface was exposed to this solution. This conclusion led to the need to understand how much Cu was taken up by the plant.

To measure Cu uptake into the plant, harvested and dried wheat shoot tissue was digested in acid and the metal content was measured using ICP-MS. There is some uncertainty with these data as, while calibration curves were successfully created on the instruments, digested NIST tomato leaf standards did not give expected results. Cu concentrations in the standards were below the manufacturer specifications with recoveries averaging 36%. While there is some uncertainty as to the accuracy of the shoot Cu concentrations, these data are precise and therefore reported. It was found that drought did not affect shoot Cu concentration (two-way ANOVA p-value > 0.05), but this variable was increased according to CuO NP concentration (Figure 3 - 5).

Results showed that plants exposed to higher CuO NP concentrations took up more Cu during the growth period. However, the highly concentrated ions in the growth matrix H_2O of drought pots, including at the highest CuO NP concentrations of 15 and 30 mg Cu/kg, did not affect Cu uptake. This may indicate similar availability of Cu to plants in watered and drought boxes or, more likely, that wheat seedlings in watered and drought conditions were able to regulate uptake and translocation of this vital micronutrient.
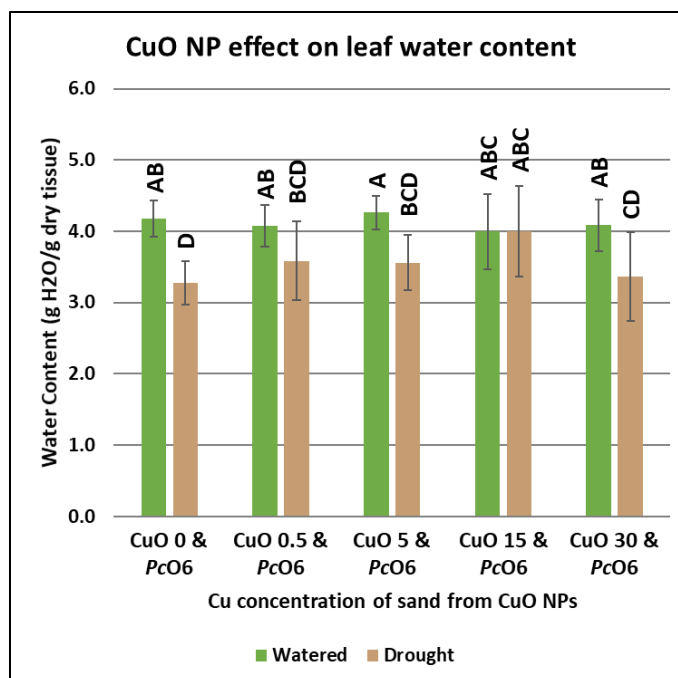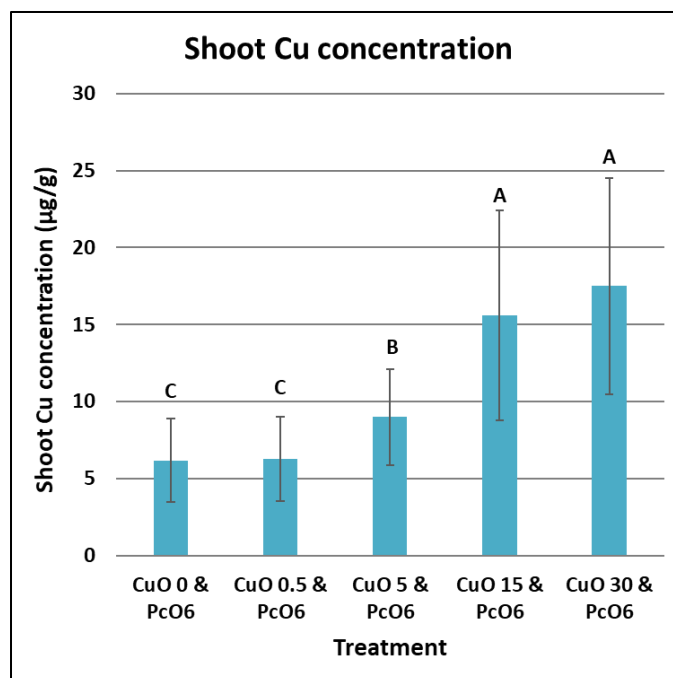
Figure 3 - 5: Shoot Cu concentration after 14 d of growth followed by 8 d of growth with or without drought (22 d of growth total). Because drought had no impact on shoot Cu concentration (log-transformed two-way ANOVA p-value > 0.05), all drought and watered pots are combined for a total of n=18 pots. Error bars denote one standard deviation. Data were log-transformed before statistical analysis to achieve a normal distribution. Treatments that share letters have no statistical differences (log-transformed Tukey p-value > 0.05). CuO NP concentrations are in units of mg Cu/kg growth matrix.

Wheat shoot rigidity during drought

Another benefit of CuO NPs for wheat was shown in an incidental observation made during these studies. Wheat seedling shoot erectness increased in wheat exposed to CuO NPs during drought, even at the lowest dose of 0.5 mg Cu/kg (Figure 3 - 6). This effect was observable during the first 4 d of drought however, most plants had fallen over due to the water stress severity after about 5 d of drought.
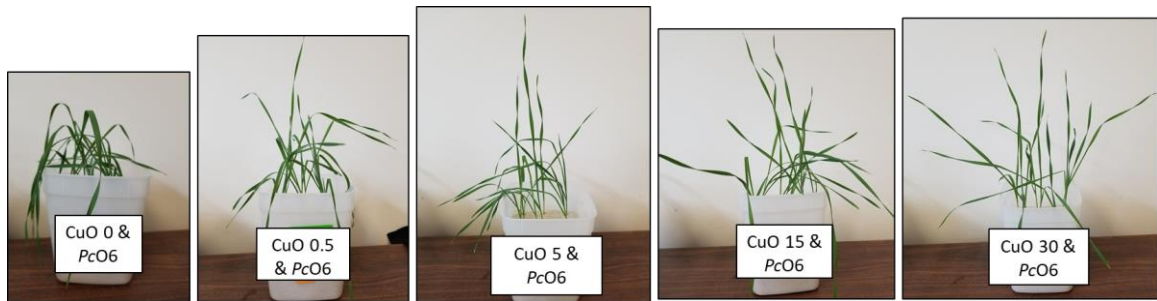
Figure 3 - 6: Images showing the differing plant stand of wheat after 4 days of drought. This effect was only observed for the first 5 d of drought under these growth conditions. CuO NP concentration is noted in each image and is in units of mg Cu/kg growth matrix.

This finding has been reported in previous studies (Yang et al. 2018) In further investigation, improved erectness of the plants was found to correspond with increased lignification, or the formation of the structural polymer lignin, in the sclerenchyma cells (Jacobson et al., 2018, Chapter 2 of this thesis- page 22). This is significant as sclerenchyma cells are considered the strengthening cells of the plant.

Conclusions

Chlorophyll fluorescence was determined to be the best method for quantifying wheat seedling drought response. Gas exchange measurements often fell below instrument detection limits for wheat plants in drought and the low surface area of wheat seedling leaves limited the accuracy of gas exchange measurements. Since PcO6 did not affect chlorophyll fluorescence, it was decided that the control without added microbes was unnecessary for further tests.

After 14 d of growth followed by 8 d of drought, CuO NP dosages from 0.5 to 30 mg Cu/kg did not affect wheat seedling drought tolerance in a Cu-sufficient growth matrix at this growth stage. While not a promising result, wheat seedlings exhibited no

signs of Cu toxicity, and *Pc*O6 colonization of wheat roots was not prevented at these

CuO NP concentrations. These outcomes raise questions as to whether CuO NPs may

affect wheat seedling drought tolerance at later growth times or if CuO NPs could affect

wheat recovery from a droughted to a well-watered state. Further investigation into

potential CuO NP-induced drought tolerance is underway in our research group,

including studies of mature wheat and soil studies.

While further investigation continues, the lack of toxicity by CuO NPs towards

wheat at these doses shows that CuO NPs can be used for other agricultural applications

without negative consequences. CuO NPs exhibit numerous beneficial effects to crops

including the release of Cu (a vital micronutrient) pesticidal activity, and improved plant

stand during drought.

Acknowledgments

References

Adams, Josh, Melanie Wright, Hannah Wagner, Jonathan Valiente, David Britt, and Anne Anderson. 2017. "Cu from Dissolution of CuO Nanoparticles Signals Changes in Root Morphology." Plant Physiology and Biochemistry 110:108–17.

Van Aken, Benoit. 2015. "Gene Expression Changes in Plants and Microorganisms Exposed to Nanomaterials." Current Opinion in Biotechnology 33:206–19.

Bowne, Jairus B., Tim A. Erwin, Juan Juttner, Thorsten Schnurbusch, Peter Langridge, Antony Bacic, and Ute Roessner. 2012. "Drought Responses of Leaf Tissues from Wheat Cultivars of Differing Drought Tolerance at the Metabolite Level." Molecular Plant 5(2):418–29.

Cioffi, Nicola, Luisa Torsi, Nicoletta Ditaranto, Luigia Sabbatini, Pier Giorgio Zambonin, Giuseppina

Tantillo, Lina Ghibelli, Maria D'Alessio, Teresa Bleve-Zacheo, and Enrico Traversa. 2004. "Antifungal Activity of Polymer-Based Copper Nanocomposite Coatings." Applied Physics Letters 85(12):2417–19.

Costa, Ohana Y. A., Jos M. Raaijmakers, and Eiko E. Kuramae. 2018. "Microbial Extracellular Polymeric Substances – Ecological Functions and Impact on Soil Aggregation." Frontiers in Microbiology 9(July):1636.

Dimkpa, Christian O., Alyssa Calder, David W. Britt, Joan E. McLean, and Anne J. Anderson. 2011. "Responses of a Soil Bacterium, Pseudomonas Chlororaphis O6 to Commercial Metal Oxide Nanoparticles Compared with Responses to Metal Ions." Environmental Pollution 159(7):1749–56.

Edwards, Gerald E. and Neil R. Baker. 1993. "Can CO2 Assimilation in Maize Leaves Be Predicted Accurately from Chlorophyll Fluorescence Analysis?" Photosynthesis Research 37:89–102.

Elmer, Wade H. and Jason C. White. 2016. "The Use of Metallic Oxide Nanoparticles to Enhance Growth of Tomatoes and Eggplants in Disease Infested Soil or Soilless Medium." Environmental Science: Nano 3(5):1072–79.

Esteban-Tejeda, L., F. Malpartida, A. Esteban-Cubillo, C. Pecharromn, and J. S. Moya. 2009. "Antibacterial and Antifungal Activity of a Soda-Lime Glass Containing Copper Nanoparticles." Nanotechnology 20.

Flexas, Jaume, Josefina Bota, José M. Escalona, Bartolomé Sampol, and Hipólito Medrano. 2002. "Effects of Drought on Photosynthesis in Grapevines under Field Conditions: An Evaluation of Stomatal and Mesophyll Limitations." Functional Plant Biology 29(4):461–71.

Fryer, Michael J., James R. Andrews, Kevin Oxborough, David A. Blowers, and Neil R. Baker. 1998. "Relationship between CO2 Assimilation, Photosynthetic Electron Transport, and Active O2 Metabolism in Leaves of Maize in the Field during Periods of Low Temperature." Plant Physiology 116(2):571–80.

Gong, Haijun and Kunming Chen. 2012. "The Regulatory Role of Silicon on Water Relations, Photosynthetic Gas Exchange, and Carboxylation Activities of Wheat Leaves in Field Drought Conditions." Acta Physiologiae Plantarum 34(4):1589–94.

Henson, I. E., C. R. Jensen, and N. C. Turner. 1989. "Leaf Gas Exchange and Xater Relations of Lupins and Wheat. III. Abscisic Acid and Drought-Induced Stomatal Closure." Australian Journal of Plant Physiology 16(5):429.

Hoagland, D. R. and D. I. Arnon. 1950. "The Water-Culture Method for Growing Plants without Soil." Circular.

Le Houerou, Henry N. 1996. "Climate Change, Drought and Desertification." Journal of Arid Environments 34(2):133–85.

Jacobson, Astrid, Stephanie Doxey, Matthew Potter, Joshua Adams, David Britt, Paul McManus, Joan McLean, and Anne Anderson. 2018. "Interactions between a Plant Probiotic and Nanoparticles on Plant Responses Related to Drought Tolerance." Industrial Biotechnology 14(3):148–56.

Kim, Ji Soo, Yong Hwan Kim, Ju Yeon Park, Anne J. Anderson, and Young Cheol Kim. 2014. "The Global Regulator GacS Regulates Biofilm Formation in Pseudomonas Chlororaphis O6 Differently with Carbon Source." Canadian Journal of Microbiology 60(3):133–38.

Kim, Young Cheol, Bernard R. Glick, Yoav Bashan, and Choong-Min Ryu. 2012. "Enhancement of Plant Drought Tolerance by Microbes." Pp. 383–413 in Plant Responses to Drought Stress: From Morphological to Molecular Features. Vol. 9783642326.

Lu, Congming and Jianhua Zhang. 1998. "Effects of Water Stress on Photosynthesis, Chlorophyll Fluorescence and Photoinhibition in Wheat Plants." Australian Journal of Plant Physiology 25:883–92.

Maxwell, Kate and Giles N. Johnson. 2000. "Chlorophyll Fluorescence—a Practical Guide." Journal of Experimental Botany 51(345):659–68.

Mengel, Konrad and Ernest A. Kirkby. 2001. "Soil Copper." Pp. 599–611 in Principles of plant nutrition. Springer Science.

Monneveux, Philippe, Djamila Rekika, Edmundo Acevedo, and Othmane Merah. 2006. "Effect of Drought on Leaf Gas Exchange, Carbon Isotope Discrimination, Transpiration Efficiency and Productivity in Field Grown Durum Wheat Genotypes." Plant Science 170(4):867–72.

Printz, Bruno, Stanley Lutts, Jean-Francois Hausman, and Kjell Sergeant. 2016. "Copper Trafficking in Plants and Its Implication on Cell Wall Dynamics." Frontiers in Plant Science 7(May):1–16.

Sánchez-Rodríguez, J., P. Pérez, and R. Martínez-Carrasco. 1999. "Photosynthesis, Carbohydrate Levels and Chlorophyll Fluorescence-Estimated Intercellular CO2 in Water-Stressed Casuarina Equisetifolia Forst. and Forst." Plant, Cell and Environment 22(7):867–73.

Shangguan, Z. P., M. A. Shao, and J. Dyckmans. 2000. "Nitrogen Nutrition and Water Stress Effects on Leaf Photosynthetic Gas Exchange and Water Use Efficiency in Winter Wheat." Environmental and Experimental Botany 44(2):141–49.

Spencer, Matthew, Choong-Min Ryu, Kwang Yeol Yang, Young Cheol Kim, Joseph W. Kloepper, and Anne J. Anderson. 2003. "Induced Defence in Tobacco by Pseudomonas Chlororaphis Strain O6 Involves at Least the Ethylene Pathway." Physiological and Molecular Plant Pathology 63(1):27–34.

Subrahmanyam, D., N. Subash, A. Haris, and A. K. Sikka. 2006. "Influence of Water Stress on Leaf Photosynthetic Characteristics in Wheat Cultivars Differing in Their Susceptibility to Drought." Photosynthetica 44(1):125–29.

Timmusk, Salme, Seong Bin Kim, Eviatar Nevo, Islam Abd El Daim, Bo Ek, Jonas Bergquist, and Lawrence Behers. 2015. "Sfp-Type PPTase Inactivation Promotes Bacterial Biofilm Formation and Ability to Enhance Wheat Drought Tolerance." Frontiers in Microbiology 6(MAY):1–13.

Valentini, R., D. Epron, P. De Angelis, G. Matteucci, and E. Dreyer. 1995. "In Situ Estimation of Net CO2assimilation, Photosynthetic Electron Flow and Photorespiration in Turkey Oak (Q. Cerris L.) Leaves: Diurnal Cycles under Different Levels of Water Supply." Plant, Cell & Environment 18(6):631–40.

Vincent, Delphine, Catherine Lapierre, Brigitte Pollet, Gabriel Cornic, Luc Negroni, and Michel Zivy. 2005. "Water Deficits Affect Caffeate O-Methyltransferase, Lignification, and Related Enzymes in Maize Leaves. A Proteomic Investigation." Plant Physiology 137(3):949–60.

Wang, Guiling. 2005. "Agricultural Drought in a Future Climate: Results from 15 Global Climate Models Participating in the IPCC 4th Assessment." Climate Dynamics 25(7–8):739–53.

Woo, Nick S., Murray R. Badger, and Barry J. Pogson. 2008. "A Rapid, Non-Invasive Procedure for Quantitative Assessment of Drought Survival Using Chlorophyll Fluorescence." Plant Methods 4(1):1–14.

Yang, Kwang Yeol, Stephanie Doxey, Joan E. McLean, David Britt, Andre Watson, Dema Al Qassy, Astrid Jacobson, and Anne J. Anderson. 2018. "Remodeling of Root Morphology by CuO and ZnO Nanoparticles: Effects on Drought Tolerance for Plants Colonized by a Beneficial Pseudomonad." Botany 96:175–86.

CHAPTER 4

ABIOTIC STRESSORS IMPACT OUTER MEMBRANE VESICLE COMPOSITION

IN A BENEFICIAL SOIL BACTERIUM: RAMAN SPECTROSCOPY

CHARACTERIZATION

Abstract

Outer membrane vesicles (OMVs) produced by Gram-negative bacteria have roles in cell-to-cell signaling, biofilm formation, and stress responses. Here, the effects of abiotic stressors on OMV contents and composition from biofilm cells of the plant-health-promoting soil bacterium *Pseudomonas chlororaphis* O6 (*Pc*O6) are examined. Two stressors relevant to this root colonizing bacterium were examined: CuO nanoparticles (NPs)- a potential fertilizer and fungicide- and H_2O_2- released from roots during plant stress responses. Atomic force microscopy revealed 40-300 nm diameter OMVs from control and stressed biofilm cells. Raman spectroscopy with linear discriminant analysis (LDA) identified *Pc*O6 cells and resultant purified OMVs according to the cellular stressor with 83.3% and 77.1% accuracies, respectively. All OMVs had higher relative concentrations of proteins, lipids, and nucleic acids than intact *Pc*O6 cells. Nucleic acid concentration increased in OMVs of stressed cells: CuO NP-induced OMVs > H_2O_2-induced OMVs > control OMVs. Biochemical assays confirmed the presence of lipopolysaccharides, nucleic acids, and protein in OMVs; however, these assays did not discriminate OMV composition according to the cellular stressor. These results demonstrate the utility of Raman spectroscopy and LDA to characterize and distinguish stress effects on OMVs from control and stressed cells.

Background

Outer membrane vesicles (OMVs) are extracellular vesicles ranging in size from 20-300 nm in diameter produced by Gram-negative bacteria (Kim et al. 2015; Li, Clarke, and Beveridge 1998; Yáñez-Mó et al. 2015). OMV composition includes numerous outer membrane and periplasmic components including proteins, lipopolysaccharide (LPS), enzymes, and in the case of pathogens, toxins (Lekmeechai et al. 2018; Schwechheimer and Kuehn 2015). OMVs may also contain DNA (Bitto et al. 2017; Grande et al. 2015) or RNA (Koeppen et al. 2016). Consequently, OMVs exhibit many unique functions including acting as a protein secretion system (Bonnington and Kuehn 2014), delivery of virulence factors by pathogenic bacteria (Bomberger et al. 2009; Ellis and Kuehn 2010; Horstman and Kuehn 2000), communication and signaling between bacteria (Berleman and Auer 2013; Renelli et al. 2004), and cross-kingdom signaling with eukaryotic cells (Bauman and Kuehn 2009; Berleman and Auer 2013; Horstman and Kuehn 2000). OMVs appear to be released during all stages of cell growth in liquid and solid culture (Beveridge 1999) and have been observed as a structural part of the biofilm matrix in naturally-occurring and laboratory-grown biofilms (Schooling and Beveridge 2006).

Relationships between OMV release and biofilm formation and maintenance are apparent with multiple potential OMV roles (Wang, Chanda, and Zhong 2015). Intact OMVs have been observed within the biofilm matrix (Schooling and Beveridge 2006) and may mediate biofilm formation (Ionescu et al. 2014). For several *Helicobacter pylori* strains, OMV production correlates with the ability to form and maintain the biofilm (Yonezawa et al. 2009). The quorum-sensing molecule 2-heptyl-3-hydroxy-4-quinolone, used for communication during biofilm formation by *Pseudomonas aeruginosa*, is

present within *P. aeruginosa*-produced OMVs (Mashburn and Whiteley 2005) and is

required for OMV formation by this bacterium (Mashburn-Warren et al. 2008).

Although OMVs are continually released, OMV production increases in response

to stress (McBroom and Kuehn 2007; van de Waterbeemd et al. 2013), possibly as a

mechanism to quickly release misfolded periplasmic proteins (Haurat, Elhenawy, and

Feldman 2015; McBroom and Kuehn 2007). OMV production under stress also appears

to have defensive roles. OMVs present bacteriophages and other membrane-binding

antimicrobial agents with decoy targets that bind these agents away from the cell

(Manning and Kuehn 2011). OMVs may contain specific enzymes and other compounds

to increase bacterial survival (Berleman et al. 2014; Kadurugamuwa and Beveridge 1996;

Li et al. 1998). For example, although exposure to reactive oxygen species (ROS), such

as H_2O_2, increases OMV release in several bacteria (Lekmeechai et al. 2018; MacDonald

and Kuehn 2013; van de Waterbeemd et al. 2013), *H. pylori* releases catalase-containing

OMVs in response to ROS stress thus protecting cells from oxidative damage

(Lekmeechai et al. 2018). Another example is packaging β-lactamase into OMVs by

Moraxella catarrhalis to lessen cell death by β-lactam antibiotics (Schaar et al. 2011).

Although OMVs have been studied from human pathogens (Ellis and Kuehn

2010; Wang et al. 2015) and plant pathogens (Bahar et al. 2016; Katsir and Bahar 2017),

the OMV roles for plant-health-promoting bacteria are currently unknown. The beneficial

relationship between the plant and its associated microbiome requires cross-kingdom

signaling that is mediated through many small metabolites, including hormones and

quorum sensing molecules (Hughes and Sperandio 2008; Schikora, Schenk, and

Hartmann 2016). OMV release presents one potential method for the secretion and

delivery of these signals.

Here, OMVs of a well-characterized plant-health-promoting soil bacterium, *Pseudomonas chlororaphis* O6 (*Pc*O6), were studied. *Pc*O6 is a Gram-negative, rod-shaped bacterium originally isolated from roots of commercial dryland wheat grown in Cache Valley, UT, USA (Spencer et al. 2003). *Pc*O6 is representative of many beneficial soil bacteria, boosting plant health through multiple protective pathways. *Pc*O6 is an aggressive root colonizer and forms robust biofilms on plant roots (Jacobson et al. 2018; Kim et al. 2014). Cell growth within the biofilm is then nurtured through root exudates (Bonebrake et al. 2018). In return, the bacterium protects the host by producing phenazines and other antibacterial and antifungal compounds (Anderson and Kim 2018). *Pc*O6 protects plants from drought, in part by producing butanediol that triggers partial stomatal closure (Cho et al. 2008). Biofilm formation may also promote crop drought tolerance as the biofilm matrix maintains moisture around plant roots (Costa, Raaijmakers, and Kuramae 2018; Timmusk et al. 2015).

OMVs have been observed in atomic force microscopy images of *Pc*O6 cells (Dimkpa, McLean, et al. 2012; Gade et al. 2016), but OMV composition and their role in *Pc*O6 signaling and stress responses are currently unknown. Two relevant stressors to the rhizosphere, or the area around plant roots, and their effects on *Pc*O6 and subsequent OMV production were examined in this study. The first stressor was CuO nanoparticles (NPs). Numerous engineered metal and metal oxide NPs are explored for agricultural applications including delivering macronutrient and micronutrient to crops (Liu and Lal 2015; Sekhon 2014), controlling pests and pathogens (Sekhon 2014), and protecting crops against various stresses (Khan et al. 2017), including drought (Anderson et al.

2017; Jacobson et al. 2018; Sekhon 2014; Yang et al. 2018). In *Pc*O6-colonized wheat,

CuO NPs upregulate genes associated with water deficiency tolerance (Yang et al. 2018)

and increase lignification in wheat sclerenchyma, considered to be the strengthening

tissue of the plant (Jacobson et al. 2018). Thus NP-induced gene expression can

contribute to crop stress tolerance (Van Aken 2015; Yang et al. 2018). NPs also change

gene expression in various beneficial and antagonistic microorganisms (Van Aken 2015).

CuO NPs are known to increase *Pc*O6 cell size (Bonebrake et al. 2018), decrease the

production of the Fe-scavenging siderophore pyoverdine (Dimkpa, Mclean, et al. 2012),

and increase the production of the plant growth regulator indole-3-acetic acid (Dimkpa,

Zeng, et al. 2012). However, sublethal CuO NP dosages do not diminish *Pc*O6 biofilm

formation (Bonebrake et al. 2018). Hydrogen peroxide (H_2O_2) was examined as a second

bacterial stressor as ROS increase OMV production (MacDonald and Kuehn 2013) and

are generated as a stress response by plant root cells (Marslin, Sheeba, and Franklin

2017), including CuO NP stress (Adams et al. 2017).

To characterize OMVs, as well as any compositional changes due to these abiotic

stressors, Raman spectroscopy was chosen as the primary characterization technique.

Compared to other spectroscopy techniques, Raman spectroscopy is well suited for

biological samples as it requires minimal sample preparation, is non-destructive, and

gives a linear correlation of compound concentration to signal strength (Momen-Heravi

et al. 2012). Raman spectroscopy is regularly used for cellular identification and

characterization, even at a single-cell level (Harz, Rösch, and Popp 2009; Huang et al.

2010; Swain and Stevens 2007). Changes in biomolecular profiles according to the

growth stage can be detected by Raman spectroscopy in mycobacterial cells (Hanson et

al. 2019). Raman spectroscopy has been used for the characterization of extracellular vesicles from eukaryotic cells (Huefner et al. 2016; Krafft et al. 2016; Tatischeff et al. 2012), but no current literature reports Raman spectroscopy characterization of OMVs.

Raman spectroscopy was used to explore the chemical signature of OMVs isolated from PcO6 cells under baseline conditions and under CuO NP or H_2O_2 stress. Raman spectra of intact PcO6 cells were compared to spectra from purified OMVs, with and without exposure to these stressors. Biochemical assays detecting protein, LPS, and DNA content were performed to measure their presence in OMVs and to further examine changes in OMV composition.

Materials and Methods

Bacterial growth conditions

PcO6 stocks were kept at -80°C in 15% glycerol and thawed before use. PcO6 biofilms were grown at 22°C on minimal medium (K_2HPO_4- 10.5 g/L, KH_2PO_4- 4.5 g, Na*citrate*$2H_2O$- 0.5 g/L, $(NH_4)_2SO_4$- 1 g/L, sucrose- 2 g/L, anhydrous $MgSO_4$- 0.125 g/L) 2% agar plates (15 x 100 mm) for 48 h to a confluent lawn (~5 x 10^4 CFUs/plate).

PcO6 biofilms were also grown on hollow fiber membranes for SEM imaging. Hollow fiber membranes were inoculated with 2 μL PcO6 suspended in sterile double distilled H_2O (ddH_2O) (resistance > 18 MΩ*cm) at a concentration of 10^6 colony forming units (CFUs)/mL, draped across wells with liquid minimal medium, and allowed to grow at 22°C for 28 h.

Abiotic stressor preparations

Sterile ddH_2O was used as the control treatment. CuO NPs (diameter < 100 nm,

purity = 99.95%) were obtained from American Elements (Los Angeles, CA, USA) as a

nanopowder and stored protected from light. NP size distribution and agglomeration

profiles were confirmed with scanning electron microscopy (FEI Quanta FEG 650)

(Figure A - 1). Elemental composition was determined by scanning electron microscopy

with energy-dispersive X-ray spectroscopy using an X-Max Detector (Oxford

Instruments). NP stress used CuO NPs suspended in sterile ddH_2O (30 mg Cu from CuO

NPs/L) through sonication (Q500, QSonica LLC) for 10 min with an alternating 10 s

on/off cycle at 25% amplitude. The ROS stress was 3% H_2O_2 (v/v).

Treatments of *Pc*O6 biofilm cells before OMV isolation

The confluent lawns of *Pc*O6 biofilm cells on minimal medium were treated by

flooding with 10 mL of ddH_2O, H_2O_2, or CuO NPs, added in 1 mL aliquots. These

conditions were maintained for 60 min, during which time the cells detached from the

surface and became suspended in the liquid. CFUs were counted with serial dilutions on

LB 2% agar petri dishes to check the effect of stressors on cell viability. CuO NPs had no

significant effect on CFUs/plate while H_2O_2 had only a minimal effect on cell viability

(<10% CFU reduction).

Isolating and purifying outer membrane vesicles

OMVs were isolated from *Pc*O6 cells using a method adapted from Zhou *et al.*

(1998). Twenty minimal medium plates with confluent *Pc*O6 lawns (a total surface area

of 0.628 m^2) were used per treatment to maximize OMV yields for analysis. The cell

suspension (10 mL/plate for a total of 200 mL/treatment) was poured from the petri

dishes into 50 mL polypropylene conical tubes and centrifuged (10,000 x g, 20 min) to

generate a cell pellet leaving OMVs and other secreted materials in the supernatant. This

step also removed CuO NPs from the solution when this stressor was used. OMVs were concentrated from the supernatant by ammonium sulfate precipitation. Ammonium sulfate (Mallinckrodt chemicals) was added over the course of two hours (240 g/L total) at 15 min intervals to the supernatant, which was left undisturbed at 22°C until precipitates formed (anywhere from 2-8 h). The precipitates were pelleted by centrifugation (10,000 x g, 10 min), resuspended in 1 mL sterile deionized H_2O, and dialyzed against ddH_2O for at least 16 h. The solution was sterile filtered (0.45 μm, Ultrafree PVDF centrifugal filter units, Beckman Coulter Inc.) to remove any remaining cells or contaminants.

To purify OMVs from flagella, pili, and secondary metabolites (Figure A - 2), density gradient ultracentrifugation was performed using methods adapted from Chutkan *et al.* (2013). The crude OMV suspension was mixed with OptiPrep iodixanol gradient medium (Sigma Aldrich) to create a 45% OptiPrep solution (vol/vol). A 2 mL aliquot was loaded into the base of each ultracentrifuge tube (Ultraclear 12.5 mL centrifuge tube, Beckman Coulter) and covered sequentially with 2 mL layers of 40, 35, 30, 25, and 20% OptiPrep before centrifugation (212,000 x g, 3 h, 4°C) (Optima LE-80K Centrifuge, Beckman). Aliquots of 1 mL were collected from the top of the gradient in a cold room to minimize diffusion. OMV-containing fractions, the top 1 mL of each tube, were pooled from each treatment, diluted at least 10 times with sterile ddH_2O, loaded into centrifuge tubes (26.3 mL Polycarbonate Bottle with Cap, Beckman Coulter), and centrifuged (40,000 x g, 3 h) to pellet the OMVs. The OMV pellet was resuspended in 750 μL sterile ddH_2O and sterile filtered (0.45 μm, Ultrafree PVDF centrifugal filter units). The presence of OMVs in the filtrate was confirmed with AFM imaging. Pure OMV preps

were stored at 4°C until used for Raman spectroscopy, which took place within 48 h of

OMV isolation and purification. Samples were frozen (-20°C) until further needed.

Atomic Force Microscopy (AFM)

AFM was performed on a Nanoscope III Bioscope (Digital Instruments, Inc.) in

tapping mode. Budget Sensors-Tap 300AL-G cantilevers with a tip radius of curvature

<10 nm, length of 125 μm, width of 30 μm, thickness of 4 μm, and a 40 N/m force

constant were employed. Images were collected at 256 x 256 resolution and 1 Hz over a

range of scan sizes and scan angles. For whole *Pc*O6 cells, a sample of the bacterial lawn

on a sterile inoculation loop was smeared on a clean glass slide and immediately imaged.

For OMVs, 20 μL purified OMV suspension was pipetted onto a clean glass slide,

allowed to dry, and immediately imaged. OMV diameter was determined using the

horizontal distance in the line cut feature in the Nanoscope software. Ten OMVs were

sized per treatment from 2 separate images of 1 x 1 μm or less.

Scanning Electron Microscopy (SEM)

SEM was performed with an FEI Quanta FEG 650 equipped with an Oxford X-

Max EDS housed in the Microscopy Core Facility at Utah State University. Hollow fiber

membranes with *Pc*O6 biofilms were dipped in sterile distilled H_2O, fixed in methanol

for 10 min, and dried in two 10 min bath of 100% ethanol. Samples were critical point

dried and sputter coated in an Au/Pd coat. Images were captured under high vacuum.

Purified OMVs were pipetted onto a clean substrate, fixed with 2.5% glutaraldehyde,

dehydrated using two 5 min washes of increasing ethanol concentrations (50, 70, & 95%)

followed by three 15 min washes with 100% ethanol. Samples were imaged under high

vacuum without coatings.

Dynamic light scattering

DLS measurements were performed on a DynaPro NanoStar (Wyatt Technology Corporation, Santa Barbara, CA) employing Dynamics Software (version 7.0.3, Wyatt Technology Corporation, Santa Barbara, CA) and a 658 nm laser. The purified OMV suspensions were diluted 1:10 in sterile deionized water, and 70 µL was transferred to DLS cuvettes. The intensity autocorrelation function (see Figure A - 3 for autocorrelation graphs) was used to calculate a hydrodynamic diameter based on the Stokes−Einstein equation using a regularization method employed in the software.

Raman spectroscopy

To examine the intact cells, confluent *Pc*O6 lawns from two minimal media plates with or without the stress treatments were centrifuged from solution (14,000 x g, 10 min), and resuspended in 1 mL sterile, deionized H_2O. This process was repeated two additional times to remove stressors. After the third centrifugation, *Pc*O6 cells were resuspended in 200 µL sterile, deionized H_2O. The majority of OMVs, cell secretions, and other cell debris remained in the supernatant which was discarded after each centrifugation. A 10 µL aliquot of the *Pc*O6 suspension was pipetted onto aluminum tape affixed to a clean glass microscope slide and allowed to dry. For OMVs, no additional preparation was needed for Raman spectroscopy after isolation and purification steps. Twenty µL purified OMV suspension was pipetted onto aluminum tape affixed to a clean glass microscope slide and allowed to dry.

Raman spectra were obtained using a Renishaw inVia Raman microscope with a 633 nm laser, 1200 g/mm grating, and 14 mW laser power. Spectra were obtained over a 30 s acquisition time with a wavenumber range of 200-3200 cm^{-1}, with 3 accumulations

per spectrum. For each of the 3 OMV isolations, 4 spectra were obtained per treatment.

Spectrogryph (Menges 2019) was used to visualize spectra, obtain peak numbers, and

average spectra. Linear discriminant analysis (LDA) of spectra was performed with R

following background subtraction (WiRE 4.1), removal of cosmic rays (WiRE 4.1), data

truncation to 750-1700 cm^{-1}, and 2670-3100 cm^{-1}, and normalization of spectra (R).

<u>260/280 ratio</u>

The nucleic acid to protein ratio was determined based on the adsorption ratio of

260/280 nm. Frozen samples were thawed and 2 μL of each sample was pipetted into

wells of a microdrop plate (Take 3 plate, BioTek Instruments Inc.) and absorbance was

read at 260 and 280 nm (Synergy HT, BioTek Instruments Inc.). Duplicates were run for

each sample.

<u>Micro-bicinchoninic acid (micro-BCA) assay</u>

OMVs protein content was quantified with a Pierce micro-BCA assay kit

(Thermo Scientific). Frozen OMV samples were thawed and prepared according to

manufacturer's instructions and absorbance was read at 562 nm (Synergy HT, BioTek

Instruments Inc.) with appropriate bovine serum albumin standards from the

manufacturer with concentrations of 0 to 200 μg protein/mL. Duplicates were run for

each standard and sample.

<u>Lipopolysaccharide (LPS) quantification</u>

LPS quantification was done with a Pierce Endotoxin Quantification Kit (Thermo

Scientific). Frozen samples were thawed and prepared according to manufacturer's

instructions and absorbance was read at 405 nm (Synergy HT, BioTek Instruments Inc.)

with LPS standards from *Escherichia coli* supplied by the manufacturer in the range of 0.1 to 1 Endotoxin Units (EU)/mL. Duplicates were run for each standard and sample.

Results

<div align="center">Physical characterization of outer membrane vesicles</div>

OMV production by *Pc*O6 biofilm cells was confirmed *in situ* with imaging by atomic force microscopy (AFM) and scanning electron microscopy (SEM). AFM images of *Pc*O6 biofilm cells, transferred from minimal media agar plates, without stressors show OMVs as aggregates between *Pc*O6 cells (Figure 4 - 1A) and as linear assemblies apart from the cells (Figure 4 - 1B). Isolated OMVs appear as aggregates in AFM images with no visible differences between control and stress-induced OMVs (Figure 4 - 2, Figure A - 4). Purified OMVs from control cells also appear as aggregates in SEM images (Figure 4 - 3A). SEM images of *Pc*O6 biofilms formed on hollow fiber membranes draped in minimal medium, representing an entirely different method for *Pc*O6 biofilm growth, also showed OMVs as part of the biofilm matrix and/or adhered to cells (Figure 4 - 3B).

Size analysis of the OMVs in the AFM images showed average diameters of individual OMVs in the range of 40-100 nm (Figure A - 5), matching size descriptions of other vesicles imaged by AFM (Kim et al. 2019). However, many aggregates appeared larger with clearly defined boundaries between OMVs. This propensity for OMV aggregation was confirmed with dynamic light scattering (DLS) results showing OMVs with hydrodynamic diameters ranging from 40-300 nm (Figure A - 6). The imaging and DLS results are consistent with literature reports of OMV diameters between 10 and 300 nm (Deatheragea and Cooksona 2012; Ellis and Kuehn 2010).
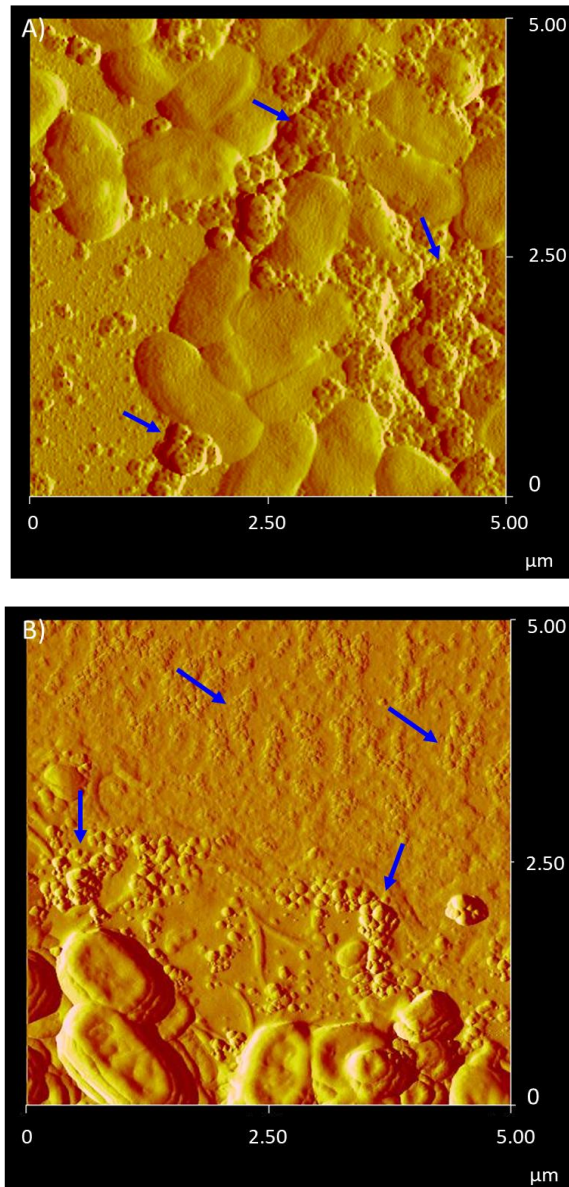
Figure 4 - 1: AFM amplitude images of cells from the edges of a *Pc*O6 smear from a biofilm grown on a 2% minimal media plate onto a clean glass slide. OMVs are visible in both images as A) aggregates between *Pc*O6 cells and B) as linear assemblies. Arrows point to examples of these OMV aggregates.
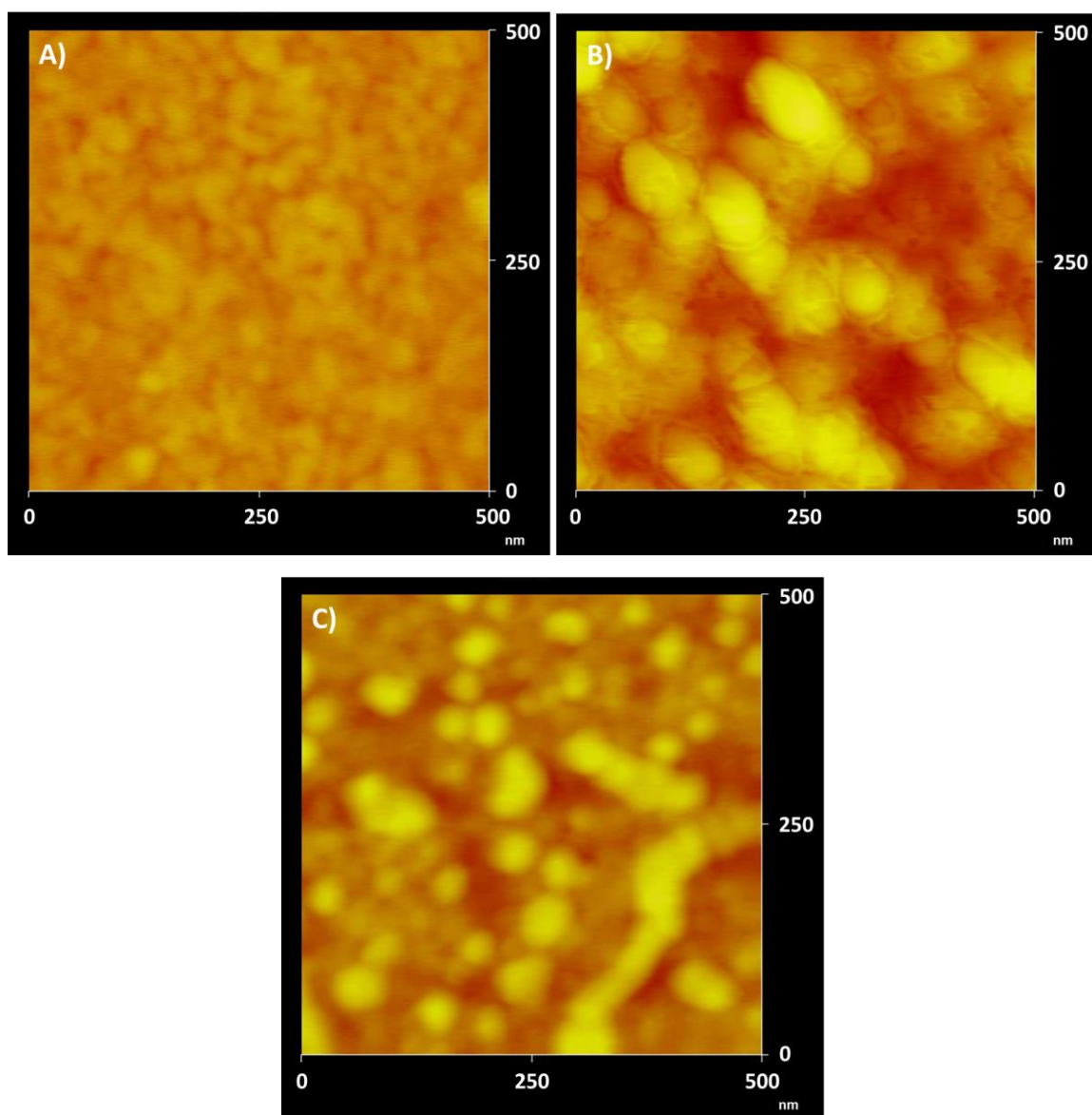
Figure 4 - 2: AFM height images of purified OMVs. Z-scales are from red to yellow from 0 to 25 nm respectively. A) OMVs harvested from *Pc*O6 without any stressors. B) OMVs harvested from *Pc*O6 under H_2O_2 stress (3% v/v). C) OMVs harvested from *Pc*O6 under CuO NP stress (30 mg Cu/L). Additional AFM images are shown in Figure A - 4.
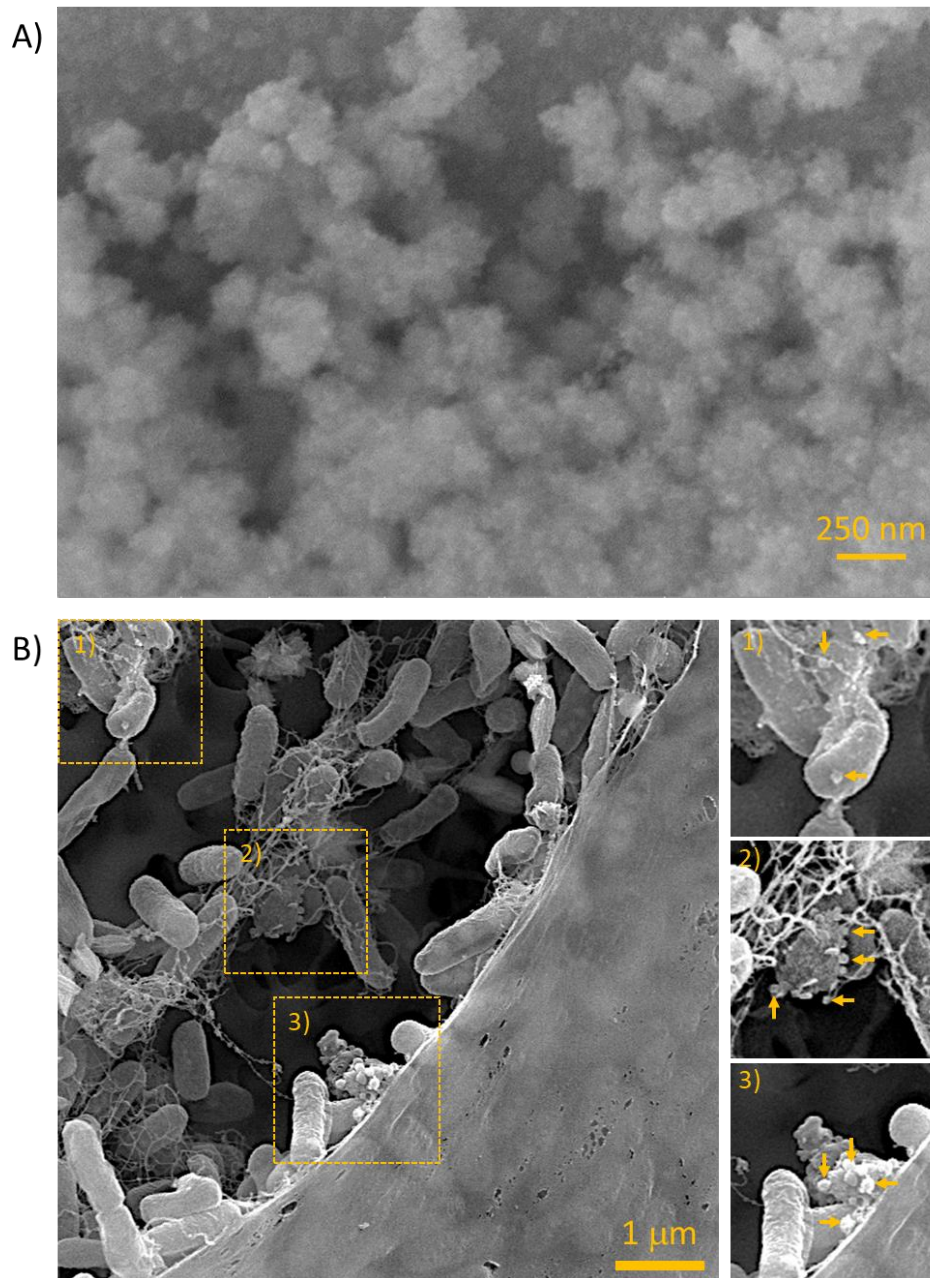
Figure 4 - 3: SEM images of *Pc*O6 and purified OMVs. A) SEM image showing aggregation of purified OMVs from *Pc*O6 biofilms without abiotic stressors after glutaraldehyde fixation and ethanol dehydration. B) SEM image showing the cross-section of a *Pc*O6 biofilm grown on a hollow fiber membrane draped in minimal medium without any added stressors. Three areas of this image are highlighted to show potential OMVs which are marked with arrows.

Chemical characterization of *Pc*O6 cells with Raman spectroscopy

Raman spectroscopy was coupled with LDA to detect differences in the chemical profiles of control and stressed *Pc*O6 cells. Raman spectra of whole *Pc*O6 cells (n=12 from 3 replicates), normalized to the highest peak of 2935 cm^{-1} (C-H bonds), from each treatment are shown in Figure 4 - 4. Peak assignments were consistent for proteins, amino acids such as phenylalanine and tyrosine, unsaturated lipids, polysaccharides, and nucleic acids such as adenine, uracil, and guanine (a full list of peak assignments is shown in Table A - 3). Although the LDA of Raman spectra misclassified a few spectra (LDA plot shown in Figure 4 - 5 and LDA confusion matrix shown in Table 4 - 1), there were still distinct chemical profiles for *Pc*O6 according to the stressor.

There were no peaks unique for any treatment nor any peaks that disappeared in any one treatment. However, peak intensities differed between treatments with the spectra of control *Pc*O6 giving the highest relative intensities, followed by H_2O_2-treated *Pc*O6, then CuO NP-treated *Pc*O6. The following peaks showed the greatest decreases in peak intensity for stressed cells relative to the control: a) 880 cm^{-1}: tryptophan and lipid N^+ $(CH_3)_3$ bonds; b) 1220-1280 cm^{-1}: amide III; c) 1330-1340 cm^{-1}: adenine, guanine, tyrosine, and tryptophan; d) 1365 cm^{-1}: lipid C-H bonds; e) 1450 cm^{-1}: protein and lipid C-H bonds; and f) 1660 cm^{-1}: unsaturated lipids.
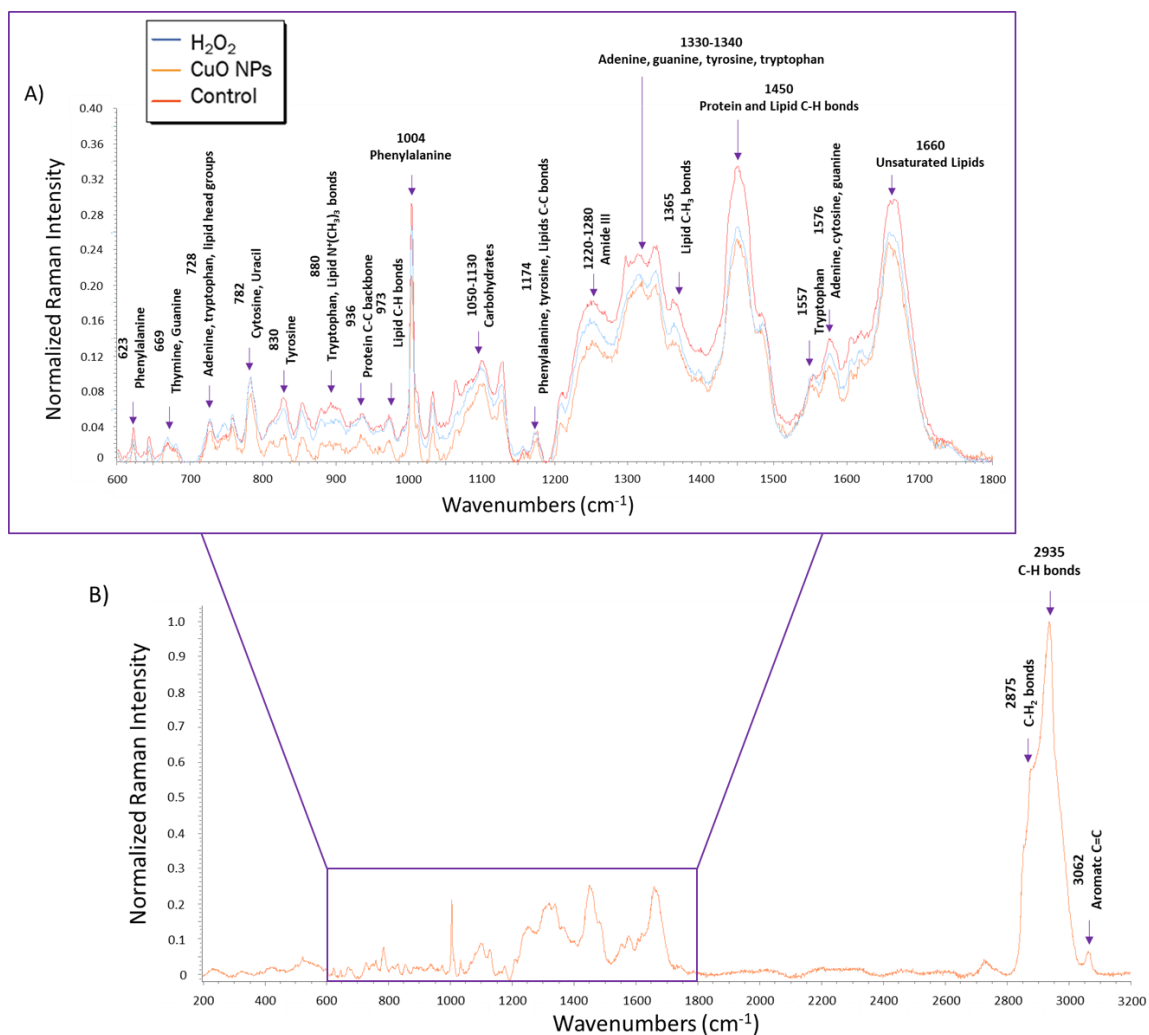
Figure 4 - 4: Averaged Raman spectra of intact *Pc*O6 cells (3 replicates with 4 spectra each for a total of n=12). A) Averaged Raman spectra of *Pc*O6 cells treated with H_2O_2 stress, CuO NP stress, and the control with no added stressor from 600 to 1800 cm^{-1}. In this region, differences are seen in relative peak intensity indicating differences in relative concentrations of various compounds. B) Averaged Raman spectra of *Pc*O6 cells without any applied stressor from 600 to 3200 cm^{-1}. No significant differences are seen in the relative peak intensities above 1800 cm^{-1} of *Pc*O6 cells of each treatment so spectra of CuO NP and H_2O_2 treated cells are not shown. In both graphs, notable peak assignments are shown with an arrow and labeled with both the peak number and peak assignment. See Table A - 3 for a list of all peak assignments and respective sources.
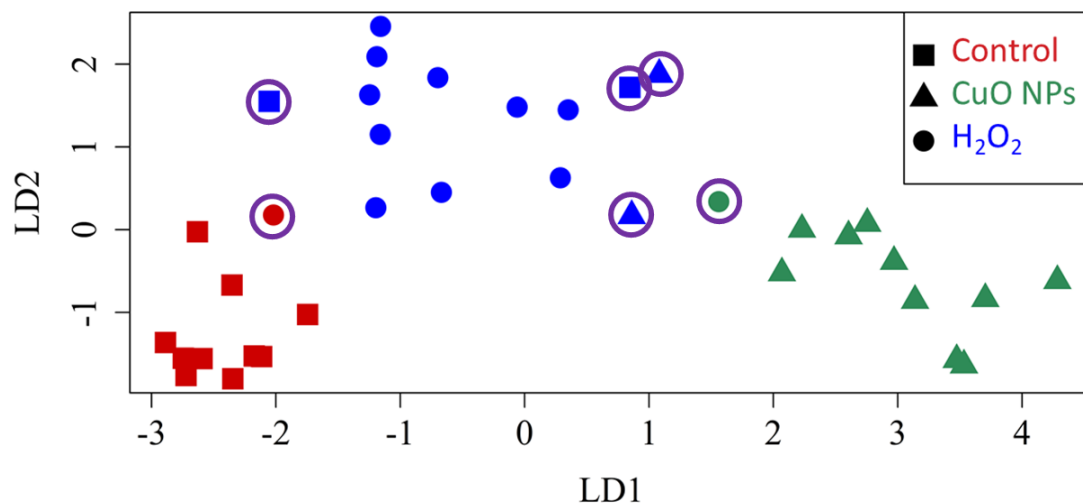
Figure 4 - 5: LDA plot of Raman spectra from PcO6 cells. Data were truncated to 750-1700 cm^{-1} and 2670-3100 cm^{-1}, where most peaks are located. The shape of the points of the plot indicates the true treatment of each spectrum whereas the color of the point indicates the predicted treatment according to LDA. Misclassified spectra are circled in purple.

Table 4 - 1: Confusion matrix showing LDA results of Raman spectra from PcO6 cells. LDA of the Raman spectra gave an 83.3% accuracy indicating that spectra of PcO6 are highly dependent on the stressor.

Confusion matrix of Raman spectra of PcO6 cells			
	Predicted Treatment		
	Control	**CuO NPs**	**H$_2$O$_2$**
Control	10	0	2
CuO NPs	0	10	2
H$_2$O$_2$	1	1	10

(True Treatment)

Comparing Raman spectra of PcO6 cells and isolated OMVs

Raman spectroscopy was used to compare the chemical profiles of PcO6 cells and isolated OMVs. Unique peaks were found in comparisons between Raman spectra of

control *Pc*O6 cells and purified OMVs from control cells (Figure 4 - 6): 27 peaks are

unique to *Pc*O6 cells, 14 peaks are unique to OMVs, and 10 peaks are shared (a full list

of peak assignments for *Pc*O6 cells and OMVs is shown in Table A - 3). Figure 4 - 6

shows these shared peak assignments, and whether relative peak intensity is higher for

control *Pc*O6 cells or resultant purified OMVs. The same trends were seen in H₂O₂ and

CuO NP-treated *Pc*O6 cells and purified OMVs of stressed cells (data not shown).
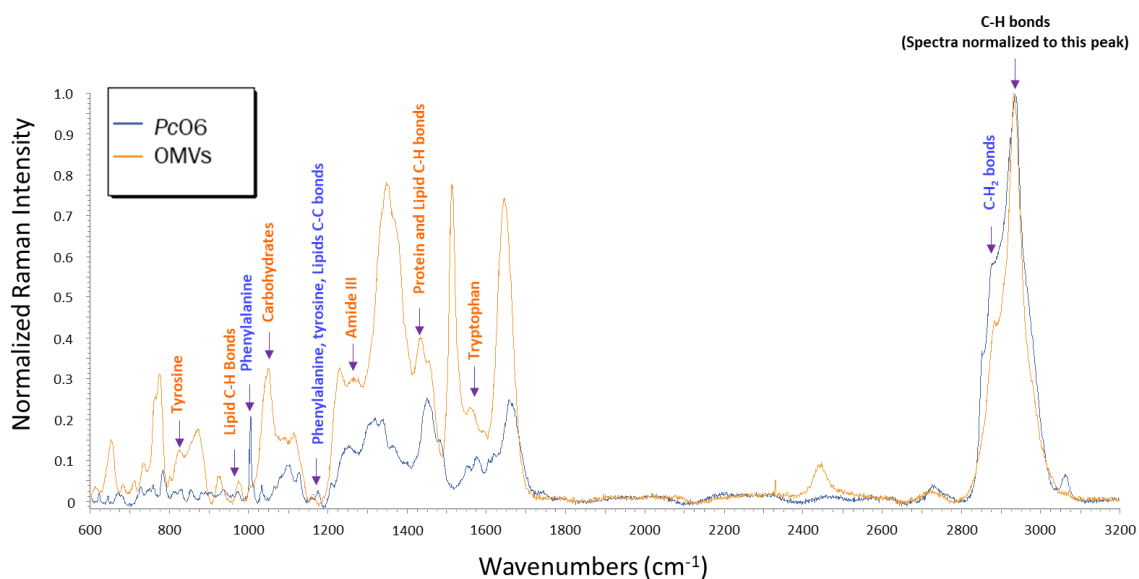
Figure 4 - 6: Comparisons between averaged Raman spectra of control *Pc*O6 cells and OMVs (3
replicates with 4 spectra each for a total of n=12). Peaks that are shared by *Pc*O6 and OMVs
Raman spectra are marked with an arrow and labeled with the peak assignment. Text color
indicates whether these peaks are higher in *Pc*O6 cells (blue text), or isolated OMVs (orange
text). See Table A - 3 for a list of all peak assignments and respective sources.

The relative intensity differed between shared peaks. All but two of these shared

peaks had higher relative intensity for the OMV spectra than spectra of intact *Pc*O6 cells.

Though there are few peaks shared by intact *Pc*O6 cells and purified OMVs, several

unique peaks for *Pc*O6 and OMV Raman spectra correspond to the same chemical

compounds: i.e. *Pc*O6 peak 644 cm^{-1} and OMV peak 870 cm^{-1} both corresponding with

tyrosine. The amino acid tryptophan and the nucleic acids adenine, cytosine, and guanine

are also present in *Pc*O6 cells and purified OMVs though different peaks give these

assignments for whole *Pc*O6 cells and isolated OMVs. Both *Pc*O6 and OMV spectra

show various lipid, carbohydrate, protein, and DNA signatures although different

signatures of these macromolecules appear in each: i.e. *Pc*O6 peak 820 cm^{-1} indicates

lipid O-P-O bonds while OMV peak 1120 cm^{-1} indicates lipid C-C bond.

Especially notable in Raman spectra of isolated OMVs was the increased intensity

of nucleic acid peaks which implies that DNA and/or RNA are selectively packaged by

*Pc*O6 into and/or onto OMVs. This conclusion was confirmed measurements of OMV

260/280 ratios, which compares the concentration of nucleic acids to the concentration of

protein which absorb light at 260 and 280 nm respectively. OMV 260/280 ratios did not

vary according to cell stressor (Table A - 4) with an overall mean of 5.91 $\pm$ 0.09.

Although the micro-BCA assay detected varying amounts of protein in OMV suspensions

(Figure A - 7), the 260/280 ratio results indicate that the amount of protein is insignificant

to the amount of DNA present within/on OMVs.

Chemical characterization of stress-induced outer membrane vesicles with Raman spectroscopy

The chemical profiles of control OMVs were compared with H_2O_2- and CuO NP-

induced OMVs with Raman spectroscopy and LDA. Averaged Raman spectra from

OMVs harvested from cells of all treatments are shown in Figure 4 - 7 (n=12 for control

and CuO NP-induced OMVs and n=11 for H_2O_2-induced OMVs from 3 OMV

isolations). Comparing the spectra according to the cellular stressor, there were no peaks unique for any treatment nor any peaks that disappeared in any one treatment. Instead, the differences between stressors are primarily in differing peak intensities. Differences are seen in the peak intensity of control OMVs and those harvested from PcO6 exposed to CuO NPs and H_2O_2, most notably: a) 1646 cm^{-1}, glycine; b) 1513 cm^{-1}, adenine, cytosine, and guanine; and c) 1348 cm^{-1}, adenine, guanine, tyrosine, and tryptophan. For these peaks, OMVs from CuO NP-treated PcO6 have the highest intensity, followed by OMVs from H_2O_2-treated PcO6 then OMVs of control cells.
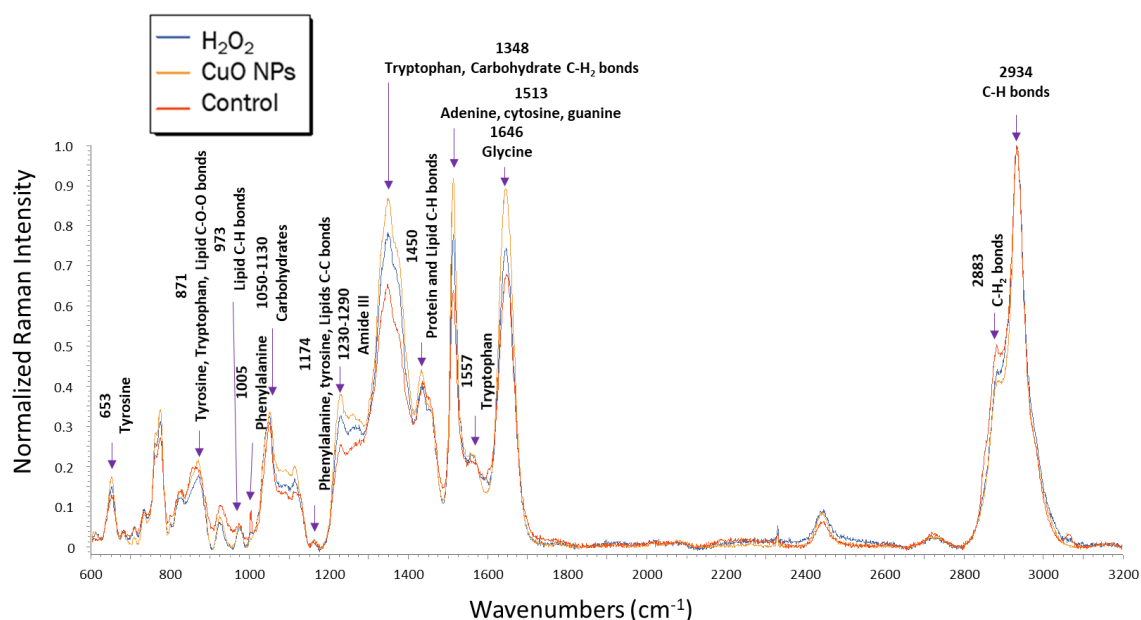
Figure 4 - 7: Averaged Raman spectra of OMVs harvested from PcO6 colonies exposed to H_2O_2, CuO NPs, or no stressor at all (n=12 for control and CuO NP-induced OMVs and n=11 for H_2O_2-induced OMVs from 3 OMV isolations) from 600 to 3200 cm^{-1}. Differences are seen in normalized peak intensities indicating large differences in relative concentrations of compounds in the OMVs. Notable peak assignments are marked with an arrow and labeled with their respective peak number and peak assignment. For a list of all peak assignments and their sources, see Table A - 3.

LDA results (LDA plot shown in Figure 4 - 8, LDA confusion matrix shown in Table 4 - 2) showed a 77.1% accuracy for pure OMVs from all treatments with several misclassified spectra in each treatment, indicating OMV composition and contents are less consistent compared to *Pc*O6 cells. This OMV heterogeneity was further confirmed with biochemical assays. LPS content (average of 15.6 ± 2.7 endotoxin units (EU)/mL solution) and protein content (average of 23.3 ± 13.4 µg/mL solution) of OMVs were not affected by cellular stressor nor trial and did not correlate with each other (Figure A - 7).
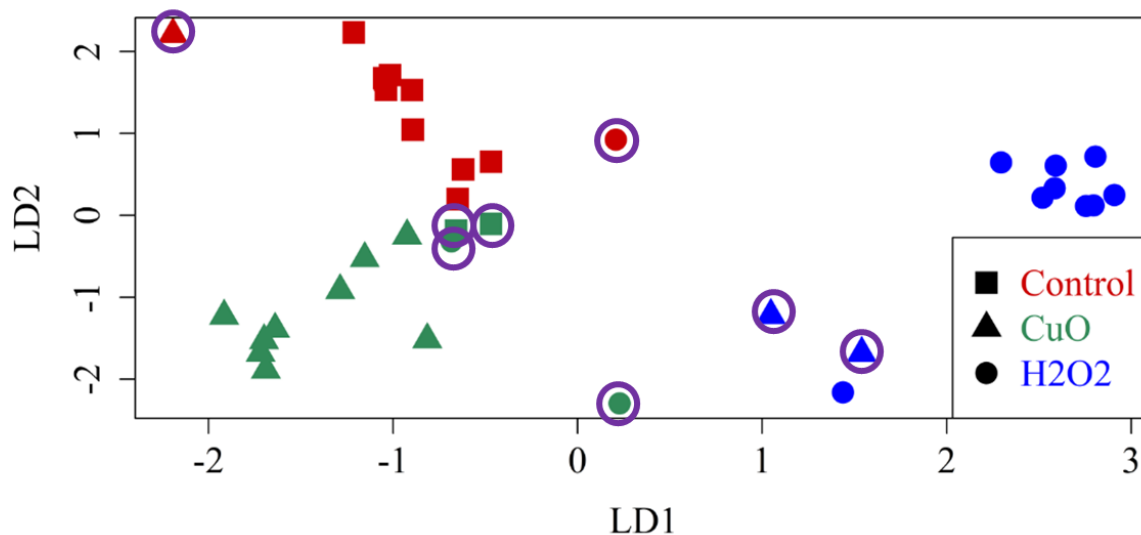
Figure 4 - 8: LDA plot of Raman spectra from purified OMVs (n=12 for control and CuO NP-induced OMVs and n=11 for H_2O_2-induced OMVs from 3 OMV isolations). Data were truncated to 750-1700 cm^{-1} and 2670-3100 cm^{-1}, where most peaks are located. The shape of the points of the plot indicates the true treatment of each spectrum whereas the color of the point indicates the predicted treatment according to LDA. Misclassified spectra are circled in purple.

Table 4 - 2: Confusion matrix from LDA plot of Raman spectra given by pure OMVs. One Raman spectrum of H_2O_2-induced OMVs was omitted from this analysis. LDA of the Raman spectra gave a 77.1% accuracy.

Confusion matrix of Raman spectra of pure OMVs				
		Predicted Treatment		
		Control	**CuO NPs**	**H$_2$O$_2$**
True Treatment	**Control**	10	2	0
	CuO NPs	1	9	2
	H$_2$O$_2$	1	2	8

Discussion

DLS and AFM measurements showed that OMV sizes were highly polydisperse regardless of the cellular stressor. Differing OMV diameter according to the analysis method has been reported in the literature (Kim et al. 2019), likely due to differences in OMV aggregation and/or hydration. Aggregation of OMVs observed in AFM and SEM images may be due to outer membrane surface features in OMVs similar to those involved in adhesion for intact cells (Berleman et al. 2016). Similar results were observed in studies of OMVs produced by *Neisseria lactamica*, where OMV aggregation was found to be a pH-dependent process. Numerous large OMV aggregates occurred at pH 7.0 with fewer aggregates occurring at pH 8.0 (Gorringe et al. 2005), implying that many OMV surface proteins reached an isoelectric equilibrium at this higher pH thus reducing the number of OMV aggregates. LPS charge may also be altered by environmental pH.

OMV aggregation is believed to be involved in biofilm formation. OMVs produced by biofilm *Myxococcus xanthus* cells form chains that tether biofilm cells together (Remis et al. 2014). *Xyllela fastidiosa* uses OMV aggregates to mediate surface

adhesion, either promoting or preventing biofilm formation by the bacterium (Ionescu et al. 2014). *Pc*O6 is a strong biofilm colonizer (Bonebrake et al. 2018) and may use OMVs in its aggressive colonization of plant roots.

This work established that Raman spectroscopy coupled with LDA was a reliable method for characterization of OMV content; the creation of libraries of the peaks could be valuable in the assessment of structural changes to cells under different exposures. Comparing Raman spectra of intact *Pc*O6 cells and isolated OMVs, it is clear that certain *Pc*O6 cell components are enriched while others are excluded in OMVs, which is reported in studies of other Gram-negative bacteria (Bonnington and Kuehn 2014; McMahon et al. 2012). The decreased peak intensity of H_2O_2-treated *Pc*O6 cells is likely because unsaturated lipids react with H_2O_2 to form lipid peroxides and reactive aldehydes (Pradenas et al. 2012). The fact that the same peaks are affected in CuO NP-stressed PcO6 cells likely indicates that ROS is formed in cells as a response to CuO NP stress, a CuO NP attribute that contributes to its dose-dependent bactericidal activity (Surapaneni et al. 2012). The relative greater content of unsaturated lipids in OMVs harvested from these stressed cells compared to OMVs produced by control cells could relate to changes in membrane integrity of cells under stress.

Also notable is the high amount of nucleic acids in OMVs compared to whole *Pc*O6 cells, implicating the potential role of OMVs to transport DNA and/or RNA in *Pc*O6 biofilms. RNA in OMVs has been reported in the forms of ribosomal RNA, mRNA, and small RNAs (Malabirade et al. 2018). OMVs released by *P. aeruginosa* may contain plasmid DNA (Renelli et al. 2004), coding chromosomal DNA (Bitto et al. 2017), or noncoding environmental DNA (eDNA) (Whitchurch et al. 2002). These nucleic acids

extend proposed OMV roles in cell-to-cell communication to both gene and transcription levels. OMVs of *P. aeruginosa* contain chromosomal DNA coding for genes related to bacterial survival under stress conditions (Bitto et al. 2017). eDNA is an important part of the biofilm matrix (Costa et al. 2018) and is involved in adhesion to surfaces, aggregation of bacterial cells, and exchange of genetic information (Flemming and Wingender 2010). In *H. pylori*, eDNA was observed on OMV surfaces, perhaps as a method for OMV aggregation and cell-to-cell binding (Grande et al. 2015) including within the biofilm matrix (Remis et al. 2014).

The biochemical assays confirmed the presence of protein, LPS, and nucleic acids in the OMVs from *Pc*O6 that are indicated from the Raman spectral peaks. The inability of these assays to discriminate among OMVs according to the cellular stressor is unsurprising: OMVs are chemically heterogeneous in nature (Deatheragea and Cooksona 2012; Grande et al. 2015; Schooling and Beveridge 2006) due to the multiple potential mechanisms and pathways that lead to OMV formation (Ellis and Kuehn 2010; Kulp and Kuehn 2010). The presence of LPS, lipoproteins, and DNA in OMVs is significant because these are among the structures known "microbe-associated molecular patterns" (MAMPs) that induce resistance responses in plants (Choi and Klessig 2016). Thus, the contents of the OMVs released from *Pc*O6 could be implicated in the induction of systemic resistance observed in plants with roots colonized with *Pc*O6.

The findings of OMV production from the plant-beneficial microbe, *Pc*O6, and the changes in their composition with NP and ROS exposure revealed features that influence plant and bacterial responses in the rhizosphere. The nature of the charge on the OMV surfaces and the eDNA content could affect biofilm formation. Proteins such as

catalase found in OMVs from other bacteria (Lekmeechai et al. 2018) could alter ROS responses at the plant-biofilm interface. DNA and RNA release through OMVs could affect gene expression and the numerous confirmed MAMPs could induce plant resilience to stress.

A more detailed understanding of OMV contents is not only justified but necessary. Further studies of the effects of CuO NPs and other agriculturally relevant NPs on the plants' bacterial microbiome should extend to their influence on OMV production. For the medical field, stress-induced changes in OMV composition may be exploited to obtain OMVs better suited for targeted delivery of vaccines and drugs. While some researchers have used bacterial stress to increase OMV production for vaccine development (van de Waterbeemd et al. 2013), composition changes in OMVs from stressed cells could modify the OMVs so that they are more effective at stimulating a host response.

Acknowledgments

References

Adams, Josh, Melanie Wright, Hannah Wagner, Jonathan Valiente, David Britt, and Anne Anderson. 2017. "Cu from Dissolution of CuO Nanoparticles Signals Changes in Root Morphology." Plant Physiology and Biochemistry 110:108–17.

Van Aken, Benoit. 2015. "Gene Expression Changes in Plants and Microorganisms Exposed to

Nanomaterials." Current Opinion in Biotechnology 33:206–19.

Anderson, Anne J. and Young Cheol Kim. 2018. "Biopesticides Produced by Plant-Probiotic Pseudomonas Chlororaphis Isolates." Crop Protection 105(November 2017):62–69.

Anderson, Anne J., Joan E. McLean, Astrid R. Jacobson, and David W. Britt. 2017. "CuO and ZnO Nanoparticles Modify Interkingdom Cell Signaling Processes Relevant to Crop Production." Journal of Agricultural and Food Chemistry acs.jafc.7b01302.

Bahar, Ofir, Gideon Mordukhovich, Dee Dee Luu, Benjamin Schwessinger, Arsalan Daudi, Anna Kristina Jehle, Georg Felix, and Pamela C. Ronald. 2016. "Bacterial Outer Membrane Vesicles Induce Plant Immune Responses." Molecular Plant-Microbe Interactions 29(5):374–84.

Bauman, Susanne J. and Meta J. Kuehn. 2009. "Pseudomonas Aeruginosa Vesicles Associate with and Are Internalized by Human Lung Epithelial Cells." BMC Microbiology 9:1–12.

Berleman, James and Manfred Auer. 2013. "The Role of Bacterial Outer Membrane Vesicles for Intra- and Interspecies Delivery." Environmental Microbiology 15(2):347–54.

Berleman, James E., Simon Allen, Megan A. Danielewicz, Jonathan P. Remis, Amita Gorur, Jack Cunha, Masood Z. Hadi, David R. Zusman, Trent R. Northen, H. Ewa Witkowska, and Manfred Auer. 2014. "The Lethal Cargo of Myxococcus Xanthus Outer Membrane Vesicles." Frontiers in Microbiology 5(September):1–11.

Berleman, James E., Marcin Zemla, Jonathan P. Remis, and Manfred Auer. 2016. "Preparation of Outer Membrane Vesicles from Myxococcus Xanthus." Bio-Protocol 6(2):e1716.

Beveridge, Terry J. 1999. "Structures of Gram-Negative Cell Walls and Their Derived Membrane Vesicles." Journal of Bacteriology 181(16):4725–33.

Bitto, Natalie J., Ross Chapman, Sacha Pidot, Adam Costin, Camden Lo, Jasmine Choi, Tanya D'Cruze, Eric C. Reynolds, Stuart G. Dashper, Lynne Turnbull, Cynthia B. Whitchurch, Timothy P. Stinear, Katryn J. Stacey, and Richard L. Ferrero. 2017. "Bacterial Membrane Vesicles Transport Their DNA Cargo into Host Cells." Scientific Reports 7(1):1–11.

Bomberger, Jennifer M., Daniel P. MacEachran, Bonita A. Coutermarsh, Siying Ye, George A. O'Toole, and Bruce A. Stanton. 2009. "Long-Distance Delivery of Bacterial Virulence Factors by Pseudomonas Aeruginosa Outer Membrane Vesicles." PLoS Pathogens 5(4).

Bonebrake, Michelle, Kaitlyn Anderson, Jonathan Valiente, Astrid Jacobson, Joan E. McLean, Anne Anderson, and David W. Britt. 2018. "Biofilms Benefiting Plants Exposed to ZnO and CuO Nanoparticles Studied with a Root-Mimetic Hollow Fiber Membrane." Journal of Agricultural and Food Chemistry 66(26):6619–27.

Bonnington, K. E. and M. J. Kuehn. 2014. "Protein Selection and Export via Outer Membrane Vesicles." Biochimica et Biophysica Acta - Molecular Cell Research 1843(8):1612–19.

Cho, Song Mi, Beom Ryong Kang, Song Hee Han, Anne J. Anderson, Ju-Young Park, Yong-Hwan Lee, Baik Ho Cho, Kwang-Yeol Yang, Choong-Min Ryu, and Young Cheol Kim. 2008. "2R,3R-Butanediol, a Bacterial Volatile Produced by Pseudomonas Chlororaphis O6, Is Involved in Induction of Systemic Tolerance to Drought in Arabidopsis Thaliana." Molecular Plant-Microbe Interactions 21(8):1067–75.

Choi, Hyong Woo and Daniel F. Klessig. 2016. "DAMPs, MAMPs, and NAMPs in Plant Innate Immunity." BMC Plant Biology 16(1):1–10.

Chutkan, Halima, Ian MacDonald, Andrew Manning, and Meta J. Kuehn. 2013. "Quantitative and Qualitative Preparations of Bacterial Outer Membrane Vesicles." Methods in Molecular Biology (Clifton, N.J.).

Costa, Ohana Y. A., Jos M. Raaijmakers, and Eiko E. Kuramae. 2018. "Microbial Extracellular Polymeric Substances – Ecological Functions and Impact on Soil Aggregation." Frontiers in Microbiology 9(July):1636.

Deatheragea, Brooke L. and Brad T. Cooksona. 2012. "Membrane Vesicle Release in Bacteria, Eukaryotes, and Archaea: A Conserved yet Underappreciated Aspect of Microbial Life." Infection and Immunity 80(6):1948–57.

Dimkpa, Christian O., Joan E. Mclean, David W. Britt, and Anne J. Anderson. 2012. "CuO and ZnO Nanoparticles Differently Affect the Secretion of Fluorescent Siderophores in the Beneficial Root Colonizer, Pseudomonas Chlororaphis O6." Nanotoxicology 6(6):635–42.

Dimkpa, Christian O., Joan E. McLean, David W. Britt, William P. Johnson, Bruce Arey, A. Scott Lea, and Anne J. Anderson. 2012. "Nanospecific Inhibition of Pyoverdine Siderophore Production in Pseudomonas Chlororaphis O6 by CuO Nanoparticles." Chemical Research in Toxicology

25(5):1066–74.

Dimkpa, Christian O., Jia Zeng, Joan E. McLean, David W. Britt, Jixun Zhan, and Anne J. Anderson. 2012. "Production of Indole-3-Acetic Acid via the Indole-3-Acetamide Pathway in the Plant-Beneficial Bacterium Pseudomonas Chlororaphis O6 Is Inhibited by ZnO Nanoparticles but Enhanced by CuO Nanoparticles." Applied and Environmental Microbiology 78(5):1404–10.

Ellis, T. N. and M. J. Kuehn. 2010. "Virulence and Immunomodulatory Roles of Bacterial Outer Membrane Vesicles." Microbiology and Molecular Biology Reviews 74(1):81–94.

Flemming, Hans Curt and Jost Wingender. 2010. "The Biofilm Matrix." Nature Reviews Microbiology 8(9):623–33.

Gade, Aniket, Joshua Adams, David W. Britt, Fen Ann Shen, Joan E. McLean, Astrid Jacobson, Young Cheol Kim, and Anne J. Anderson. 2016. "Ag Nanoparticles Generated Using Bio-Reduction and -Coating Cause Microbial Killing without Cell Lysis." BioMetals 29(2):211–23.

Gorringe, Andrew, Denise Halliwell, Mary Matheson, Karen Reddin, Michelle Finney, and Michael Hudson. 2005. "The Development of a Meningococcal Disease Vaccine Based on Outer Membrane Vesicles." Vaccine 23(17–18):2210–13.

Grande, Rossella, Maria C. Di Marcantonio, Iole Robuffo, Arianna Pompilio, Christian Celia, Luisa Di Marzio, Donatella Paolino, Marilina Codagnone, Raffaella Muraro, Paul Stoodley, Luanne Hall-Stoodley, and Gabriella Mincione. 2015. "Helicobacter Pylori ATCC 43629/NCTC 11639 Outer Membrane Vesicles (OMVs) from Biofilm and Planktonic Phase Associated with Extracellular DNA (EDNA)." Frontiers in Microbiology 6(DEC).

Hanson, Cynthia, Morgan M. Bishop, Jacob T. Barney, and Elizabeth Vargis. 2019. "Effect of Growth Media and Phase on Raman Spectra and Discrimination of Mycobacteria." Journal of Biophotonics.

Harz, M., P. Rösch, and J. Popp. 2009. "Vibrational Spectroscopy-A Powerful Tool for the Rapid Identification of Microbial Cells at the Single-Cell Level." Cytometry Part A 75(2):104–13.

Haurat, M. Florencia, Wael Elhenawy, and Mario F. Feldman. 2015. "Prokaryotic Membrane Vesicles: New Insights on Biogenesis and Biological Roles." Biological Chemistry 396(2):95–109.

Horstman, Amanda L. and Meta J. Kuehn. 2000. "Enterotoxigenic Escherichia Coli Secretes Active Heat-Labile Enterotoxin via Outer Membrane Vesicles." Journal of Biological Chemistry 275(17):12489–96.

Huang, Wei E., Mengqiu Li, Roger M. Jarvis, Royston Goodacre, and Steven A. Banwart. 2010. "Shining Light on the Microbial World the Application of Raman Microspectroscopy." Advances in Applied Microbiology 70:153–86.

Huefner, Anna, Wei Li Kuan, Karin H. Müller, Jeremy N. Skepper, Roger A. Barker, and Sumeet Mahajan. 2016. "Characterization and Visualization of Vesicles in the Endo-Lysosomal Pathway with Surface-Enhanced Raman Spectroscopy and Chemometrics." ACS Nano 10(1):307–16.

Hughes, David T. and Vanessa Sperandio. 2008. "Inter-Kingdom Signalling: Communication between Bacteria and Their Hosts." Nature Reviews Microbiology 6(February):111–20.

Ionescu, Michael, Paulo A. Zaini, Clelia Baccari, Sophia Tran, Aline M. da Silva, and Steven E. Lindow. 2014. "Xyllela Fastidiosa Outer Membrane Vesicles Modulate Plant Colonization by Blocking Attachment to Surfaces." Proceedings of the National Academy of Sciences 111(37):E3910–18.

Jacobson, Astrid, Stephanie Doxey, Matthew Potter, Joshua Adams, David Britt, Paul McManus, Joan McLean, and Anne Anderson. 2018. "Interactions between a Plant Probiotic and Nanoparticles on Plant Responses Related to Drought Tolerance." Industrial Biotechnology 14(3):148–56.

Kadurugamuwa, Jagath L. and Terry J. Beveridge. 1996. "Bacteriolytic Effect of Membrane Vesicles from Pseudomonas Aeruginosa on Other Bacteria Including Pathogens: Conceptually New Antibiotics." Journal of Bacteriology 178(10):2767–74.

Katsir, Leron and Ofir Bahar. 2017. "Bacterial Outer Membrane Vesicles at the Plant–Pathogen Interface." PLOS Pathogens 13(6):e1006306.

Khan, M. Nasir, M. Mobin, Zahid Khorshid Abbas, Khalid A. AlMutairi, and Zahid H. Siddiqui. 2017. "Role of Nanomaterials in Plants under Challenging Environments." Plant Physiology and Biochemistry 110:194–209.

Kim, Ji Hyun, Jaewook Lee, Jaesung Park, and Yong Song Gho. 2015. "Gram-Negative and Gram-Positive Bacterial Extracellular Vesicles." Seminars in Cell and Developmental Biology 40:97–104.

Kim, Ji Soo, Yong Hwan Kim, Ju Yeon Park, Anne J. Anderson, and Young Cheol Kim. 2014. "The Global Regulator GacS Regulates Biofilm Formation in Pseudomonas Chlororaphis O6

Differently with Carbon Source." Canadian Journal of Microbiology 60(3):133–38.

Kim, Sally Yunsun, Dipesh Khanal, Bill Kalionis, and Wojciech Chrzanowski. 2019. "High-Fidelity Probing of the Structure and Heterogeneity of Extracellular Vesicles by Resonance-Enhanced Atomic Force Microscopy Infrared Spectroscopy." Nature Protocols 14(2):576–93.

Koeppen, Katja, Thomas H. Hampton, Michael Jarek, Maren Scharfe, Scott A. Gerber, Daniel W. Mielcarz, Elora G. Demers, Emily L. Dolben, John H. Hammond, Deborah A. Hogan, and Bruce A. Stanton. 2016. "A Novel Mechanism of Host-Pathogen Interaction through SRNA in Bacterial Outer Membrane Vesicles." PLoS Pathogens 12(6):1–22.

Krafft, Christoph, Konrad Wilhelm, Anna Eremin, Sigrun Nestel, Nikolas von Bubnoff, Wolfgang Schultze-Seemann, Juergen Popp, and Irina Nazarenko. 2016. "A Specific Spectral Signature of Serum and Plasma-Derived Extracellular Vesicles for Cancer Screening." Nanomedicine: Nanotechnology, Biology and Medicine 13(3):835–41.

Kulp, Adam and Meta J. Kuehn. 2010. "Biological Functions and Biogenesis of Secreted Bacterial Outer Membrane Vesicles." Annual Review of Microbiology 64(1):163–84.

Lekmeechai, Sujinna, Yu Ching Su, Marta Brant, Maria Alvarado-Kristensson, Anna Vallström, Ikenna Obi, Anna Arnqvist, and Kristian Riesbeck. 2018. " Helicobacter Pylori Outer Membrane Vesicles Protect the Pathogen from Reactive Oxygen Species of the Respiratory Burst." Frontiers in Microbiology 9(SEP):1–6.

Li, Z., A. J. Clarke, and T. J. Beveridge. 1998. "Gram-Negative Bacteria Produce Membrane Vesicles Which Are Capable of Killing Other Bacteria." Journal of Bacteriology 180(20):5478–83.

Liu, Ruiqiang and Rattan Lal. 2015. "Potentials of Engineered Nanoparticles as Fertilizers for Increasing Agronomic Productions." Science of the Total Environment 514:131–39.

MacDonald, Ian A. and Meta J. Kuehn. 2013. "Stress-Induced Outer Membrane Vesicle Production by Pseudomonas Aeruginosa." Journal of Bacteriology 195(13):2971–81.

Malabirade, Antoine, Janine Habier, Anna Heintz-Buschart, Patrick May, Julien Godet, Rashi Halder, Alton Etheridge, David Galas, Paul Wilmes, and Joëlle V. Fritz. 2018. "The RNA Complement of Outer Membrane Vesicles from Salmonella Enterica Serovar Typhimurium under Distinct Culture Conditions." Frontiers in Microbiology 9(AUG):1–21.

Manning, Andrew J. and Meta J. Kuehn. 2011. "Contribution of Bacterial Outer Membrane Vesicles to Innate Bacterial Defense." BMC Microbiology 11(1):258.

Marslin, Gregory, Caroline J. Sheeba, and Gregory Franklin. 2017. "Nanoparticles Alter Secondary Metabolism in Plants via ROS Burst." Frontiers in Plant Science 8(May):1–8.

Mashburn-Warren, Lauren, Jörg Howe, Patrick Garidel, Walter Richter, Frank Steiniger, Manfred Roessle, Klaus Brandenburg, and Marvin Whiteley. 2008. "Interaction of Quorum Signals with Outer Membrane Lipids: Insights into Prokaryotic Membrane Vesicle Formation." Molecular Microbiology 69(2):491–502.

Mashburn, Lauren M. and Marvin Whiteley. 2005. "Membrane Vesicles Traffic Signals and Facilitate Group Activities in a Prokaryote." Nature 437(7057):422–25.

McBroom, Amanda J. and Meta J. Kuehn. 2007. "Release of Outer Membrane Vesicles by Gram-Negative Bacteria Is a Novel Envelope Stress Response." Molecular Microbiology 63(2):545–58.

McMahon, Kenneth J., Maria E. Castelli, Eleonora García Vescovi, and Mario F. Feldman. 2012. "Biogenesis of Outer Membrane Vesicles in Serratia Marcescens Is Thermoregulated and Can Be Induced by Activation of the Rcs Phosphorelay System." Journal of Bacteriology 194(12):3241–49.

Menges, Friedrich. 2019. "Spectragryph."

Momen-Heravi, Fatemeh, Leonora Balaj, Sara Alian, John Tigges, Vasilis Toxavidis, Maria Ericsson, Robert J. Distel, Alexander R. Ivanov, Johan Skog, and Winston Patrick Kuo. 2012. "Alternative Methods for Characterization of Extracellular Vesicles." Frontiers in Physiology 3(September):1–8.

Pradenas, Gonzalo A., Braulio A. Paillavil, Sebastián Reyes-Cerpa, José M. Pérez-Donoso, and Claudio C. Vásquez. 2012. "Reduction of the Monounsaturated Fatty Acid Content of Escherichia Coli Results in Increased Resistance to Oxidative Damage." Microbiology 158(5):1279–83.

Remis, Jonathan P., Dongguang Wei, Amita Gorur, Marcin Zemla, Jessica Haraga, Simon Allen, H. Ewa Witkowska, J. William Costerton, James E. Berleman, and Manfred Auer. 2014. "Bacterial Social Networks: Structure and Composition of Myxococcus Xanthus Outer Membrane Vesicle Chains." Environmental Microbiology 16(2):598–610.

Renelli, Marika, Valério Matias, Reggie Y. Lo, and Terry J. Beveridge. 2004. "DNA-Containing Membrane Vesicles of Pseudomonas Aeruginosa PAO1 and Their Genetic Transformation Potential." Microbiology 150(7):2161–69.

Schaar, Viveka, Therése Nordström, Matthias Mörgelin, and Kristian Riesbeck. 2011. "Moraxella Catarrhalis Outer Membrane Vesicles Carry β-Lactamase and Promote Survival of Streptococcus Pneumoniae and Haemophilus Influenzae by Inactivating Amoxicillin." Antimicrobial Agents and Chemotherapy 55(8):3845–53.

Schikora, Adam, Sebastian T. Schenk, and Anton Hartmann. 2016. "Beneficial Effects of Bacteria-Plant Communication Based on Quorum Sensing Molecules of the N-Acyl Homoserine Lactone Group." Plant Molecular Biology 90(6):605–12.

Schooling, Sarah R. and Terry J. Beveridge. 2006. "Membrane Vesicles: An Overlooked Component of the Matrices of Biofilms." Journal of Bacteriology 188(16):5945–57.

Schwechheimer, Carmen and Meta J. Kuehn. 2015. "Outer-Membrane Vesicles from Gram-Negative Bacteria: Biogenesis and Functions." Nature Reviews Microbiology 13(10):605–19.

Sekhon, Bhupinder Singh. 2014. "Nanotechnology in Agri-Food Production : An Overview." Nanotechnology, Science and Applications 7:31–53.

Spencer, Matthew, Choong-Min Ryu, Kwang Yeol Yang, Young Cheol Kim, Joseph W. Kloepper, and Anne J. Anderson. 2003. "Induced Defence in Tobacco by Pseudomonas Chlororaphis Strain O6 Involves at Least the Ethylene Pathway." Physiological and Molecular Plant Pathology 63(1):27–34.

Surapaneni, Meghana, Prachi Kabra, Swati Chakraborty, and Padmavathy Nagarajan. 2012. "Understanding the Pathway of Antibacterial Activity of Copper Oxide Nanoparticles." RCS Advanced.

Swain, R. J. and M. M. Stevens. 2007. "Raman Microspectroscopy for Non-Invasive Biochemical Analysis of Single Cells." Biochemical Society Transactions 35(3):544–49.

Tatischeff, Irène, Eric Larquet, Juan M. Falcón-Pérez, Pierre-Yves Turpin, and Sergei G. Kruglik. 2012. "Fast Characterisation of Cell-Derived Extracellular Vesicles by Nanoparticles Tracking Analysis, Cryo-Electron Microscopy, and Raman Tweezers Microspectroscopy." Journal of Extracellular Vesicles 1(1):19179.

Timmusk, Salme, Seong Bin Kim, Eviatar Nevo, Islam Abd El Daim, Bo Ek, Jonas Bergquist, and Lawrence Behers. 2015. "Sfp-Type PPTase Inactivation Promotes Bacterial Biofilm Formation and Ability to Enhance Wheat Drought Tolerance." Frontiers in Microbiology 6(MAY):1–13.

Wang, Wendong, Warren Chanda, and Mintao Zhong. 2015. "The Relationship between Biofilm and Outer Membrane Vesicles: A Novel Therapy Overview." FEMS Microbiology Letters 362(15):1–6.

van de Waterbeemd, Bas, Gijsbert Zomer, Jan van den IJssel, Lonneke van Keulen, Michel H. Eppink, Peter van der Ley, and Leo A. van der Pol. 2013. "Cysteine Depletion Causes Oxidative Stress and Triggers Outer Membrane Vesicle Release by Neisseria Meningitidis; Implications for Vaccine Development." PLoS ONE 8(1).

Whitchurch, Cynthia B., Tim Tolker-Nielsen, Paula C. Ragas, and John S. Mattick. 2002. "Extracellular DNA Required for Bacterial Biofilm Formation." Science 295(5559):1487.

Yáñez-Mó, María, Pia R. M. Siljander, Andreu Zoraida, Apolonija Bedina Zavec, Francesc E. Borràs, Edit I. Buzas, Krisztina Buzas, Enriqueta Casal, Francesco Cappello, Joana Carvalho, Eva Colás, Anabela Cordeiro-Da Silva, Stefano Fais, Juan M. Falcon-Perez, Irene M. Ghobrial, Bernd Giebel, Mario Gimona, Michael Graner, Ihsan Gursel, Mayda Gursel, Niels H. H. Heegaard, An Hendrix, Peter Kierulf, Katsutoshi Kokubun, Maja Kosanovic, Veronika Kralj-Iglic, Eva Maria Krämer-Albers, Saara Laitinen, Cecilia Lässer, Thomas Lener, Erzsébet Ligeti, Aija Line, Georg Lipps, Alicia Llorente, Jan Lötvall, Mateja Manček-Keber, Antonio Marcilla, Maria Mittelbrunn, Irina Nazarenko, Esther N. M. Nolte-'t Hoen, Tuula A. Nyman, Lorraine O'Driscoll, Mireia Olivan, Carla Oliveira, Éva Pállinger, Hernando A. Del Portillo, Jaume Reventós, Marina Rigau, Eva Rohde, Marei Sammar, Francisco Sánchez-Madrid, N. Santarém, Katharina Schallmoser, Marie Stampe Ostenfeld, Willem Stoorvogel, Roman Stukelj, Susanne G. Van Der Grein, M. Helena Vasconcelos, Marca H. M. Wauben, and Olivier De Wever. 2015. "Biological Properties of Extracellular Vesicles and Their Physiological Functions." Journal of Extracellular Vesicles 4(2015):1–60.

Yang, Kwang Yeol, Stephanie Doxey, Joan E. McLean, David Britt, Andre Watson, Dema Al Qassy, Astrid Jacobson, and Anne J. Anderson. 2018. "Remodeling of Root Morphology by CuO and

ZnO Nanoparticles: Effects on Drought Tolerance for Plants Colonized by a Beneficial Pseudomonad." Botany 96:175–86.

Yonezawa, Hideo, Takako Osaki, Satoshi Kurata, Minoru Fukuda, Hayato Kawakami, Kuniyasu Ochiai, Tomoko Hanawa, and Shigeru Kamiya. 2009. "Outer Membrane Vesicles of Helicobacter Pylori TK1402 Are Involved in Biofilm Formation." BMC Microbiology 9:1–12.

Zhou, Leah, Ratchapin Srisatjaluk, D. E. Justus, and R. J. Doyle. 1998. "On the Origin of Membrane Vesicles in Gram-Negative Bacteria." FEMS Microbiology Letters 163(2):223–28.

CHAPTER 5

CONCLUSIONS AND FUTURE WORK

Summary

The goal of this research was to understand the potential of CuO nanoparticles (NPs) in protecting wheat from abiotic stresses by studying the effects of CuO NPs on wheat seedlings and a beneficial rhizobacterium, *Pseudomonas chlororaphis* O6 (*Pc*O6). Three specific aims were developed from this overarching goal for this thesis: 1) investigate the effects of CuO NPs on wheat seedling lignification, 2) investigate the effects of CuO NPs on wheat seedling drought tolerance, and 3) investigate the effects of CuO NPs on outer membrane vesicle (OMV) formation by *Pc*O6.

Effects of CuO nanoparticles on wheat seedling lignification

Lignin stains showed that wheat seedlings exposed to CuO NPs (10 and 300 mg Cu/kg growth medium) have higher lignin content in the leaf sclerenchyma cells. This finding is significant as the sclerenchyma cells are considered the primary strengthening tissue of the plant. Leaves of wheat exposed to CuO NPs (300 mg Cu/kg) showed a 12% higher ultimate tensile strength and 17% higher toughness than wheat without NPs (ANOVA with posthoc student t-test p-value $\ll 0.05$). CuO NP-induced lignification has advantages over the creation of new cultivars with higher lignin content, which is a time-consuming trial-and-error process.

Effects of CuO nanoparticles on wheat seedling drought tolerance

Methods were developed to quantify wheat seedling drought tolerance with leaf gas exchange and chlorophyll fluorescence. It was found that the chlorophyll

fluorescence parameters of F_v/F_m, a ratio of the maximum photosystem II activity, and

Φ_{PSII}, a ratio of the operating photosystem II activity, were the most reliable

measurements of drought response in wheat seedlings. Using chlorophyll fluorescence

parameters, three wheat growth studies were performed to determine the effect of CuO

NPs on wheat. Low CuO NP dosages had no statistically significant effect on wheat

seedling drought tolerance under these experimental conditions (restricted maximum

likelihood p-value > 0.05). While CuO NPs did not enhance wheat seedling drought

tolerance under these conditions, these CuO NP dosages exhibited no apparent phytotoxic

effects and may be employed as fungicides, micronutrient sources, and other agricultural

applications without negative effects on wheat growth.

<u>Effects of CuO nanoparticles on outer membrane vesicle formation</u>

It was evident from atomic force microscopy (AFM) images that OMVs have

aggregative properties. This property was observed in AFM and SEM images of *Pc*O6

where OMVs were visible and in images of purified OMVs. Individual OMVs in AFM

images measured 40-100 nm in diameter. DLS results showed evidence of OMV

aggregation also, as hydrodynamic diameters ranged from 40-300 nm. OMV aggregation

has been observed in OMVs of other bacteria and may be related to biofilm formation.

Raman spectroscopy coupled with linear discriminant analysis (LDA) was able to

differentiate *Pc*O6 cells according to the stressor with an 83.3% accuracy. Comparing

spectra of *Pc*O6 cells and OMVs: 27 peaks are unique for *Pc*O6 cells, 14 are unique to

purified OMVs, and 10 peaks are shared. For shared peaks, the intensity of these peaks is

usually greater in purified OMVs. These results show that certain *Pc*O6 cell components

are enriched in OMVs while others are excluded, a finding reported in other Gram-

negative bacteria. Raman spectra also implied a high concentration of nucleic acids in OMVs which was confirmed by measuring OMV 260/280 ratios, a ratio of the concentration of nucleic acids (which absorb light at 260 nm) to the concentration of proteins (which absorb light at 280 nm).

Raman spectroscopy of OMVs showed high chemical heterogeneity. However, Raman spectroscopy coupled with LDA still discriminated OMVs according to the cellular stressor with a 77.1% accuracy. Nucleic acid peaks of OMVs were further increased in those OMVs isolated from cells exposed to CuO NPs or H_2O_2, which may indicate changes in signaling between bacteria.

Conclusions

<u>Copper oxide nanoparticles and wheat leaf lignification</u>

CuO NPs increased lignin content in wheat seedling leaf sclerenchyma cells which corresponded with increased ultimate tensile strength and toughness. Increased lignin content is correlated with increased to lodging in mature wheat (Zheng et al. 2017) and increased resistance to pathogens in other crops (Hammerschmidt and Kuć 1982). These results are promising, but several questions need answers before CuO NP-induced lignification be considered for agriculture.

Lodging is a concern for mature wheat, not wheat seedlings. It will be important to see if these early differences in lignification between wheat with and without exposure to CuO NPs are still significantly different at later growth stages. Additionally, no bulk or ionic controls were used in these studies and the number of CuO NP doses were limited (0, 10, and 300 mg Cu/kg for lignin staining tests; 0 and 300 mg Cu/kg for tensile tests). A larger number of CuO NP dosages should be used centered around more realistic field

application rates. Bulk and ionic controls may then be applied to test whether the observed results are truly NP effects or a result of Cu ion release from the NPs.

<u>Copper oxide nanoparticles and wheat seedling drought tolerance</u>

Under the studied conditions, CuO NPs did not affect wheat seedling drought tolerance. These results conflict with previous data published by our research group where multiple genes relating to water stress tolerance were upregulated in wheat exposed to CuO NPs and *Pc*O6 (Yang et al. 2018). There are several potential reasons for the discrepancies between these studies.

These transcriptional level changes may not be measurable in wheat until later stages of growth. Different CuO NP dosages were used in each study: Yang et al. used 0 and 300 mg Cu/kg whereas the studies in chapter 3 used a range of concentrations from 0 to 30 mg Cu/kg. The presence *of Pc*O6, which was applied to the seeds in both studies, may also explain why no changes were seen in wheat seedling drought tolerance when exposed to CuO NPs. *Pc*O6 promotes drought tolerance in crops primarily through the release of 2R,3R-butanediol that triggers stomatal closure in plants (Cho et al., 2008), and formation of a biofilm matrix on the plant root (Kim et al., 2014; Jacobson et al., 2018) which may help maintain moisture around plant roots (Costa, Raaijmakers, and Kuramae 2018; Timmusk et al. 2015). Perhaps this plant-health-promoting bacterium overshadowed any change in drought tolerance due to the CuO NP dosages applied.

Whether or not CuO NPs affect wheat drought tolerance, plant stand was noticeably improved for plants exposed to CuO NPs compared to plants without NPs during the early stages of drought. While promising, these observations are not necessarily NP effects. Additional ionic and bulk controls are necessary to show whether

these benefits are due to CuO NPs or simply due to the release of Cu ions.

Outer membrane vesicles

This first attempt to characterize OMVs of a plant-health-promoting bacterium showed that OMV contents and composition are affected by abiotic stress including CuO NP stress. Raman spectroscopy, coupled with LDA, was a valuable tool in discriminating between bacteria and OMVs according to the cellular stressor. The downstream effects of these findings require further investigation. It will be important to see what roles OMVs have in biofilm bacteria relationships and plant-bacteria relationships as well as how CuO NPs and other stressors may affect these relationships.

Future work

Copper oxide nanoparticle effects on plants and their mechanisms

Despite all of the positive effects seen with CuO NPs, the mechanisms behind these changes are still debated. NPs are known to alter gene expression in plants (Van Aken 2015) but the exact mechanisms behind these changes are not known with exactness. Furthermore, the mechanisms of NP uptake by plants are still not known with certainty although endocytosis pathways have been proposed (reviewed by Miralles, Church, and Harris 2012). The effects of NP dosage on NP-induced gene expression changes have not been well-studied which is troubling since NPs have differing dose-dependent toxicity according to size and chemical composition (Dimkpa et al. 2013).

Ionic copper and bulk copper oxide controls

To discern discrete nano-scale effects of CuO NPs, ionic Cu and bulk CuO controls need to be included at some stage of future CuO NP agricultural studies. It is

important to know whether or not CuO NP effects are truly NP effects or if these results are merely due to Cu ion release from the NPs. Comparisons with other metallic and non-metallic NPs will also be needed as CuO NPs are not the only NPs considered for agricultural applications. Drought studies using the same methods described in Chapter 3 using ZnO and SiO_2 NPs are already underway in our research group.

Soil studies of copper oxide nanoparticles

In further research into the use of CuO NPs in agriculture, soil studies will need to be performed. Though sand provides an ideal growth system for laboratory experiments, this model system is limited in representing wheat growth in agricultural fields. The complex structure, compositions, and microbiomes present different agriculture settings are all variables that will need to be considered in future studies.

Outer membrane vesicles of planktonic cells

Studies comparing OMVs harvested from PcO6 in a planktonic state and a biofilm state will be necessary as bacteria are present in both forms in the soil. Previous studies of other bacteria have shown that qualitative and quantitative differences are seen in OMVs produced by bacteria in these different phases (Grande et al. 2015; Schooling and Beveridge 2006). Nutrient availability also affects OMV formation (Klimentová and Stulík 2015; van de Waterbeemd et al. 2013). Therefore, studies into the effects of nutrition on OMV formation of PcO6 will also be needed including studies into the effects of different media types and changes in nutrients of defined media.

Roles and applications of outer membrane vesicles in the rhizosphere

The next step in the ongoing OMV research by our research group will be to

investigate the roles of OMVs in the rhizosphere. Understanding the roles of OMVs in the rhizosphere will show how these bacterial products may be applied in agriculture. *Pc*O6 is already included with several other soil bacteria isolates in a bioprotectant produced in South Korea (Anderson and Kim 2018). Perhaps OMVs could be used to induce plant immune responses and prevent infection by pathogens.

Research into the pathways of OMV production and OMV-mediated communication of *Pc*O6 will be required. To test the roles of OMVs in bacteria-bacteria communication by *Pc*O6, it will be necessary to test the effects of OMVs on doubling time. Doubling times may be measured by creating growth curves of *Pc*O6 cultures in liquid minimal medium. Cell density can be determined with absorbance readings at 600 nm. A calibration curve should be made beforehand to convert absorbance units to CFUs/mL. Doubling time and the onset of stationary phase by the bacteria can be determined with this method. OMVs are added at previously determined stages of growth. Changes in growth curves are then be compared. The effects of OMVs isolated from bacteria in differing conditions can be compared.

It will also be necessary to understand whether OMVs signal changes in the production of secondary metabolites during stationary phase. OMVs are added at previously determined stages of growth. Once *Pc*O6 cultures are at stationary phase for a set amount of time, absorbance and fluorescence spectroscopy are used to assess changes in the production of secondary metabolites including phenazines (absorbance of 367 nm (Kim et al. 2014)), and pyoverdines (fluorescence with 398 nm excitation and 430-540 nm emission (Anderson et al. 2017)). The effects of OMVs isolated from bacteria in differing conditions can be compared. Purified OMVs of all induction methods should

also be tested for the presence of these secondary metabolites.

To test the roles of OMVs in quorum sensing and biofilm formation, purified OMVs can be added to liquid cultures of WT *Pc*O6 and cultures of biofilm deficient *Pc*O6 mutants. Four mutants have already been obtained for these potential studies. The mutation protocols and first characterization tests of these mutants are included in Appendix B of this thesis.

Biofilm architecture and formation can be quantified using methods by J. S. Kim et al. (2014). After 4 days of growth in liquid medium, planktonic cells are removed by pipetting the liquid solution out of the container leaving only the biofilm cells. Wells are stained with 0.25% crystal violet that is then washed out with a set volume of ethanol. Absorbance readings at 570 nm are measured on all crystal violet solutions.

<u>Outer membrane vesicle-mediated cross-kingdom signaling</u>

OMVs are known to mediate cross-kingdom including between human pathogens and their hosts (Berleman and Auer 2013; Horstman and Kuehn 2000) and plant pathogens and their hosts (Katsir and Bahar 2017). It will be important to test whether OMVs of plant-health-promoting bacteria, including *Pc*O6, interact with plant hosts. This relationship may be studied using plants such as *Arabidopsis thaliana* either in laboratory conditions or with plant cell cultures. *A. thaliana* is ideal for such studies because the entire genome is known and assessing changes in gene expression is a simple task with that knowledge.

<u>Outer membrane vesicles in drug delivery</u>

The potential of cellular vesicles in drug delivery has long been discussed in the literature (Van Dommelen et al. 2012), including OMVs (Wang, Gao, and Wang 2019).

OMVs could be engineered to carry needed drugs in the human body through synthetic biological engineering, engineering bacteria to produce OMVs with specific qualities, or downstream processing, labeling, and modifying isolated OMVs. This approach was demonstrated in a study by Gujrati et al. (2014). *Escherichia coli* were engineered to have low pathogenicity and isolated OMVs were loaded with small interfering RNA through electroporation. The engineered OMVS were able to silence cancer cell genes and induced highly significant tumor regression in mice.

OMVs from soil bacteria, including *Pc*O6, may be ideal candidates for drug delivery as most soil bacteria exhibit low to no pathogenicity towards humans, although lipopolysaccharide on OMVs will still induce immune responses. This potential OMV application could be explored through the human immune responses to OMVs of soil bacteria. One experiment exposing mammalian cells to OMVs from *Pc*O6 has been performed (results in Appendix C of this thesis).

<u>Outer membrane vesicle isolation and purification</u>

If OMVs prove marketable and mass production is necessary, methods of production and isolation will need to be improved. Current methods outlined in Chapter 4 of this thesis are time-consuming and expensive and difficult to upscale. More efficient methods would be needed for manufacturing applications.

Tangential flow filtration may be a preferable method for the isolation of OMVs. This method would allow for easier upscale than current precipitation methods previously explained. Designing bioreactors specially designed to allow the release of OMVs from the batch while maintaining bacteria at stationary phase is another potential method. Such a bioreactor would likely need to use microfluidic chambers for the release of OMVs.

Though much more efficient than precipitation, these methods still do not separate OMVs from flagella, pili, secreted biomolecules, and other cellular debris. Affinity or gel chromatography are two potential solutions for the purification of OMVs from other cell components. These processes allow upscaling to manufacturing levels whereas density gradient ultracentrifugation is not easy to upscale due to the rotor speed required for this process.

References

Van Aken, Benoit. 2015. "Gene Expression Changes in Plants and Microorganisms Exposed to Nanomaterials." Current Opinion in Biotechnology 33:206–19.

Anderson, Anne J. and Young Cheol Kim. 2018. "Biopesticides Produced by Plant-Probiotic Pseudomonas Chlororaphis Isolates." Crop Protection 105(November 2017):62–69.

Anderson, Anne J., Joan E. McLean, Astrid R. Jacobson, and David W. Britt. 2017. "CuO and ZnO Nanoparticles Modify Interkingdom Cell Signaling Processes Relevant to Crop Production." Journal of Agricultural and Food Chemistry acs.jafc.7b01302.

Berleman, James and Manfred Auer. 2013. "The Role of Bacterial Outer Membrane Vesicles for Intra- and Interspecies Delivery." Environmental Microbiology 15(2):347–54.

Costa, Ohana Y. A., Jos M. Raaijmakers, and Eiko E. Kuramae. 2018. "Microbial Extracellular Polymeric Substances – Ecological Functions and Impact on Soil Aggregation." Frontiers in Microbiology 9(July):1636.

Dimkpa, Christian O., Drew E. Latta, Joan E. Mclean, David W. Britt, Maxim I. Boyanov, and Anne J. Anderson. 2013. "Fate of CuO and ZnO Nano and Micro Particles in the Plant Environment." Environmental Science & Technology 47:4734–42.

Van Dommelen, Susan M., Pieter Vader, Samira Lakhal, S. A. A. Kooijmans, Wouter W. Van Solinge, Matthew J. A. Wood, and Raymond M. Schiffelers. 2012. "Microvesicles and Exosomes: Opportunities for Cell-Derived Membrane Vesicles in Drug Delivery." Journal of Controlled Release 161(2):635–44.

Grande, Rossella, Maria C. Di Marcantonio, Iole Robuffo, Arianna Pompilio, Christian Celia, Luisa Di Marzio, Donatella Paolino, Marilina Codagnone, Raffaella Muraro, Paul Stoodley, Luanne Hall-Stoodley, and Gabriella Mincione. 2015. "Helicobacter Pylori ATCC 43629/NCTC 11639 Outer Membrane Vesicles (OMVs) from Biofilm and Planktonic Phase Associated with Extracellular DNA (EDNA)." Frontiers in Microbiology 6(DEC).

Gujrati, Vipul, Sunghyun Kim, Sang Hyun Kim, Jung Joon Min, Hyon E. Choy, Sun Chang Kim, and Sangyong Jon. 2014. "Bioengineered Bacterial Outer Membrane Vesicles as Cell-Specific Drug-Delivery Vehicles for Cancer Therapy." ACS Nano 8(2):1525–37.

Hammerschmidt, R. and J. Kuć. 1982. "Lignification as a Mechanism for Induced Systemic Resistance in Cucumber." Physiological Plant Pathology.

Horstman, Amanda L. and Meta J. Kuehn. 2000. "Enterotoxigenic Escherichia Coli Secretes Active Heat-Labile Enterotoxin via Outer Membrane Vesicles." Journal of Biological Chemistry 275(17):12489–96.

Katsir, Leron and Ofir Bahar. 2017. "Bacterial Outer Membrane Vesicles at the Plant–Pathogen Interface." PLOS Pathogens 13(6):e1006306.

Kim, Ji Soo, Yong Hwan Kim, Ju Yeon Park, Anne J. Anderson, and Young Cheol Kim. 2014. "The Global Regulator GacS Regulates Biofilm Formation in Pseudomonas Chlororaphis O6 Differently with Carbon Source." Canadian Journal of Microbiology 60(3):133–38.

Klimentová, Jana and Jiří Stulík. 2015. "Methods of Isolation and Purification of Outer Membrane Vesicles

from Gram-Negative Bacteria." *Microbiological Research* 170:1–9.

Miralles, Pola, Tamara L. Church, and Andrew T. Harris. 2012. "Toxicity, Uptake, and Translocation of Engineered Nanomaterials in Vascular Plants." *Environmental Science and Technology* 46(17):9224–39.

Schooling, Sarah R. and Terry J. Beveridge. 2006. "Membrane Vesicles: An Overlooked Component of the Matrices of Biofilms." *Journal of Bacteriology* 188(16):5945–57.

Timmusk, Salme, Seong Bin Kim, Eviatar Nevo, Islam Abd El Daim, Bo Ek, Jonas Bergquist, and Lawrence Behers. 2015. "Sfp-Type PPTase Inactivation Promotes Bacterial Biofilm Formation and Ability to Enhance Wheat Drought Tolerance." *Frontiers in Microbiology* 6(MAY):1–13.

Wang, Sihan, Jin Gao, and Zhenjia Wang. 2019. "Outer Membrane Vesicles for Vaccination and Targeted Drug Delivery." *Wiley Interdisciplinary Reviews: Nanomedicine and Nanobiotechnology* 11(2):1–16.

van de Waterbeemd, Bas, Gijsbert Zomer, Jan van den IJssel, Lonneke van Keulen, Michel H. Eppink, Peter van der Ley, and Leo A. van der Pol. 2013. "Cysteine Depletion Causes Oxidative Stress and Triggers Outer Membrane Vesicle Release by Neisseria Meningitidis; Implications for Vaccine Development." *PLoS ONE* 8(1).

Yang, Kwang Yeol, Stephanie Doxey, Joan E. McLean, David Britt, Andre Watson, Dema Al Qassy, Astrid Jacobson, and Anne J. Anderson. 2018. "Remodeling of Root Morphology by CuO and ZnO Nanoparticles: Effects on Drought Tolerance for Plants Colonized by a Beneficial Pseudomonad." *Botany* 96:175–86.

Zheng, Mengjing, Jin Chen, Yuhua Shi, Yanxia Li, Yanping Yin, Dongqing Yang, Yongli Luo, Dangwei Pang, Xu Xu, Wenqian Li, Jun Ni, Yuanyuan Wang, Zhenlin Wang, and Yong Li. 2017. "Manipulation of Lignin Metabolism by Plant Densities and Its Relationship with Lodging Resistance in Wheat." *Scientific Reports*.

CHAPTER 6

ENGINEERING SIGNIFICANCE

Copper oxide nanoparticles in agriculture

The potential benefits of CuO nanoparticles (NPs) in agriculture are numerous. CuO NPs upregulate genes in wheat associated with the crop's ability to withstand stresses associated with drought (Yang et al. 2018). In Chapter 2 of this thesis, CuO NPs induced lignification of sclerenchyma cells, which can produce a more upright plant during drought stress. This lignification was quantified using tensile testing. The quantification of plant stand through Instron tensile strength measurements and calculation of the plant material toughness is a demonstration of engineering techniques and principles applied to a biological system, which is the definition of biological engineering.

Cu salts are often used as pesticides and the pesticidal potential of CuO NPs (Elmer and White 2016) and CuO NP composites (Cioffi et al. 2004; Esteban-Tejeda et al. 2009) have been well documented. Cu is also an essential micronutrient for plants and CuO NPs can serve as micronutrient sources (Monreal et al. 2016). The growth studies presented in this thesis used a model system, including a model microbiome, to more accurately study the influence of CuO NPs.

Most NP-agriculture studies ignore the crop microbiome, an important determinant of crop health and yield. Not only is this an oversight, but it prevents study into a potentially synergistic NP-crop-microbiome relationship. In chapter 3 of this thesis, it was observed that CuO NPs (0 to 30 mg Cu/kg) did not prevent *Pseudomonas chlororaphis* O6 (*Pc*O6), a plant-health-promoting bacterium, from colonizing wheat

seedling roots. Raman spectroscopy of *Pc*O6 cells in chapter 4 of this thesis revealed that the chemical profile of this bacterium was altered when exposed to CuO NPs. Other studies have observed that CuO NPs increase *Pc*O6 cell size (Bonebrake et al. 2018), decrease the production of the Fe-scavenging siderophore pyoverdine (Dimkpa, Mclean, et al. 2012), and increase the production of the plant growth regulator indole-3-acetic acid (Dimkpa, Zeng, et al. 2012). These changes are likely due to the ability of NPs to alter gene expression in microorganisms (Van Aken 2015). As NP-induced changes in *Pc*O6 and other plant-health-promoting microbes, NP formulations may be engineered that not only enhance crop health and yield but also increase microbiome activity that further strengthens these same crops.

NPs applied to crops may also be engineered to have specific plant-health-promoting properties. Altering surface properties of NPs through coatings may allow better adhesion to plant roots for soil-applied NPs or plant leaves for foliar-applied NPs. Abamectin, a pesticide, NPs with poly(lactic acid) coatings adsorbed to cucumber leaves (Yu et al. 2017). This adhesion prevents NP pesticides from being washed away in the rain which is a large source of pollution from traditional chemical pesticides (Sekhon 2014). Chitosan NPs can be coated with the essential plant nutrients N, P, and K (Corradini, de Moura, and Mattoso 2010) which may allow the slow and direct release of these macronutrients to the plant. The results presented in this thesis provide a foundation of native CuO NP interactions with wheat roots and root-colonizing beneficial bacteria. Using this basic systems biology model consisting of plant, microbiome, and engineered NP it has been established that for the investigated concentrations, commercial CuO NPs in a sand growth matrix do not inhibit seed germination or development of wheat

seedlings. The plant beneficial bacteria present in the sand growth matrix were also able

to thrive under the investigated CuO NP dosing. This is important in establishing a

baseline for CuO NP dosing and long-term growth studies in the lab and research fields,

before introduction to farms.

Upscaling NP applications for agriculture will have additional challenges. With

CuO NPs, one challenge to their agricultural application is soil Cu buildup. The use of Cu

in agriculture, primarily as a pesticide, has led to high Cu buildup in many crop fields

(Printz et al. 2016) which may prevent crop growth (Mengel and Kirkby 2001) and

greatly decreases soil microbial diversity (Nunes et al. 2016). One benefit of CuO NPs is

a less pronounced effect on agricultural fields than Cu ions. It has been demonstrated that

wheat has a higher toxicity threshold for CuO NPs than Cu ions (Adams et al. 2017).

*Pc*O6 also has a higher toxicity threshold for CuO NPs than Cu salts (Dimkpa et al.

2011). However, careless applications of CuO NPs that do not account for the soil

bioavailable Cu, the crop to be planted, and the soil microbial community will still lead to

toxic buildup of Cu.

Outer membrane vesicles

<u>Outer membrane vesicle characterization</u>

The results in chapter 4 of this thesis also have implications for OMV

characterization techniques. Raman spectroscopy proved to be a rapid and reproducible

method for characterizing OMVs and understanding their contents and composition.

Linear discriminant analysis of Raman spectra allowed classification of spectra and

showed that OMVs and *Pc*O6 cells had highly consistent chemical profiles according to

the cellular stressor. Raman spectroscopy has been used in the characterization of

eukaryotic extracellular vesicles (Huefner et al. 2016; Krafft et al. 2016; Tatischeff et al. 2012) but no current literature has used Raman spectroscopy for OMV characterization. Raman spectroscopy has the potential to be a first-line method for OMV characterization. Raman spectra can detect protein, lipid, nucleic acid, and carbohydrate signatures and these results may be used to determine which characterization methods are most valuable in subsequent experiments.

For example, if Raman spectra show high nucleic acid peaks then the step should identify whether these nucleic acids are present as DNA or RNA. The form of the DNA- which may be present in OMVs as plasmid DNA (Renelli et al. 2004), coding chromosomal DNA (Bitto et al. 2017), or noncoding environmental DNA (eDNA) (Whitchurch et al. 2002)- or RNA- which may be present in OMVs as ribosomal RNA, mRNA, and small RNAs (Malabirade et al. 2018)- will give insight as to how the bacteria uses OMVs. As another example, if OMV Raman spectra show different amino acid signatures or differing concentrations of those amino acids according to some environmental stimulus then protein identification through mass spectroscopy may be an appropriate next step. The identity of the proteins will lead to insight as to how the bacterium responds to differing environments.

Outer membrane vesicles and agriculture

Soil bacteria are known to communicate with host plants through various methods including hormones and quorum sensing molecules (Schikora, Schenk, and Hartmann 2016). OMVs are another potential communication method that remains largely unstudied for soil bacteria. Most OMV studies have a medical focus such as their role in host-pathogen interactions (Koeppen et al. 2016; Lekmeechai et al. 2018), and their

potential application in vaccines (Gorringe et al. 2005; Vianzon, Illek, and Moe 2017).

Research of OMVs from soil bacteria are few and focus on pathogenic bacteria (Bahar et

al. 2016; Katsir and Bahar 2017) including *Xyllela fastidiosa* (Ionescu et al. 2014),

Xanthomonas campestris (Sidhu et al. 2008; Solé et al. 2015), and *Pseudomonas syringae*

(Chowdhury and Jagannadham 2013). While important, these studies tell us little about

beneficial soil microbes which are important in agriculture as they impact crop quality

and yield (Dodd and Ruiz-Lozano 2012; Timmusk et al. 2017) and crop stress tolerance

(Kim et al. 2012; Wright et al. 2016).

In chapter 4 of this thesis, it was observed that *Pc*O6 secretes OMVs and that

OMV composition and contents varied according to the type of abiotic stressor. This first

step of understanding OMVs from plant-health-promoting bacteria is important however,

the roles of OMVs for beneficial bacteria still need analysis. Further studies will examine

potential OMV functions in biofilm formation and maintenance, communication between

microbes, DNA and RNA transfer, and communication with eukaryotic cells including

plant cells. This supports microbiome engineering to enhance plant vigor and agricultural

output.

As the OMV roles in soil bacteria are better understood, this research will lead to

research of potential OMV applications in agriculture. Several potential methods could be

used to apply OMVs to crop fields if this avenue of research proves profitable. Isolated

OMVs could be included in fertilizers and/or other soil amendments though more

inexpensive OMV isolation and purification processes would be needed. Another

potential use is including OMV-producing bacteria in these same soil amendments with

conditions engineered to cultivate increased OMV production. Soil amendments could

even contain factors that induce OMV production in naturally occurring soil bacteria in crop fields, which may be an unintended consequence of introducing engineered NPs such as CuO into agricultural settings.

Upscaling outer membrane vesicle isolation and purification

One difficulty experienced during the experiments detailed in chapter 4 of this thesis was the amount of time and effort required for OMV isolation and purification. Methods used were time-intensive: around 4 to 5 d elapsed from the time that *Pc*O6 was inoculated on solid media until purified OMVs were obtained. Furthermore, while methods used were acceptable for small-scale experiments, many methods are not easily upscaled including bacterial growth on solid medium, OMV concentration by precipitation, and OMV purification by density-gradient ultracentrifugation.

OMV precipitation can be upscaled to some degree, but other methods may be more appropriate for higher throughput. Ultrafiltration and density-gradient ultracentrifugation are standard methods for OMV concentration and isolation respectively, but these processes are difficult to economically upscale. Tangential flow filtration is perhaps the best option for high throughput processes. Gel filtration is also a commonly used OMV purification technique (Klimentová and Stulík 2015) and this technique can be upscaled for much higher throughput processes.

Bacterial growth is perhaps the easiest process to upscale as bioreactor growth is already widely practiced in the biotechnology industry. These instruments allow harvesting of various cellular products and OMVs should be no exception. OMVs could be harvested from planktonic bacteria that can be grown in continuously fed-batch bioreactors (Figure 6 - 1). Biofilm bacteria could also be grown with this assay if grown

on microbeads or encapsulated in alginate or other polymers. Another method for OMV

isolation from biofilm bacteria is growth in hollow fiber membrane bioreactors (Figure 6

- 2). Previously, our research group has demonstrated that *Pc*O6 grows robust,

multilayered biofilms on hollow fiber membranes (in the form of a root mimetic system)

and the biofilm density and properties, including the production of extracellular

polymeric substances, could be tuned through the growth medium composition

(Bonebrake et al. 2018). A similarly designed hollow fiber membrane bioreactor for

harvesting eukaryotic extracellular vesicles was recently proposed in a review by Patel et

al. 2018.
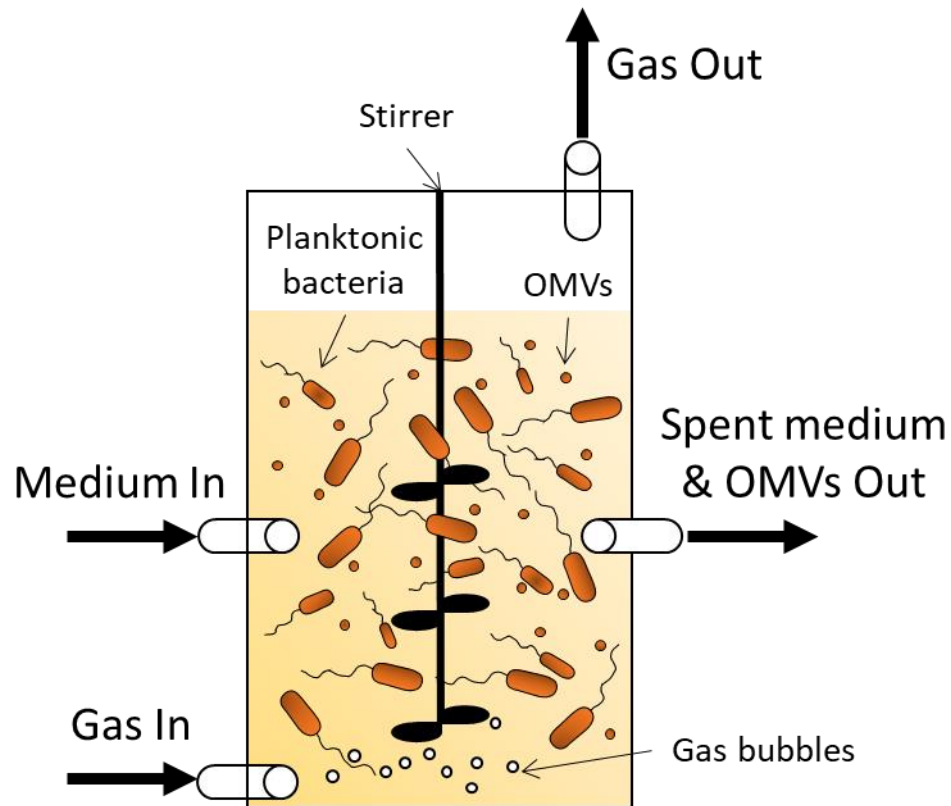
Figure 6 - 1: Diagram of a continuously fed-batch bioreactor that could be used for harvesting outer membrane vesicles.
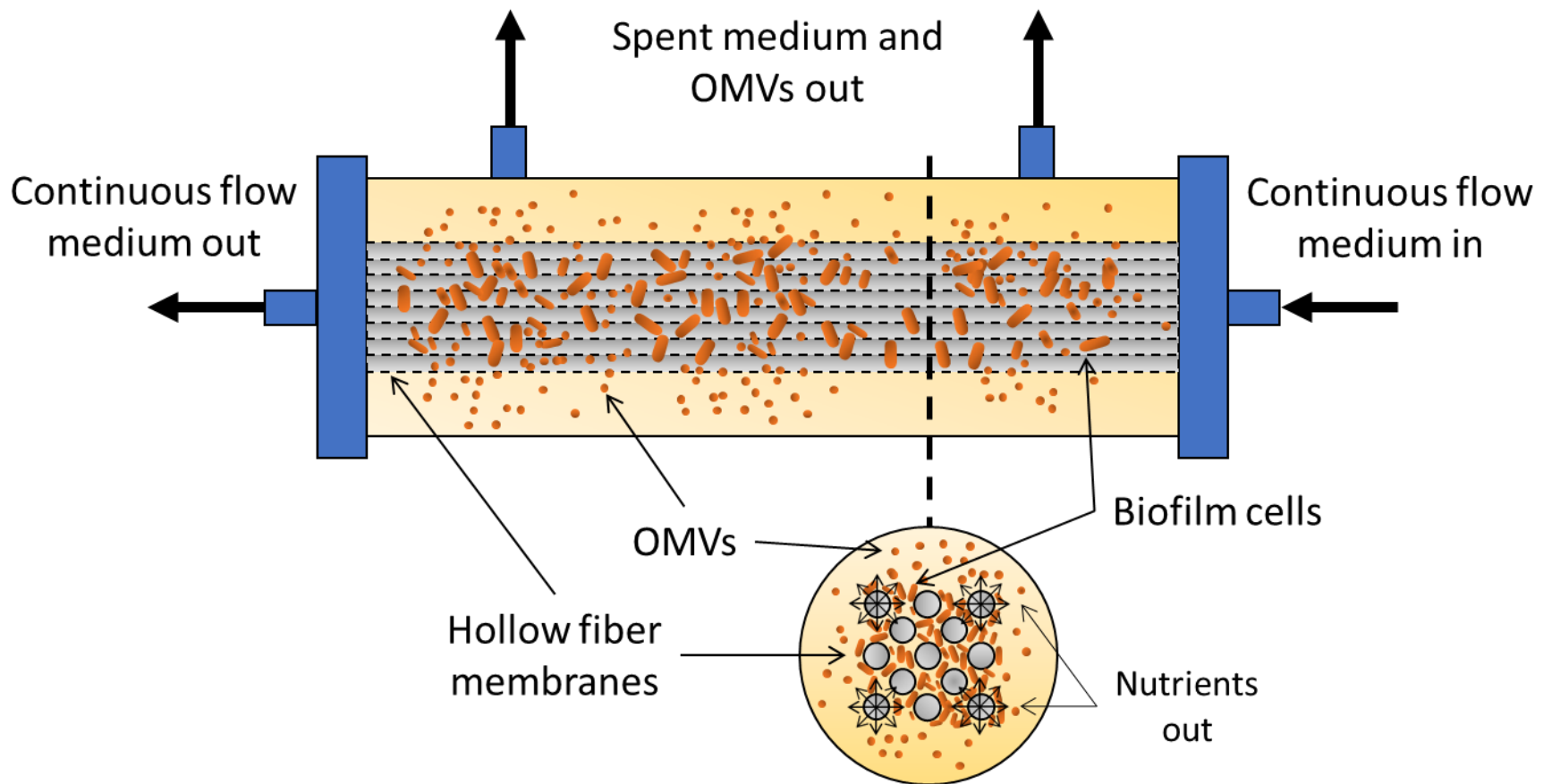
Figure 6 - 2: Diagram of a hollow fiber membrane bioreactor that could be used for harvesting outer membrane vesicles.

Conclusions

During my research, I have applied mathematics, material science, mass balances, downstream processing, and other engineering principles to biological systems in an attempt to add to the scientific body of knowledge. This work and the results I have seen with my own eyes has been exciting and led me to the decision to further my research as a Ph.D. student. I sincerely hope that this thesis will hold answers to other researchers' questions and guide them to novel discoveries and innovations in the fields of sustainable agriculture, nanotechnology, and microbiology.

References

Adams, Josh, Melanie Wright, Hannah Wagner, Jonathan Valiente, David Britt, and Anne Anderson. 2017. "Cu from Dissolution of CuO Nanoparticles Signals Changes in Root Morphology." Plant Physiology and Biochemistry 110:108–17.

Van Aken, Benoit. 2015. "Gene Expression Changes in Plants and Microorganisms Exposed to Nanomaterials." Current Opinion in Biotechnology 33:206–19.

Bahar, Ofir, Gideon Mordukhovich, Dee Dee Luu, Benjamin Schwessinger, Arsalan Daudi, Anna Kristina Jehle, Georg Felix, and Pamela C. Ronald. 2016. "Bacterial Outer Membrane Vesicles Induce Plant Immune Responses." Molecular Plant-Microbe Interactions 29(5):374–84.

Bitto, Natalie J., Ross Chapman, Sacha Pidot, Adam Costin, Camden Lo, Jasmine Choi, Tanya D'Cruze, Eric C. Reynolds, Stuart G. Dashper, Lynne Turnbull, Cynthia B. Whitchurch, Timothy P. Stinear, Katryn J. Stacey, and Richard L. Ferrero. 2017. "Bacterial Membrane Vesicles Transport Their DNA Cargo into Host Cells." Scientific Reports 7(1):1–11.

Bonebrake, Michelle, Kaitlyn Anderson, Jonathan Valiente, Astrid Jacobson, Joan E. McLean, Anne Anderson, and David W. Britt. 2018. "Biofilms Benefiting Plants Exposed to ZnO and CuO Nanoparticles Studied with a Root-Mimetic Hollow Fiber Membrane." Journal of Agricultural and Food Chemistry 66(26):6619–27.

Chowdhury, Chiranjit and Medicharla Venkata Jagannadham. 2013. "Virulence Factors Are Released in Association with Outer Membrane Vesicles of Pseudomonas Syringae Pv. Tomato T1 during Normal Growth." Biochimica et Biophysica Acta - Proteins and Proteomics 1834(1):231–39.

Cioffi, Nicola, Luisa Torsi, Nicoletta Ditaranto, Luigia Sabbatini, Pier Giorgio Zambonin, Giuseppina Tantillo, Lina Ghibelli, Maria D'Alessio, Teresa Bleve-Zacheo, and Enrico Traversa. 2004. "Antifungal Activity of Polymer-Based Copper Nanocomposite Coatings." Applied Physics Letters 85(12):2417–19.

Corradini, E., M. R. de Moura, and L. H. C. Mattoso. 2010. "A Preliminary Study of the Incorparation of NPK Fertilizer into Chitosan Nanoparticles." Express Polymer Letters 4(8):509–15.

Dimkpa, Christian O., Alyssa Calder, David W. Britt, Joan E. McLean, and Anne J. Anderson. 2011. "Responses of a Soil Bacterium, Pseudomonas Chlororaphis O6 to Commercial Metal Oxide Nanoparticles Compared with Responses to Metal Ions." Environmental Pollution 159(7):1749–56.

Dimkpa, Christian O., Joan E. Mclean, David W. Britt, and Anne J. Anderson. 2012. "CuO and ZnO Nanoparticles Differently Affect the Secretion of Fluorescent Siderophores in the Beneficial Root Colonizer, Pseudomonas Chlororaphis O6." Nanotoxicology 6(6):635–42.

Dimkpa, Christian O., Jia Zeng, Joan E. McLean, David W. Britt, Jixun Zhan, and Anne J. Anderson. 2012.

"Production of Indole-3-Acetic Acid via the Indole-3-Acetamide Pathway in the Plant-Beneficial Bacterium Pseudomonas Chlororaphis O6 Is Inhibited by ZnO Nanoparticles but Enhanced by CuO Nanoparticles." Applied and Environmental Microbiology 78(5):1404–10.

Dodd, Ian C. and Juan Manuel Ruiz-Lozano. 2012. "Microbial Enhancement of Crop Resource Use Efficiency." Current Opinion in Biotechnology 23(2):236–42.

Elmer, Wade H. and Jason C. White. 2016. "The Use of Metallic Oxide Nanoparticles to Enhance Growth of Tomatoes and Eggplants in Disease Infested Soil or Soilless Medium." Environmental Science: Nano 3(5):1072–79.

Esteban-Tejeda, L., F. Malpartida, A. Esteban-Cubillo, C. Pecharromn, and J. S. Moya. 2009. "Antibacterial and Antifungal Activity of a Soda-Lime Glass Containing Copper Nanoparticles." Nanotechnology 20.

Gorringe, Andrew, Denise Halliwell, Mary Matheson, Karen Reddin, Michelle Finney, and Michael Hudson. 2005. "The Development of a Meningococcal Disease Vaccine Based on Outer Membrane Vesicles." Vaccine 23(17–18):2210–13.

Huefner, Anna, Wei Li Kuan, Karin H. Müller, Jeremy N. Skepper, Roger A. Barker, and Sumeet Mahajan. 2016. "Characterization and Visualization of Vesicles in the Endo-Lysosomal Pathway with Surface-Enhanced Raman Spectroscopy and Chemometrics." ACS Nano 10(1):307–16.

Ionescu, Michael, Paulo A. Zaini, Clelia Baccari, Sophia Tran, Aline M. da Silva, and Steven E. Lindow. 2014. "Xyllela Fastidiosa Outer Membrane Vesicles Modulate Plant Colonization by Blocking Attachment to Surfaces." Proceedings of the National Academy of Sciences 111(37):E3910–18.

Katsir, Leron and Ofir Bahar. 2017. "Bacterial Outer Membrane Vesicles at the Plant–Pathogen Interface." PLOS Pathogens 13(6):e1006306.

Kim, Young Cheol, Bernard R. Glick, Yoav Bashan, and Choong-Min Ryu. 2012. "Enhancement of Plant Drought Tolerance by Microbes." Pp. 383–413 in Plant Responses to Drought Stress: From Morphological to Molecular Features. Vol. 9783642326.

Klimentová, Jana and Jiří Stulík. 2015. "Methods of Isolation and Purification of Outer Membrane Vesicles from Gram-Negative Bacteria." Microbiological Research 170:1–9.

Koeppen, Katja, Thomas H. Hampton, Michael Jarek, Maren Scharfe, Scott A. Gerber, Daniel W. Mielcarz, Elora G. Demers, Emily L. Dolben, John H. Hammond, Deborah A. Hogan, and Bruce A. Stanton. 2016. "A Novel Mechanism of Host-Pathogen Interaction through SRNA in Bacterial Outer Membrane Vesicles." PLoS Pathogens 12(6):1–22.

Krafft, Christoph, Konrad Wilhelm, Anna Eremin, Sigrun Nestel, Nikolas von Bubnoff, Wolfgang Schultze-Seemann, Juergen Popp, and Irina Nazarenko. 2016. "A Specific Spectral Signature of Serum and Plasma-Derived Extracellular Vesicles for Cancer Screening." Nanomedicine: Nanotechnology, Biology and Medicine 13(3):835–41.

Lekmeechai, Sujinna, Yu Ching Su, Marta Brant, Maria Alvarado-Kristensson, Anna Vallström, Ikenna Obi, Anna Arnqvist, and Kristian Riesbeck. 2018. " Helicobacter Pylori Outer Membrane Vesicles Protect the Pathogen from Reactive Oxygen Species of the Respiratory Burst." Frontiers in Microbiology 9(SEP):1–6.

Malabirade, Antoine, Janine Habier, Anna Heintz-Buschart, Patrick May, Julien Godet, Rashi Halder, Alton Etheridge, David Galas, Paul Wilmes, and Joëlle V. Fritz. 2018. "The RNA Complement of Outer Membrane Vesicles from Salmonella Enterica Serovar Typhimurium under Distinct Culture Conditions." Frontiers in Microbiology 9(AUG):1–21.

Mengel, Konrad and Ernest A. Kirkby. 2001. Principles of Plant Nutrition. 5th Editio. Springer Science.

Monreal, C. M., M. Derosa, S. C. Mallubhotla, P. S. Bindraban, and C. Dimkpa. 2016. "Nanotechnologies for Increasing the Crop Use Efficiency of Fertilizer-Micronutrients." Biology and Fertility of Soils 52(3):423–37.

Nunes, Inês, Samuel Jacquiod, Asker Brejnrod, Peter E. Holm, Anders Johansen, Kristian K. Brandt, Anders Priemé, and Søren J. Sørensen. 2016. "Coping with Copper: Legacy Effect of Copper on Potential Activity of Soil Bacteria Following a Century of Exposure." FEMS Microbiology Ecology 92(11):1–12.

Patel, Divya B., Marco Santoro, Louis J. Born, John P. Fisher, and Steven M. Jay. 2018. "Towards Rationally Designed Biomanufacturing of Therapeutic Extracellular Vesicles: Impact of the Bioproduction Microenvironment." Biotechnology Advances 36(8):2051–59.

Printz, Bruno, Stanley Lutts, Jean-Francois Hausman, and Kjell Sergeant. 2016. "Copper Trafficking in Plants and Its Implication on Cell Wall Dynamics." Frontiers in Plant Science 7(May):1–16.

Renelli, Marika, Valério Matias, Reggie Y. Lo, and Terry J. Beveridge. 2004. "DNA-Containing Membrane Vesicles of Pseudomonas Aeruginosa PAO1 and Their Genetic Transformation Potential." Microbiology 150(7):2161–69.

Schikora, Adam, Sebastian T. Schenk, and Anton Hartmann. 2016. "Beneficial Effects of Bacteria-Plant Communication Based on Quorum Sensing Molecules of the N-Acyl Homoserine Lactone Group." Plant Molecular Biology 90(6):605–12.

Sekhon, Bhupinder Singh. 2014. "Nanotechnology in Agri-Food Production : An Overview." Nanotechnology, Science and Applications 7:31–53.

Sidhu, Vishaldeep K., Frank-Jörg Vorhölter, Karsten Niehaus, and Steven A. Watt. 2008. "Analysis of Outer Membrane Vesicle Associated Proteins Isolated from the Plant Pathogenic Bacterium Xanthomonas Campestris Pv. Campestris." BMC Microbiology 8(1):87.

Solé, Magali, Felix Scheibner, Anne Katrin Hoffmeister, Nadine Hartmann, Gerd Hause, Annekatrin Rother, Michael Jordan, Martine Lautier, Matthieu Arlat, and Daniela Büttner. 2015. "Xanthomonas Campestris Pv. Vesicatoria Secretes Proteases and Xylanases via the Xps Type II Secretion System and Outer Membrane Vesicles." Journal of Bacteriology 197(17):2879–93.

Tatischeff, Irène, Eric Larquet, Juan M. Falcón-Pérez, Pierre-Yves Turpin, and Sergei G. Kruglik. 2012. "Fast Characterisation of Cell-Derived Extracellular Vesicles by Nanoparticles Tracking Analysis, Cryo-Electron Microscopy, and Raman Tweezers Microspectroscopy." Journal of Extracellular Vesicles 1(1):19179.

Timmusk, Salme, Lawrence Behers, Julia Muthoni, Anthony Muraya, and Anne-Charlotte Aronsson. 2017. "Perspectives and Challenges of Microbial Application for Crop Improvement." Frontiers in Plant Science 8(February):1–10.

Vianzon, Vianca, Beate Illek, and Gregory R. Moe. 2017. "Effect of Vaccine-Elicited Antibodies on Colonization of Neisseria Meningitidis Serogroup B and C Strains in a Human Bronchial Epithelial Cell Culture Model." Clinical and Vaccine Immunology 24(10):1–12.

Whitchurch, Cynthia B., Tim Tolker-Nielsen, Paula C. Ragas, and John S. Mattick. 2002. "Extracellular DNA Required for Bacterial Biofilm Formation." Science 295(5559):1487.

Wright, Melanie, Joshua Adams, Kwang Yang, Paul McManus, Astrid Jacobson, Aniket Gade, Joan McLean, David Britt, and Anne Anderson. 2016. "A Root-Colonizing Pseudomonad Lessens Stress Responses in Wheat Imposed by CuO Nanoparticles." PLoS ONE 11(10):1–19.

Yang, Kwang Yeol, Stephanie Doxey, Joan E. McLean, David Britt, Andre Watson, Dema Al Qassy, Astrid Jacobson, and Anne J. Anderson. 2018. "Remodeling of Root Morphology by CuO and ZnO Nanoparticles: Effects on Drought Tolerance for Plants Colonized by a Beneficial Pseudomonad." Botany 96:175–86.

Yu, Manli, Junwei Yao, Jie Liang, Zhanghua Zeng, Bo Cui, Xiang Zhao, Changjiao Sun, Yan Wang, Guoqiang Liu, and Haixin Cui. 2017. "Development of Functionalized Abamectin Poly(Lactic Acid) Nanoparticles with Regulatable Adhesion to Enhance Foliar Retention." RSC Advances 7(19):11271–80.

APPENDICES

APPENDIX A

SUPPLEMENTAL TABLES AND FIGURES
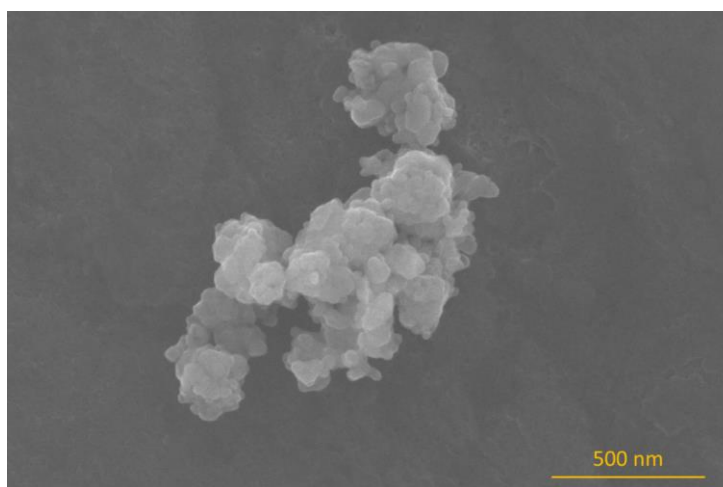
Figure A - 1: SEM image of CuO NPs. The scale bar is shown in the lower right corner. This image and other similar images were used to confirm the CuO NP size range given by the manufacturer.

Table A - 1: Compounds and dosages used in the full strength modified Hoagland's solution (Hoagland and Arnon 1950) ($FeCl_3$ was used as the Fe source). The solution was diluted to half strength for these studies. Concentrations in the half-strength solution are shown in the final column.

Compound	Stock solution	Stock/L of solution	Final Concentration (full strength)	Final Concentration (half strength)
KNO_3	202 g/L	2.5 mL	0.505 g/L	0.253g/L
$Ca(NO_3)_2*4H_2O$	472 g/L	2.5 mL	1.18 g/L	0.59 g/L
$MgSO_4*7H_2O$	493 g/L	1 mL	0.493 g/L	0.247 g/L
NH_4NO_3	80 g/L	1 mL	0.08 g/L	0.04 g/L
KH_2PO_4	136 g/L	0.5 mL	0.068 g/L	0.034 g/L
H_3BO_3	2.86 g/L	1 mL	0.00286 g/L	0.00143 g/L
$MnCl_2*4H_2O$	1.81 g/L	1 mL	0.00181 g/L	0.000905 g/L
$FeCl_3 * 6H_2O$	11.76 g/L	1.5 mL	0.0176 g/L	0.00880 g/L
$ZnSO_4*7H_2O$	0.22 g/L	1 mL	0.00022 g/L	0.00011 g/L
$CuSO_4*5H_2O$	0.051 g/L	1 mL	0.000051 g/L	0.000026 g/L
$Na_2MoO_4*2H_2O$	0.12 g/L	1 mL	0.00012 g/L	0.000060 g/L

Table A - 2: Statistical results for restricted maximum likelihood method analysis of the method for repeated measures from results from LI-6800 Portable Photosynthesis Unit chlorophyll fluorescence measurements during an 8 d period with or without drought following 14 d of growth.

Variable or interacting variables	Φ_{PSII}	F_v/F_m
CuO	0.2540	0.4671
Day	< 0.0001	< 0.0001
CuO*Day	0.3787	0.6459
Drought	< 0.0001	< 0.0001
Drought*CuO	0.0181	0.5411
Drought*Day	< 0.0001	< 0.0001
Drought*CuO*Day	0.3547	0.2449
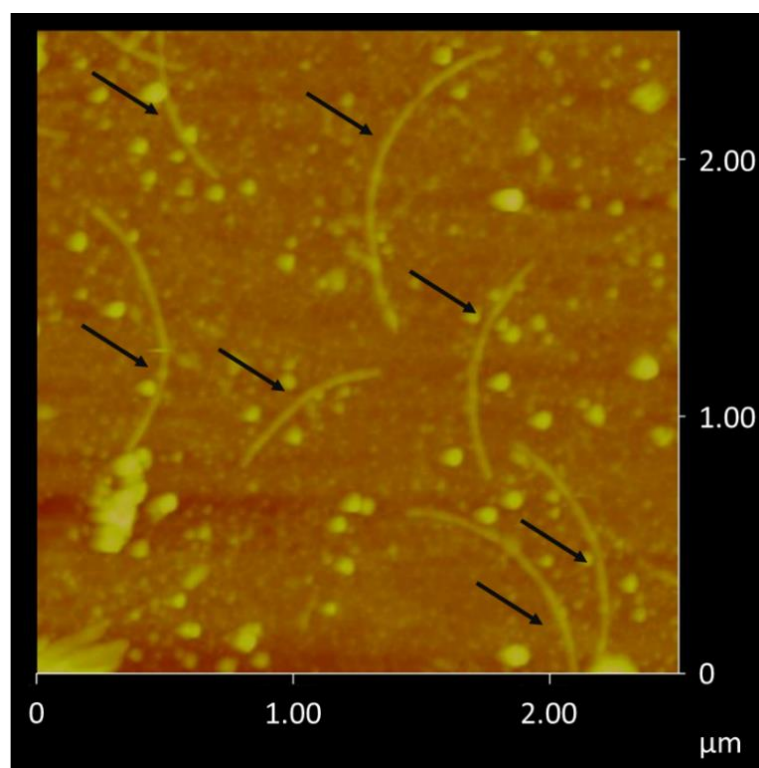
Figure A - 2: AFM topography image of an unpurified OMV suspension. Several flagella are visible, marked with black arrows. Pili and proteins are also present though these cell debris are indistinguishable from OMVs in this image. The x- and y- scales are indicated in the image. The z-scale is from red to yellow with 0 to 75 nm respectively.
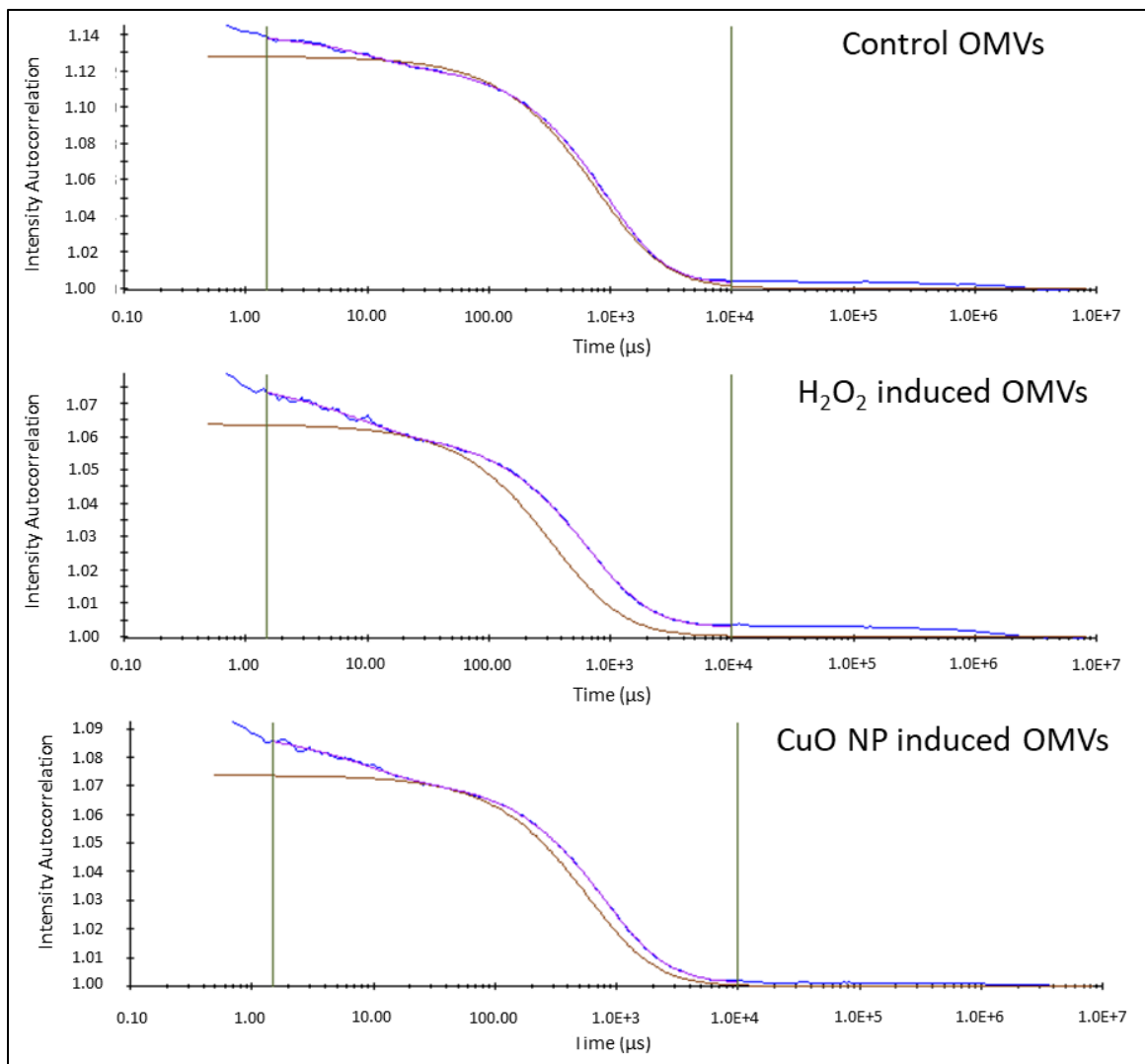
Figure A - 3: Autocorrelation graphs given by DLS during measurements of OMV size.
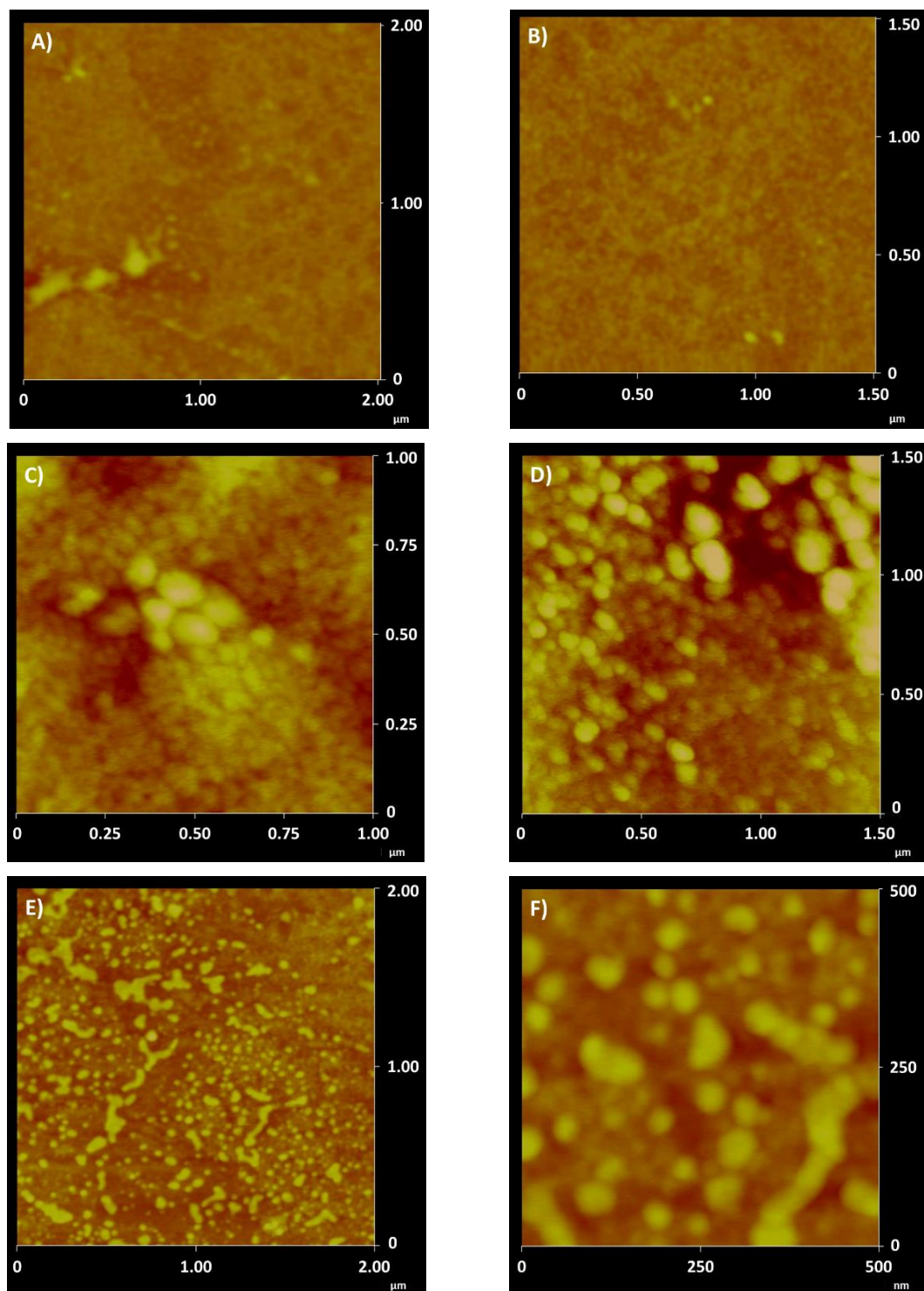
Figure A - 4: AFM height images of purified OMVs. X- and y- scales are indicated in each image. Z-scales are from red to yellow from 0 to 25 nm respectively. A) & B) OMVs harvested from *Pc*O6 without any stressors. C) & D) OMVs harvested from *Pc*O6 under H_2O_2 stress (3% v/v). E) & F) OMVs harvested from *Pc*O6 under CuO NP stress (30 mg Cu/L).
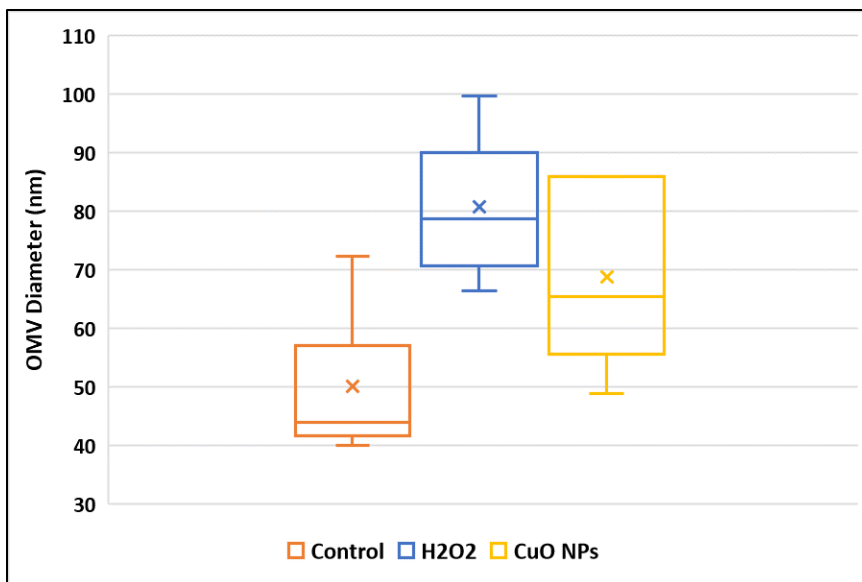
Figure A - 5: Size ranges of OMVs purified from *Pc*O6 cells subjected to the indicated stressors. Diameters measured by the AFM line cutting function (n=10).
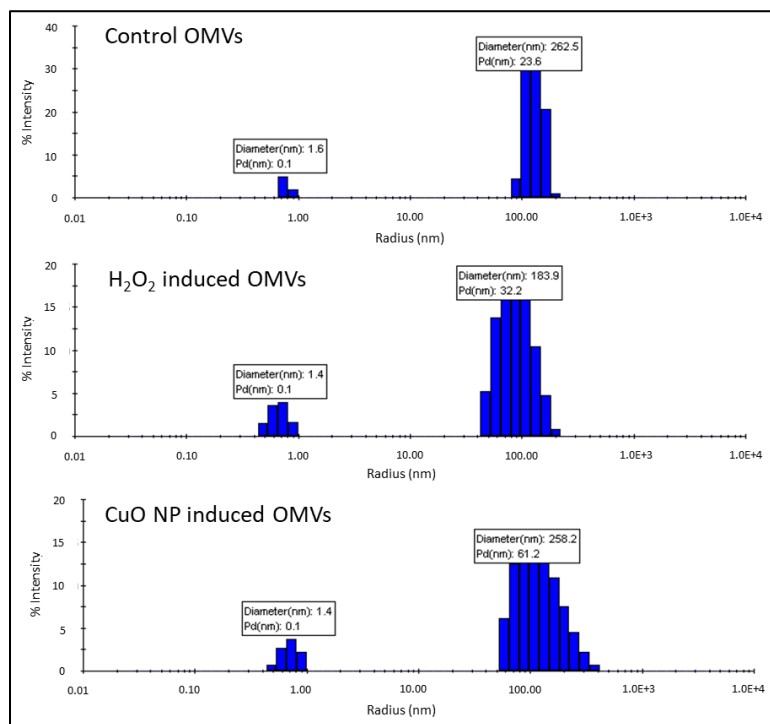
Figure A - 6: Dynamic light scattering measurements of OMVs

Table A - 3: Peaks from Raman spectra of intact PcO6 cells and purified OMVs of control cells with corresponding wave assignments from the literature. Other treatments are not shown because all treatments have the same peaks though with differing intensities.

*Pc*O6 Peak (cm⁻¹)	OMV Peak (cm⁻¹)	Literature Peak (cm⁻¹)	Assignment from Literature	Source
623	-	623	Phenylalanine (C-C bond twist)	(Notingher et al. 2003)
644	-	644, 645	Tyrosine (C-C bond twist)	(Notingher et al. 2003; Rygula et al. 2013)
-	653	654	Tyrosine	(Rygula et al. 2013)
669	-	669	Thymine and guanine	(Notingher et al. 2003)
-	685	683	Guanine (ring breath)	(Sockalingum et al. 2003)
728	-	728	Adenine, and tryptophan (ring breath)	(Notingher et al. 2003)
			Lipid C-N head groups	(Uzunbajakava et al. 2003)
-	734	-	-	-
749	749	748	Tryptophan	(Rygula et al. 2013)
758	-	758	Carbohydrate C-O ring (stretching) Carbohydrate C-O-C, C-C-O, and O-C-O bonds (in-plane bending)	(Wiercigroch et al. 2017)
		759	Tryptophan	(Rygula et al. 2013)
		760	Tyrosine (ring breath)	(Notingher et al. 2003)
			Lipid N⁺(CH₃)₃ bonds (symmetric stretching)	(Czamara et al. 2015)
-	775	-	-	-
782	-	782	Uracil, cytosine, and thymine (ring breath)	(Notingher et al. 2003)
810	-	811	Lipid O-P-O bonds	(Notingher et al. 2003)
829	826	827	Tyrosine	(Rygula et al. 2013)
		828	DNA O-P-O bonds (stretching) Tyrosine (out of plane ring breath)	(Notingher et al. 2003)
		829	Tyrosine	(Rygula et al. 2013)
		830	Exposed tyrosine	(Maquelin et al. 2002)
853	-	853	Tyrosine	(Rygula et al. 2013)
			Tyrosine (ring breath)	(Notingher et al. 2003)
-	871	870	Tyrosine	(Rygula et al. 2013)
		871	C-O-O lipid bonds (skeletal)	(Czamara et al. 2015)
880	-	880	Tryptophan	(Rygula et al. 2013)
		882	Lipid N⁺(CH₃)₃ bonds (asymmetric stretching)	(Czamara et al. 2015)

Table A - 3 continued: Peaks from Raman spectra of intact PcO6 cells and purified OMVs of control cells with corresponding wave assignments from the literature. Other treatments are not shown because all treatments have the same peaks though with differing intensities.

*Pc*O6 Peak (cm^{-1})	OMV Peak (cm^{-1})	Literature Peak (cm^{-1})	Assignment from Literature	Source
890-900	-	897	DNA deoxyribose phosphate backbone	(Notingher et al. 2003)
			Proline	(Moritz et al. 2010)
-	924	924	Protein N-C$_\alpha$-C bonds	(Rygula et al. 2013)
936	-	934	Protein C-C backbone	(Moritz et al. 2010)
		936	Protein N-C$_\alpha$-C bonds	(Rygula et al. 2013)
		936	Carbohydrate C-O in-glycosidic linkage (stretching)	(Wiercigroch et al. 2017)
		937	Protein C-C α helix backbone (stretching)	(Notingher et al. 2003)
973	974	974	Lipid C-H bonds (bending)	(Czamara et al. 2015)
1004	1005	1004 1005	Phenylalanine	(Maquelin et al. 2002; Notingher et al. 2003; Rygula et al. 2013)
1050-1130	1030-1150	1030-1130	Carbohydrates	(Schuster et al. 2000)
1064	-	1061	C-N and C-C bonds (stretching)	(Maquelin et al. 2002)
		1064	Lipid C-C bonds (stretching)	(Czamara et al. 2015)
		1066	Protein C-N bond (stretching) Lipid C-C chain bond (stretching)	(Notingher et al. 2003)
-	1092	1095	DNA PO$_2^-$ bond (stretching) Lipid C-C chain bond (stretching) Carbohydrate C-C bond (stretching)	(Notingher et al. 2003)
		1090,1091,1094	Lipid C-C bond (stretching)	(Czamara et al. 2015)
1100	-	1102	> PO$_2^-$ (symmetrical stretching)	(Maquelin et al. 2002)
-	1120	1120	Lipid C-C bond (stretching)	(Czamara et al. 2015)
1127	-	1127	Carbohydrate C-O bond (stretching)	(Wiercigroch et al. 2017)
		1127	Protein C-N bond	(Rygula et al. 2013)
		1128	Protein C-N bond stretching Lipid C-C chain bond stretching	(Notingher et al. 2003)
		1130	Unsaturated fatty acid =C-C= bonds	(Schuster et al. 2000)

Table A - 3 continued: Peaks from Raman spectra of intact PcO6 cells and purified OMVs of control cells with corresponding wave assignments from the literature. Other treatments are not shown because all treatments have the same peaks though with differing intensities.

PcO6 Peak (cm⁻¹)	OMV Peak (cm⁻¹)	Literature Peak (cm⁻¹)	Assignment from Literature	Source
1156	-	1145-1160	C-C and C-O bonds (ring breath, asymmetrical)	(Rösch et al. 2005; Schenzel and Fischer 2001)
		1154	C-C, C-N, and C-H$_3$ bonds (stretching)	(Maquelin et al. 2002)
		1156	Protein C-C & C-N bonds (stretching)	(Notingher et al. 2003)
		1155-1157	Sarcinaxanthin and carotenoids C-C bonds (stretching)	(Rösch et al. 2005)
-	1162	1161	Sucrose fructosyl unit	(Wiercigroch et al. 2017)
1174	1172	1175	Tyrosine, phenylalanine	(Uzunbajakava et al. 2003)
		1175	Lipid C-C bond (stretching)	(Czamara et al. 2015)
		1176	Tyrosine C-H in plane bend	(Notingher et al. 2003)
1209	-	1209	Phenylalanine and Tryptophan C-C$_6$H$_5$ bond (stretching)	(Notingher et al. 2003)
		1211	Tyrosine	(Rygula et al. 2013)
1220-1280	1230-1290	1220-1290	Amide III	(Schuster et al. 2000)
1252	-	1252	Lipid =CH bond (deformation)	(Czamara et al. 2015)
1330-1340	-	1336-1339	Adenine, guanine, tyrosine, tryptophan	(Harz et al. 2009; Uzunbajakava et al. 2003)
-	1348	1348	Tryptophan C$_\alpha$-H bond (deformation)	(Rygula et al. 2013)
		1348	Carbohydrate C-H$_2$ bonds (wagging)	(Wiercigroch et al. 2017)
1365	-	1367	Lipid CH$_3$ bonds (symmetrical stretching)	(Notingher et al. 2003)
1450	1430-1455	1440-1460	C-H$_2$ bonds (deformation)	(Maquelin et al. 2002)
1482	-	1482	Protein C-H bonds (deformation)	(Rygula et al. 2013)
-	1513	1518	Adenine, cytosine, guanine	(Uzunbajakava et al. 2003)
1553	1557	1553, 1557	Tryptophan (indole ring)	(Rygula et al. 2013)
1576	-	1575-1578	Guanine, and adenine (ring stretching)	(Maquelin et al. 2002)
		1578	Guanine, and adenine	(Notingher et al. 2003)
1605	-	1605-1606	Phenylalanine	(Maquelin et al. 2002)
		1605	Tyrosine, tryptophan, and phenylalanine	(Rygula et al. 2013)
1620	-	1617	Tyrosine and tryptophan C=C bonds	(Notingher et al. 2003)
		1620	Tyrosine, tryptophan, phenylalanine	(Rygula et al. 2013)

Table A - 3 continued: Peaks from Raman spectra of intact PcO6 cells and purified OMVs of control cells with corresponding wave assignments from the literature. Other treatments are not shown because all treatments have the same peaks though with differing intensities.

PcO6 Peak (cm^{-1})	OMV Peak (cm^{-1})	Literature Peak (cm^{-1})	Assignment from Literature	Source
-	1646	1647	Glycine C=O bond	(Lagant et al. 1984)
1660	-	1658	Unsaturated lipids	(van Manen et al. 2005)
		1659	Amide I protein α helix	(Notingher et al. 2003)
			Lipid C=C bonds (stretching)	
		1660	C=C lipid bond (stretching)	(Czamara et al. 2015)
		1660	Protein amide I bond	(Rygula et al. 2013)
		1650-1680	Amide I	(Maquelin et al. 2002)
		1663	Amide I	(van Manen et al. 2005)
-	2446	-	-	-
2700-2770	2700-2790	-	-	-
2855	-	2855	Lipid C=H$_2$ bonds (asymmetric stretching)	(Czamara et al. 2015)
2875	2883	2870-2890	C-H$_2$ bonds (stretching)	(Maquelin et al. 2002)
		2875, 2883	Lipid C=H$_2$ bonds (asymmetric stretching)	(Czamara et al. 2015)
2935	2934	2935	C-H bonds (stretching)	(Harz et al. 2009; Maquelin et al. 2002)
		2935	Lipid C=H$_3$ bonds (symmetric stretching)	(Czamara et al. 2015)
3062	-	3059	Aromatic C=C-H bonds (stretching)	(Maquelin et al. 2002)
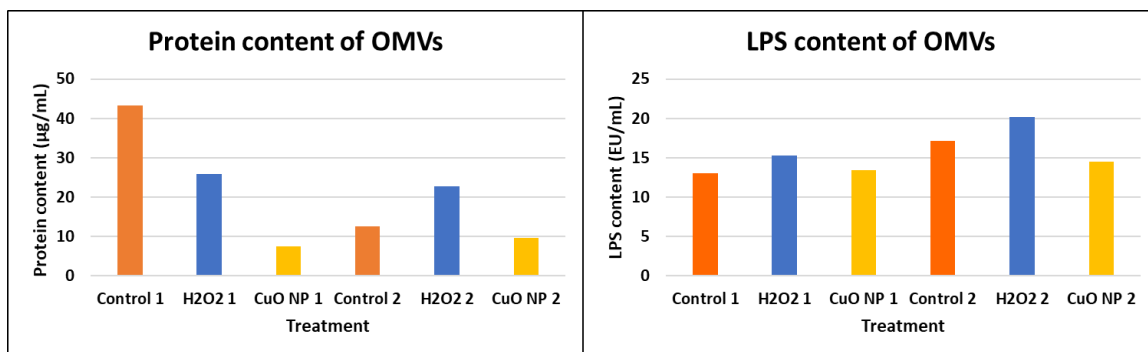
Figure A - 7: Protein content (in µg Protein/mL solution) and LPS content (in endotoxin units (EU)/mL of solution) of purified OMVs.

Table A - 4: 260/280 ratios of OMVs which quantify the nucleic acid to protein ratio respectively.

Treatment	260/280
Control 1	5.886
	5.999
Control 2	5.92
	5.637
H_2O_2 1	5.987
	5.905
H_2O_2 2	5.945
	5.935
CuO NPs 1	5.969
	5.928
CuO NPs 2	5.884
	5.911

References

Czamara, K., K. Majzner, M. Z. Pacia, K. Kochan, Agnieszka Kaczor, and M. Baranska. 2015. "Raman Spectroscopy of Lipids: A Review." Journal of Raman Spectroscopy 46(1):4–20.

Harz, M., P. Rösch, and J. Popp. 2009. "Vibrational Spectroscopy-A Powerful Tool for the Rapid Identification of Microbial Cells at the Single-Cell Level." Cytometry Part A 75(2):104–13.

Hoagland, D. R. and D. I. Arnon. 1950. "The Water-Culture Method for Growing Plants without Soil." Circular.

Lagant, Philippe, Gerard Vergoten, Guy Fleury, and Marie-H. Loucheux-Lefebvre. 1984. "Raman Spectroscopy and Normal Vibrations of Peptides." European Journal of Biochemistry 148(1):137–48.

van Manen, Henk-Jan, Yvonne M. Kraan, Dirk Roos, and Cees Otto. 2005. "Single-Cell Raman and Fluorescence Microscopy Reveal the Association of Lipid Bodies with Phagosomes in Leukocytes." Proc. Natl. Acad. Sci. USA 102(29):10159–64.

Maquelin, K., C. Kirschner, L. P. Choo-Smith, N. Van Den Braak, H. Ph. Endtz, D. Naumann, and G. J. Puppels. 2002. "Identification of Medically Relevant Microorganisms by Vibrational Spectroscopy." Journal of Microbiological Methods 51(3):255–71.

Moritz, Tobias J., Douglas S. Taylor, Christopher R. Polage, Denise M. Krol, Stephen M. Lane, and James W. Chan. 2010. "Effect of Cefazolin Treatment on the Nonresonant Raman Signatures of the Metabolic State of Individual Escherichia Coli Cells." Biophysical Journal 98(3):742a.

Notingher, I., S. Verrier, S. Haque, J. M. Polak, and L. L. Hench. 2003. "Spectroscopic Study of Human Lung Epithelial Cells (A549) in Culture: Living Cells versus Dead Cells." Biopolymers - Biospectroscopy Section 72(4):230–40.

Rösch, Petra, Michaela Harz, Michael Schmitt, Klaus Dieter Peschke, Olaf Ronneberger, Hans Burkhardt, Hans-Walter Motzkus, Markus Lankers, Stefan Hofer, Hans Thiele, and Jürgen Popp. 2005. "Chemotaxonomic Identification of Single Bacteria by Micro-Raman Spectroscopy: Application to Clean-Room-Relevant Biological Contaminations." Applied and Environmental Microbiology.

Rygula, A., K. Majzner, K. M. Marzec, A. Kaczor, M. Pilarczyk, and M. Baranska. 2013. "Raman Spectroscopy of Proteins: A Review." Journal of Raman Spectroscopy 44(8):1061–76.

Schenzel, Karla and Steffen Fischer. 2001. "NIR FT Raman Spectroscopy - A Rapid Analytical Tool for Detecting the Transformation of Cellulose Polymorphs." Cellulose 8(1):49–57.

Schuster, K. C., I. Reese, E. Urlaub, J. R. Gapes, and B. Lendl. 2000. "Multidimensional Information on the Chemical Composition of Single Bacterial Cells by Confocal Raman Microspectroscopy." Analytical Chemistry 72(22):5529–34.

Sockalingum, Ganesh D., Hasnae Lamfarraj, Abdelilah Beljebbar, Patrick Pina, Marc Delavenne, Fabienne Witthuhn, Pierre Allouch, and Michel Manfait. 2003. "Vibrational Spectroscopy as a Probe to Rapidly Detect, Identify, and Characterize Micro-Organisms." Biomedical Applications of Raman Spectroscopy 3608(April 1999):185–94.

Uzunbajakava, N., A. Lenferink, Y. Kraan, E. Volokhina, G. Vrensen, J. Greve, and C. Otto. 2003. "Nonresonant Confocal Raman Imaging of DNA and Protein Distribution in Apoptotic Cells." Biophysical Journal 84(6):3968–81.

Wiercigroch, Ewelina, Ewelina Szafraniec, Krzysztof Czamara, Marta Z. Pacia, Katarzyna Majzner, Kamila Kochan, Agnieszka Kaczor, Malgorzata Baranska, and Kamilla Malek. 2017. "Raman and Infrared Spectroscopy of Carbohydrates: A Review." Spectrochimica Acta - Part A: Molecular and Biomolecular Spectroscopy 185:317–35.

APPENDIX B

BIOFILM DEFICIENT MUTANT CHARACTERIZATION

Generation of mutants

A kanamycin resistance gene was inserted randomly into *Pc*O6 genomes using an

Ez::TN transposon kit (Epicentre Inc., Madison, WI). The methods for electroporation

into *Pc*O6 were:

<u>Making competent cells</u>

1.   Streak bacteria to get single colonies.

2.   After overnight incubation, pick a single colony. Inoculate 50 mL of LB medium

and incubate overnight at an appropriate temperature.

3.   Subculture to 1 L of LB medium with 5 mL of LB medium of the overnight

culture.

4.   Grow to OD 600 = 0.8 at appropriate temperature.

5.   Pellet cells by centrifuging at 5000 rpm for 10 minutes.

6.   Resuspend the cells in 500 mL of cold sterile 10% glycerol (v/v) and centrifuge

again. Repeat one more time.

7.   Pour off the supernatant and resuspend the cells in any remaining glycerol. If

necessary, adjust the volume up to 4 mL with cold sterile 10% glycerol (v/v).

8.   Transfer 200 μL aliquots into microcentrifuge tubes and store at -70°C.

<u>Electroporation</u>

9.   Gently thaw cells to room temperature then put on ice.

10.   In a pre-chilled microcentrifuge tube, mix 40 μL of cells with 1 μL (10 pg/μL of

10 ng/μL) of DNA. Mix the suspension well and place on ice for 30 s to 1 min.

11.   Set electroporator to 20 μF, 2.5 kV, and 200 Ω.

12.   Transfer the cell solution to a pre-chilled 0.2 cm cuvette (sterilized with ethanol

and washed with sterile H$_2$O). Shake the suspension to the bottom of the cuvette.

13.   Pulse the cells for 405 ms.

14.   Remove the cuvette and immediately add 1 mL of cold LB medium and resuspend the cells with a Pasteur pipette.

15.   Transfer the cells to a new tube and incubate them at room temperature for 1 h.

16.   Dilute the cells in PBS or SS and plate them on selective medium.

Biofilm formation

Over 5,000 mutants were isolated from 63 of 96 12-well plates. Biofilm formation was then screened for plastic surfaces in liquid medium after 4 D of growth on a rocker shaker at 100 rpm with a crystal violet stain which detects biofilm as pellicles and structures on well sides and bases. Various media were attempted (Figure B - 1) and various carbon sources (Figure B - 2).

Figure B - 1: Biofilm stains of various *Pc*O6 mutants on various media. Note that mutants still form biofilms on KB media which has casamino acids and glycerol.

SUCROSE

MANNITOL

GLUCOSE

CASAMINO ACIDS

Strain B4 E2 E11 F3 O6
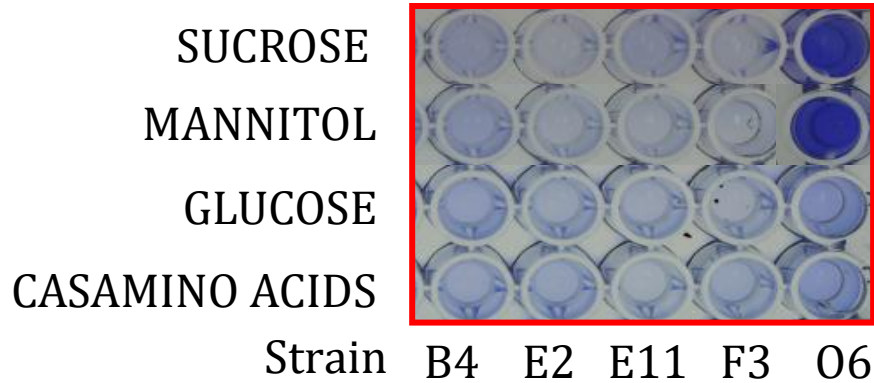
Figure B - 2: All mutants were negative for biofilm formation. WT was also negative on glucose and casamino acids. Glycerol may account for biofilms in the KB medium.

Growth in liquid media

250 mL Erlenmeyer flasks were filled with 50 mL of minimal or LB medium. WT *Pc*O6 and each strain of mutant *Pc*O6 were inoculated into two minimal medium flasks and two LB medium flasks. One flask per medium was shaken at 100 rpm for two days and one flask per medium was left sitting on a benchtop. Cell density was found by performing optical density readings at 600 nm.

There were no significant differences in growth time between wild type (WT) and mutant *Pc*O6 mutants (Figure B - 3). Differences in phenazine production (Figure B - 4) and pellicle formation (Figure B - 5) were noted. Phenazine production was altered in WT as well which may indicate that it became a GacS mutant. B4 overproduced phenazines and F3 was defective in phenazine production. E2 and E11 showed greater phenazine production when unshaken whereas B4 and F3 showed similar production in both conditions.
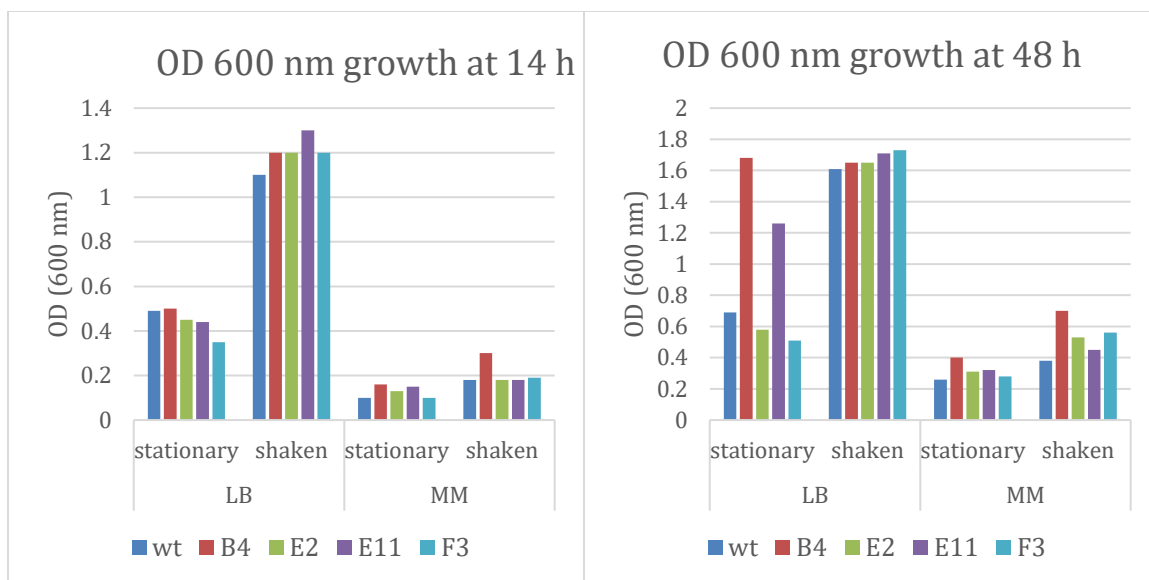
Figure B - 3: Growth of WT and mutant *Pc*O6 in LB media and minimal media (MM) after 14 h of growth and 48 h of growth.
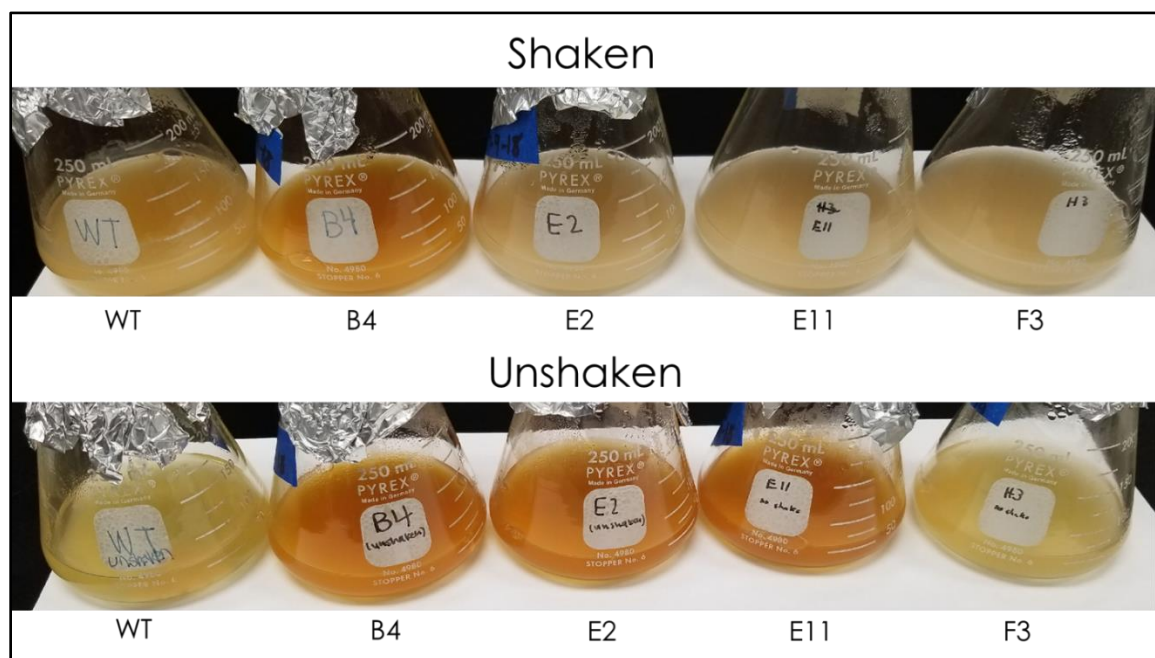
Figure B - 4: Shaken and unshaken LB flasks inoculated with WT or mutant *Pc*O6 after two days of growth.
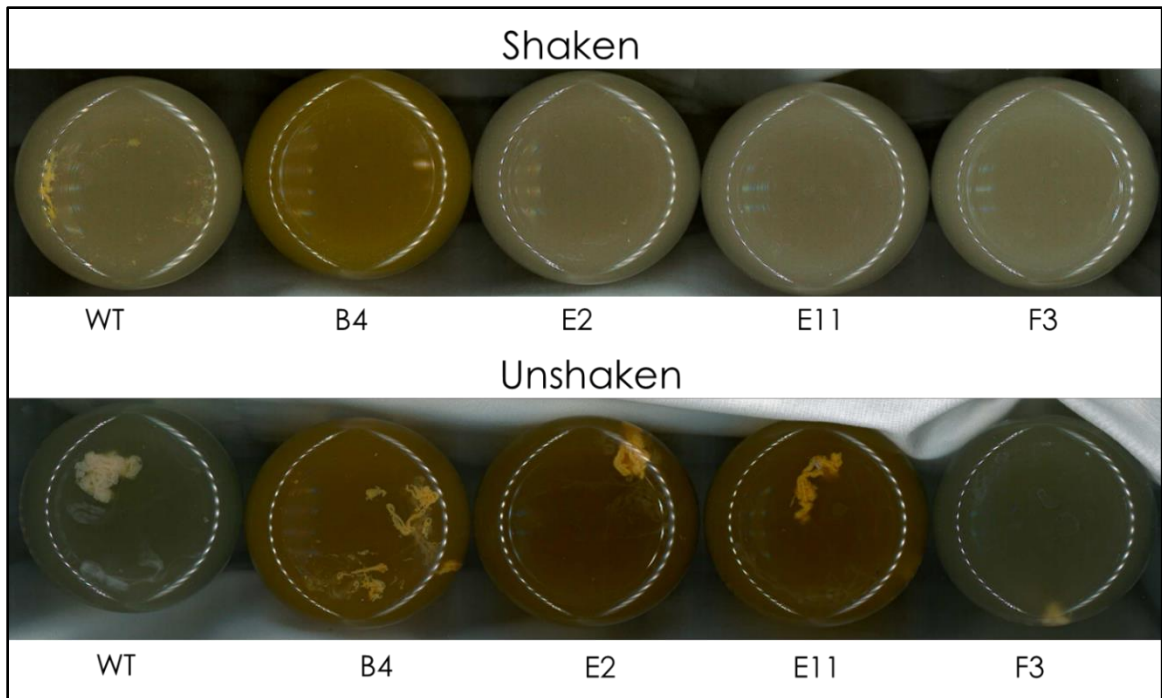
Figure B - 5: Pellicle formation in LB flasks inoculated with WT or mutant *Pc*O6 after two days of growth.

Motility

Pili and flagella involved in biofilm formation. For this reason, it was imperative to test the motility of the biofilm deficient mutants. 10 μL drops of inoculum were dropcast on an LB 0.5% agar plate or an LB 2% agar plate. After 48 h, the diameter of the bacterial growth was measured. Three plates of each agar concentration were used for the WT and mutant *Pc*O6 strains. The average diameters of each agar concentration for each *Pc*O6 strain are shown in Figure B - 6. Images of one plate of each treatment are shown in Figure B - 7.

E2 and E11 were hypermotile compared to the WT possibly due to additional flagella though imaging is needed to confirm this hypothesis. These results indicate that the inability of these bacteria to form biofilms is not correlated with motility. B4 and H3

were hypomotile compared to the WT which may indicate a lack of flagella in these

*Pc*O6 strains.
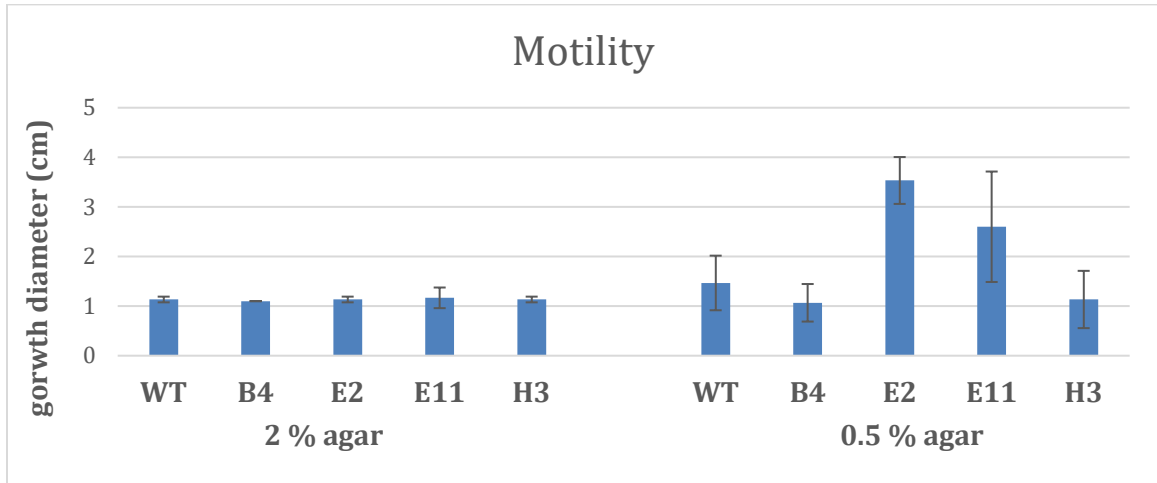
Figure B - 6: Motility of *Pc*O6 strains as measured by the average growth diameters (n=3) of 10 μL drops of WT and mutant *Pc*O6 strains on LB 2% agar plates and LB 0.5% agar plates.
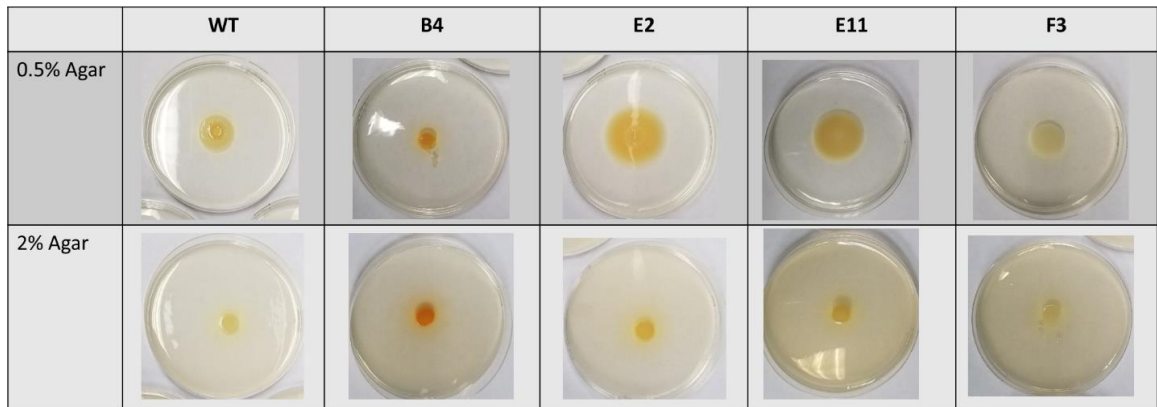
Figure B - 7: Images illustrating the motility of WT and mutant *Pc*O6 strains as measured by the growth of 10 μL drops on LB 2% agar plates and LB 0.5% agar plates.

Root Colonization

Wheat seeds (Juniper) were surface sterilized with 10% H_2O_2 for 10 minutes,

rinsed thoroughly with sterile deionized H_2O, and exposed to WT or mutant PcO6 (10^4 CFUs/mL) for 5 minutes. A control was also performed by soaking seeds for 5 minutes in sterile deionized H_2O. Seeds were planted in sand previously sterilized in closed, clear plastic containers by autoclaving for 50 minutes at 221°C. Plants were grown for 5 days before analysis. Colonization of wheat roots was assessed through two methods: 1) wheat was removed from the sand and placed on LB 2% agar petri dishes for 48 hours and 2) root sections were fixed by submersion in methanol followed by ethanol, critical point dried, and imaged with a scanning electron microscope (SEM) under low vacuum. Images from these assays are shown in Table B - 1.

The control plants showed root colonization by an unknown bacterium, possibly an endophyte of the wheat seeds. This unknown bacterium appears in images from E2 (Table B - 1), oftentimes with an endospore, though this endospore is very distinct from those formed by *Bacillus subtilis* previously seen by members of this group (data not shown). Results from the two assays disagree in all wheat colonized by WT or mutant PcO6. Bright orange colonies characteristic of PcO6 are seen on all roots however bacteria seem to be very scarce in SEM images. This may indicate that many bacteria were washed off the roots during the fixation process or that the LB agar plate assay overstates the degree of colonization. Further tests are needed to resolve this question.

Table B - 1: Images of the assays used to determine colonization of wheat roots by WT and mutant *Pc*O6.
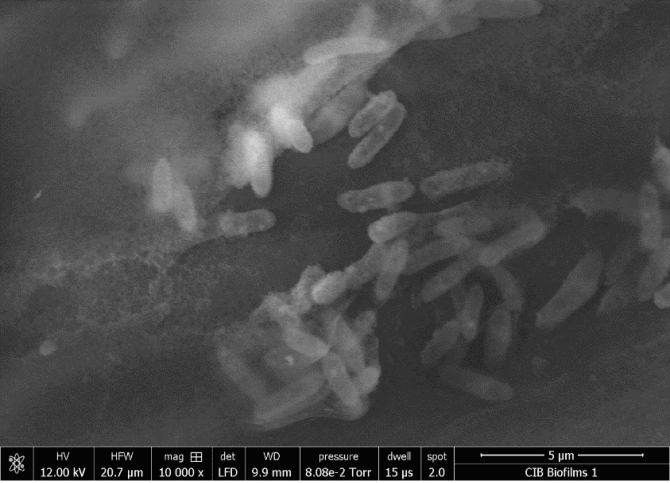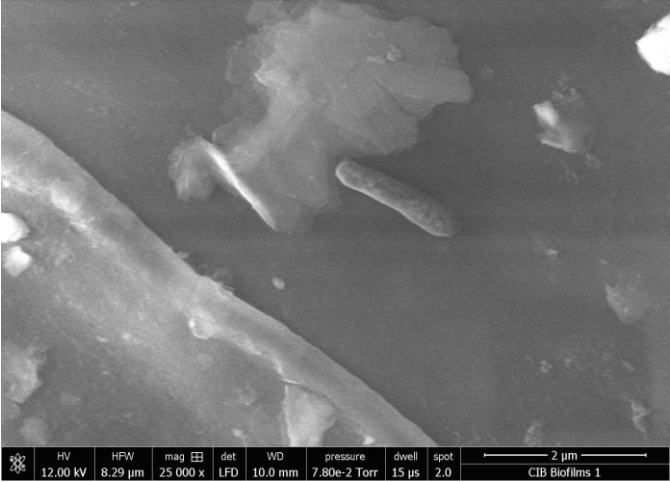
*Pc*O6 strain	Wheat root on LB 2% agar plate	SEM image
Control		
WT		

Table B - 1: Images of the assays used to determine colonization of wheat roots by WT and mutant *Pc*O6.
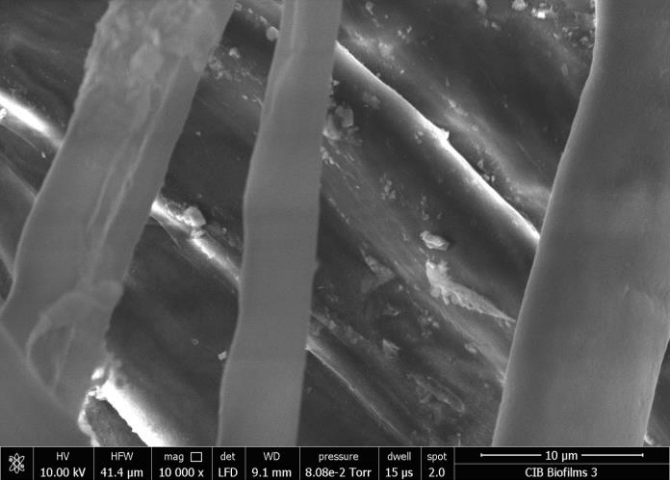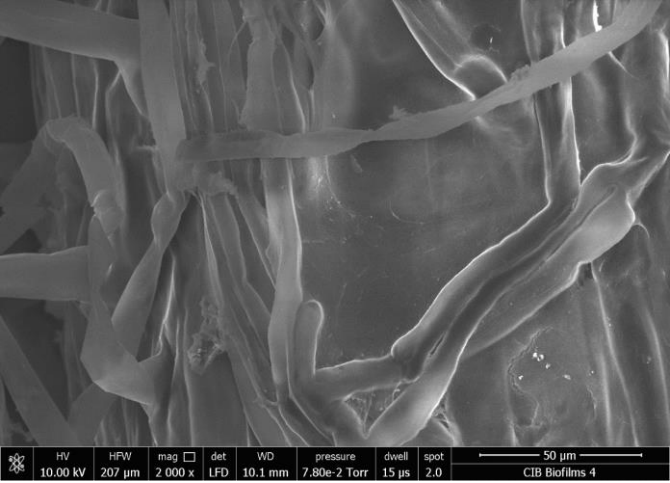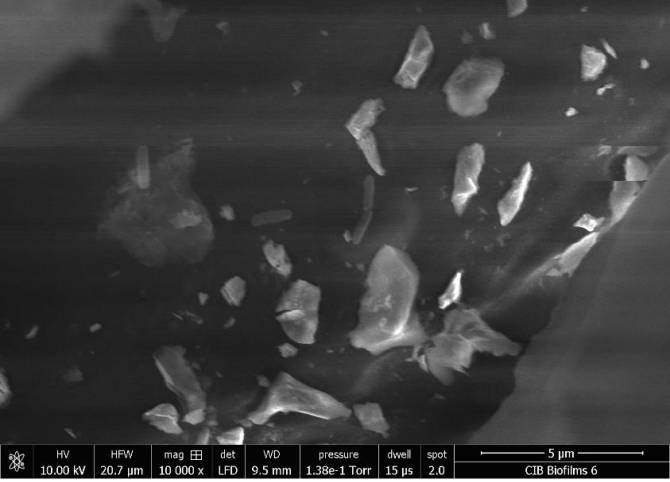
*Pc*O6 strain	Wheat root on LB 2% agar plate	SEM image
B4		
E2		

Table B - 1: Images of the assays used to determine colonization of wheat roots by WT and mutant *Pc*O6.

*Pc*O6 strain	Wheat root on LB 2% agar plate	SEM image
E11		
F3		

APPENDIX C

IMMUNE RESPONSES OF MAMMALIAN CELLS TO OUTER MEMBRANE

VESICLES

Significance

OMVs have been isolated from human pathogenic bacteria such as *Neisseria meningitidis* serogroup B to produce vaccines. *Pseudomonas chlororaphis* O6 (*Pc*O6) is a common soil bacterium found at the root of plants that help keep plants hydrated and protect the roots by producing antibiotic and antifungal products. *Pc*O6 was used as a source to obtain OMVs because it was readily available and was already being studied by one of our group. Since OMVs of *Pc*O6 are being studied as a method to protect plants from stressors such as drought, it is important to know what effects OMVs may have on human health.

Methods

OMVs for this experiment were isolated from *Pc*O6 using methods explained in Chapter 4. Three sets of cultures in quadruplicate were used. The treatments were: 1) A negative control culture of just ARPE-19 cells (2 wells standard, 2 wells with microfiltered DI water), 2) A positive control culture of the ARPE-19 cells exposed to lysed *Pc*O6 fragments (4 wells), and 3) A culture ARPE-19 cells exposed to OMVs (4 wells).

Cultures were grown to confluency (2 d) then observed daily for 7 d. Cultures were photographed under a microscope every other day to observe density and morphology. 100 uL of media were pulled every other day from each well and frozen. At the end of the 7 days, the cell density was determined using a hemocytometer and

compared to the initial viability. All samples were run on a multiplexed Cytokine Screen assay from Quansys biosciences using instructions from the manufacturer to quantify levels of various analytes indicative of an inflammatory response.

Expected outcomes

Cells that are not exposed to any bacterial components (the negative control) were expected to show little if any immune response. Cells exposed to lysed bacteria (the positive control) were expected to exhibit an immune response and lower cell viability. Cells exposed to OMVs were expected to exhibit an immune response and possibly lower cell viability.

Results

Cell density

Final cell densities are shown in Figure C - 1. Overgrowth occurred in the control cells, the cells exposed to DI H_2O, and the cells exposed to lysed PcO6 though no overgrowth occurred in the cells exposed to OMVs (Table C - 1). The addition of DI water, which the OMVs and the lysed PcO6 cells were suspended in, made no difference in the cell density or morphology. In hemocytometer assays, very few dead cells were observed despite the overgrowth (data not shown).

The lack of overgrowth in control #1, which did occur in control #2, possibly indicates that control #1 was contaminated with a mycoplasma bacterium. No visible bacteria were present in control #1 during imaging and no changes in media color were observed ruling out the possibility of contamination by another class of bacteria.

Table C - 1: Images of ARPE-19 cells in all wells just before the addition of the treatment (day 0) and on subsequent days.
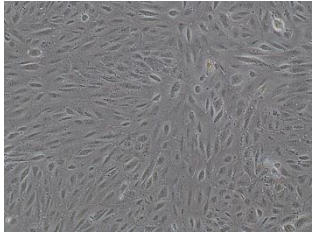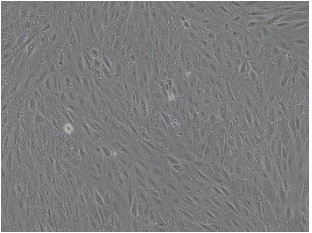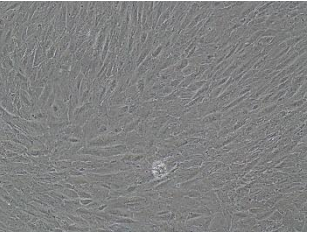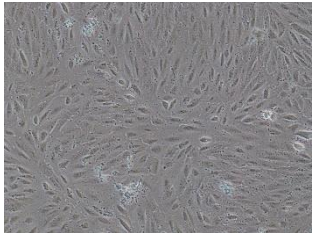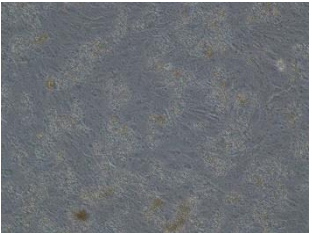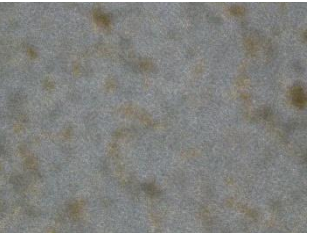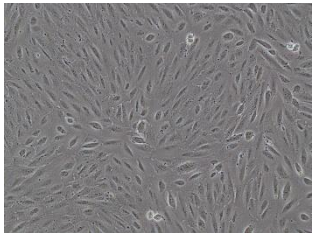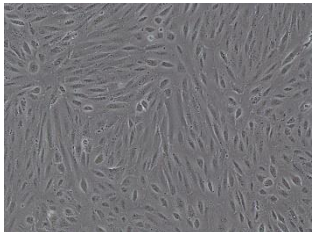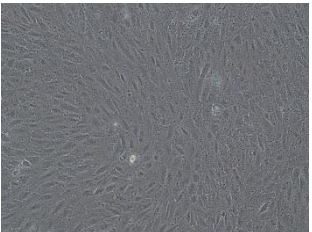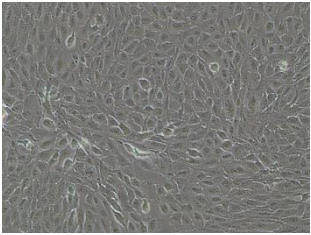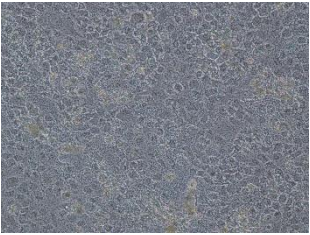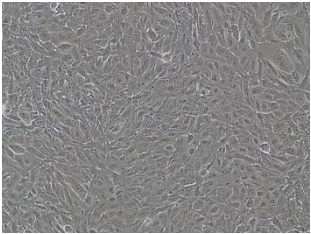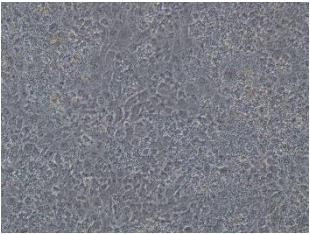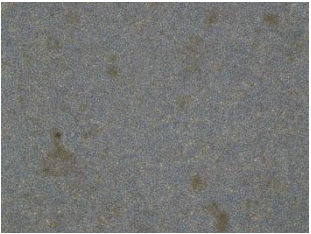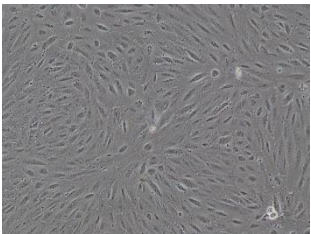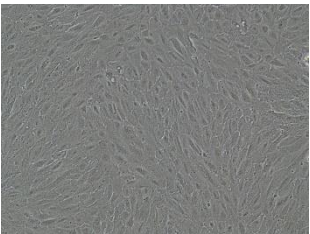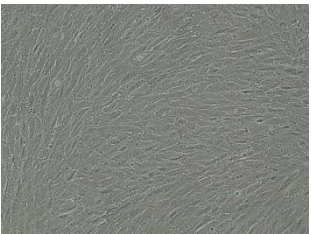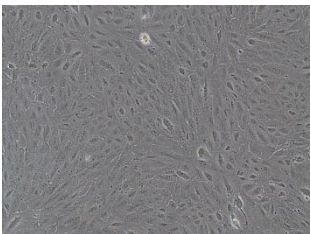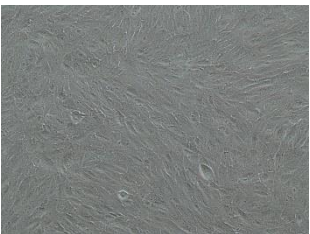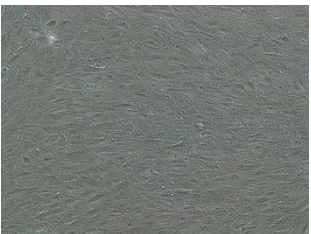
	Day 0	Day 2	Day 5	Day 7
Control Well #1				
Control Well #2				
Sterile H_2O Well #1				
Sterile H_2O Well #2				

Table C - 1: Images of ARPE-19 cells in all wells just before the addition of the treatment (day 0) and on subsequent days.

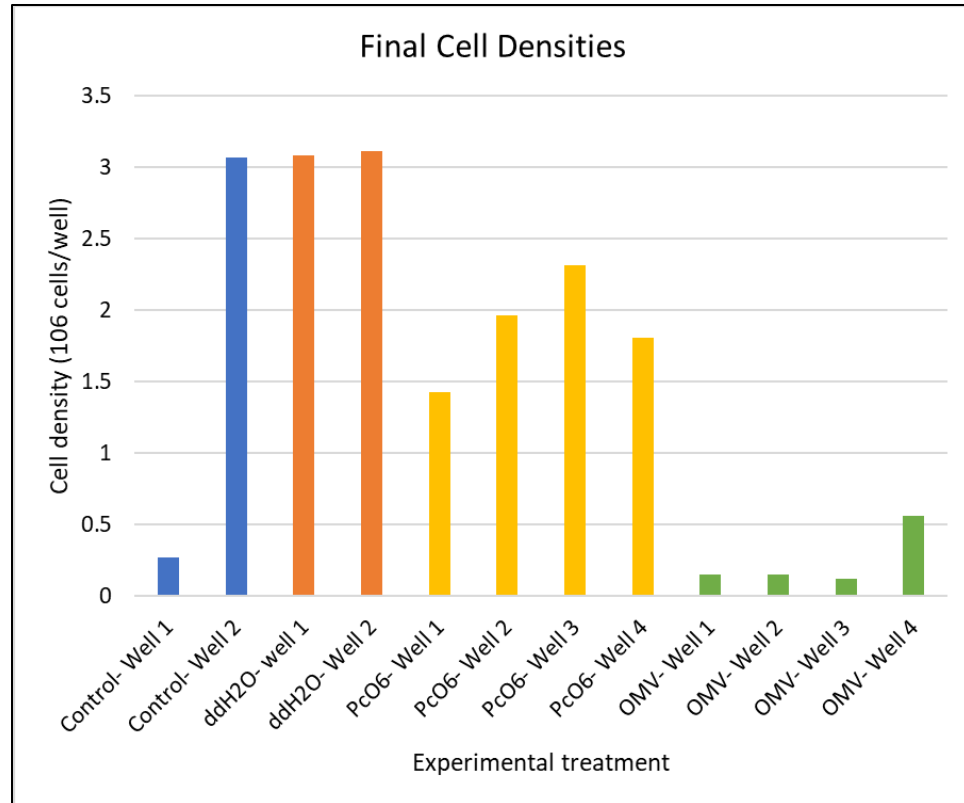|	Day 0	Day 2	Day 5	Day 7
Lysed *Pc*O6 Well #1				
Lysed *Pc*O6 Well #4				
OMVs Well #2				
OMVs Well #4				

Figure C - 1: Final ARPE-19 cell densities in each well after being grown to confluency (2 d) followed by 7 d exposed to lysed PcO6, isolated OMVs, sterile distilled H_2O, or none of these.

Cytokine analysis

Final cytokine concentrations are shown in Figure C - 2. Cytokine levels over the course of the experiment are shown in Figure C - 3. OMVs elicited an increased expression of IL-1a, IL-4, IL-5, IL-6, IL-10, and IL-15 from ARPE-19 cells. ARPE-19 exposed to lysed PcO6 showed low levels of cytokine expression in only IL-1a and IL-6. Control ARPE-19 (with and without DI H_2O) also showed low levels of IL-1a and IL-6. Cytokine analysis results supported the conclusion that control well #1 was contaminated due to the levels of IL-1a, IL-4, IL-5, IL-6, and IL-15 in that well. IL-6 was the most expressed cytokine in all cultures.
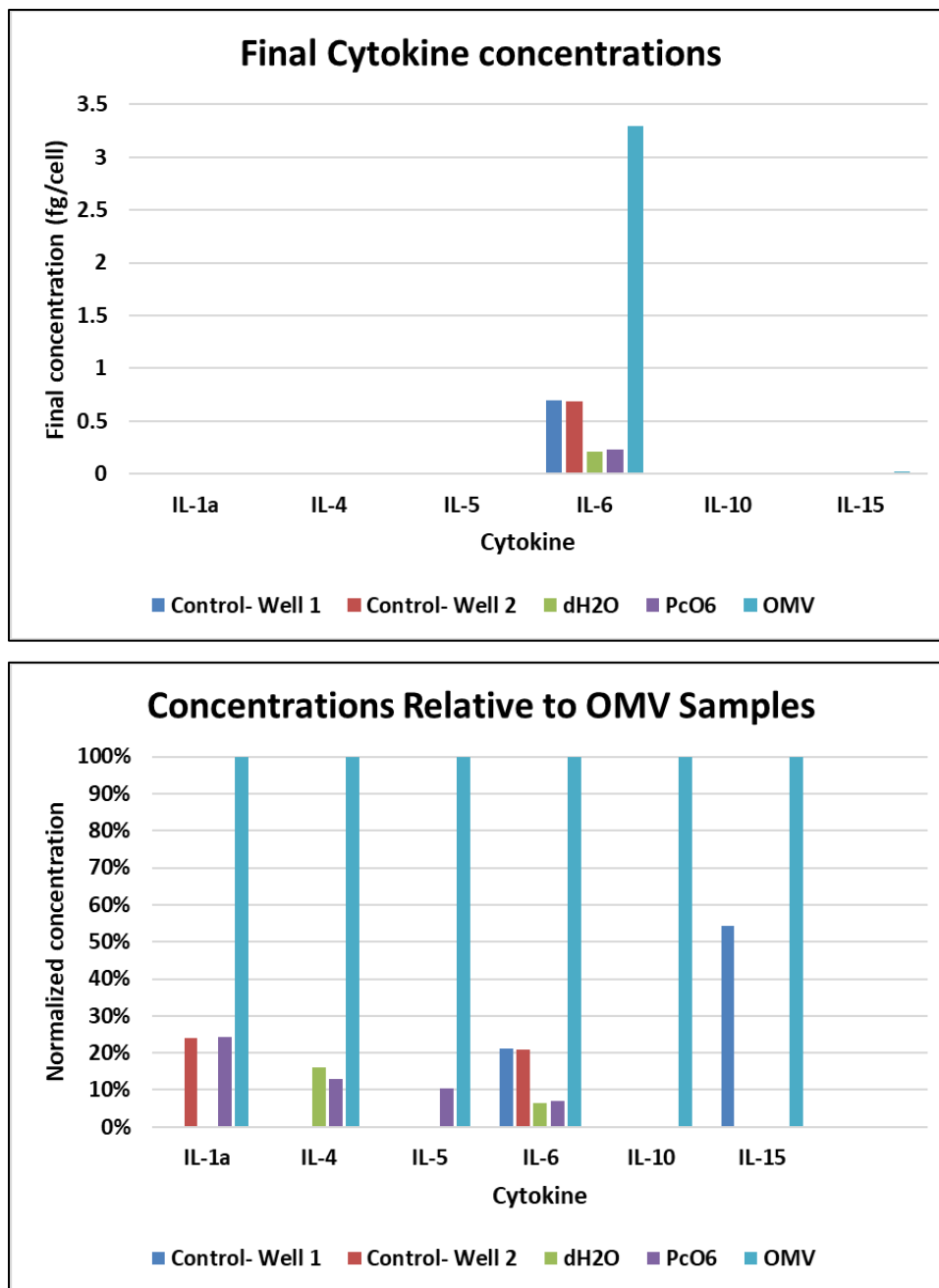
Figure C - 2: Cytokine concentrations after cells had been grown to confluency (2 days) then exposed to lysed *Pc*O6, isolated OMVs, sterile distilled water, or none of these for 7 d.
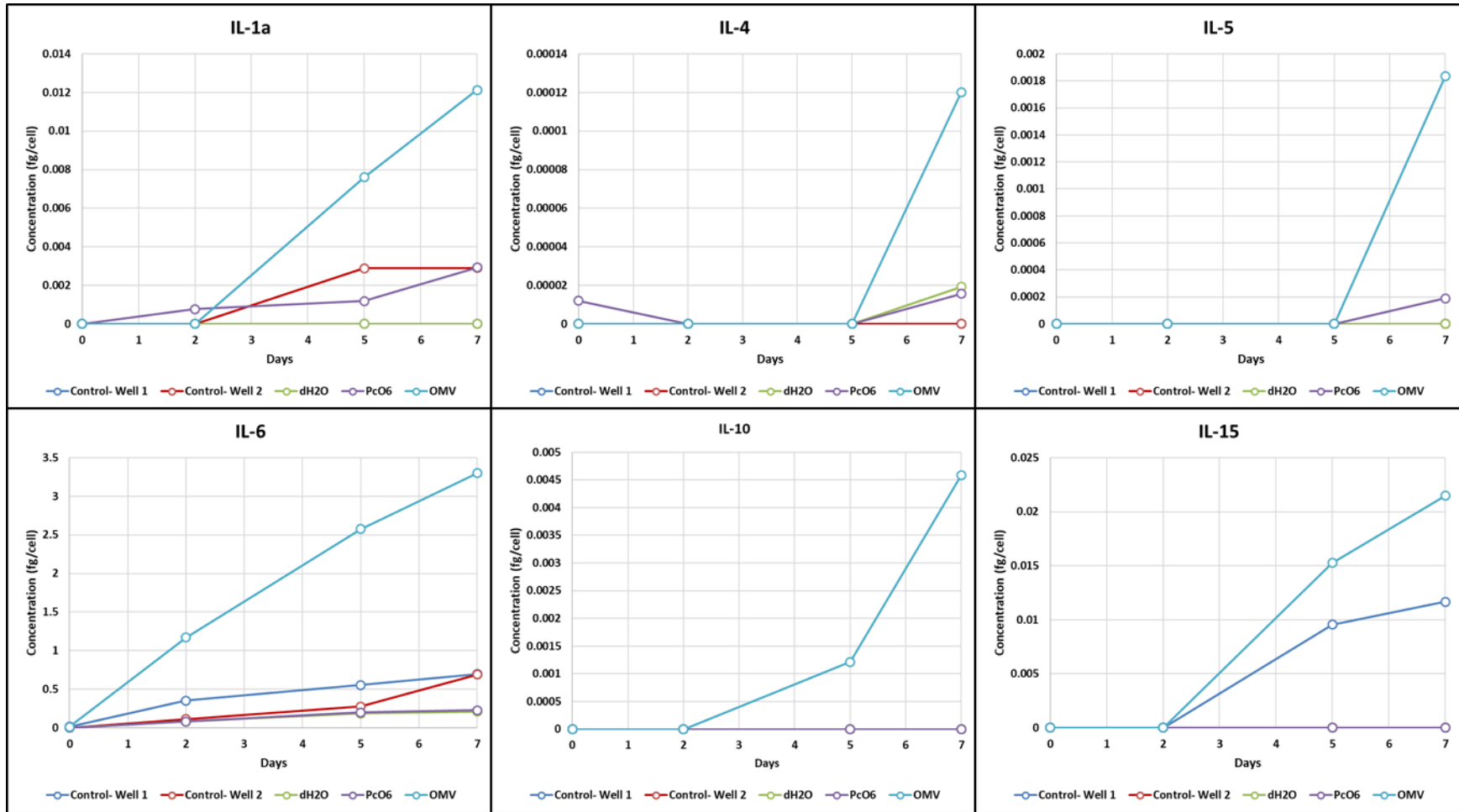
Figure C - 3: Concentrations of cytokines over the course of 7 d exposed to lysed *Pc*O6, isolated OMVs, sterile distilled water, or none of these.

Conclusions

OMVs from *Pc*O6 elicit an immune response in ARPE-19 cells. A larger response was expected from cells exposed to lysed *Pc*O6 bacteria though this may be due to the concentration of the bacterial fragments rather than chemical differences between *Pc*O6 cells and OMVs.

Future Work

The overgrowth of ARPE-19 may be prevented by shortening the growth time, not waiting for a confluent layer, or changing the media every 2 days. In this study, the media was not changed to observe a greater change in cytokine levels. Fully isolate OMVs from other secreted bacterial material to further study their effect on mammalian cells

OMV and lysed *Pc*O6 densities were not quantified in this study. In future work, tests should be performed with OMVs from a culture of *Pc*O6 of known density and compare with lysed *Pc*O6 of a culture with the same density to observe the changes from varying OMV and lysed *Pc*O6 concentrations.